Exploring the mechanisms of sexual dimorphism in oxygen delivery-to-utilization matching in skeletal muscle

by

Jesse Charles Craig

B.A., Washburn University, 2011
M.S., Kansas State University, 2015

AN ABSTRACT OF A DISSERTATION

submitted in partial fulfillment of the requirements for the degree

DOCTOR OF PHILOSOPHY

Department of Kinesiology
College of Human Ecology

KANSAS STATE UNIVERSITY
Manhattan, Kansas

2018

Abstract

The onset of skeletal muscle contractions induces rapid and robust increases in metabolic rate ($\dot{V}O_2$) and blood flow ($\dot{Q}$) in order to supply the energetic demands of the muscle. In young healthy populations, these variables increase proportionally to maintain oxygen flux into the myocyte for both sexes. However, while the resultant changes in $\dot{V}O_2$ and $\dot{Q}$ conflate to establish adequate driving pressures of oxygen (PO_2), it appears that the underlying control processes express distinct sexual dimorphism. Estrogen is crucial for cardiovascular control for young women through its relationship with nitric oxide (NO) and results in lower blood pressure and risk of cardiovascular disease for women. However, in post-menopausal women and some disease states, such as heart failure (HF), these protections are lost due to reductions in estrogen and NO bioavailability which causes women to catch and surpass men in rates of hypertension and cardiovascular disease. The purpose of this dissertation is to explore the mechanisms responsible for establishing the oxygen delivery-to-utilization matching ($\dot{Q}O_2/\dot{V}O_2$) necessary for skeletal muscle contractions in health and disease.

In the first investigation (Chapter 1), we explored the effect of altered NO bioavailability on spinotrapezius muscle interstitial space PO_2 (PO_2*is*; determined by $\dot{Q}O_2/\dot{V}O_2$) of healthy male and female rats. We show that both sexes regulate PO_2*is* to similar levels at rest and during skeletal muscle contractions. However, modulating NO bioavailability exposes sex differences in this regulation with females having greater reliance on basal NO bioavailability and males having greater responsiveness to exogenous NO. In the second investigation (Chapter 2), we sought to determine whether measures of central and peripheral function in HF rats predicted exercise tolerance (as critical speed (CS)). We showed for the first time, that CS can be resolved in HF animals and that decrements in central cardiac (echocardiography) and peripheral skeletal muscle function (PO_2*is*) predicted CS. Building upon these findings, the third investigation (Chapter 3) aimed to determine if the sex differences in the control of PO_2*is* seen in healthy rats translated to greater deficits in HF for females. Furthermore, this investigation sought to determine if five days of dietary nitrate supplementation (an exogenous NO source) would raise PO_2*is* in HF rats, with a greater effect seen in females. We revealed that HF reduces PO_2*is* at rest and during skeletal muscle contractions and this negative effect is exacerbated for females. However, elevating NO bioavailability with dietary nitrate increases resting PO_2*is* and alters the

dynamic response during contractions with females potentially being more responsive than males.

The results herein reveal the importance of NO in the control of $\dot{Q}O_2/\dot{V}O_2$ in health. The onset of HF results in deleterious declines in exercise tolerance, which are mediated through reductions in central and peripheral function, due, in part, to attenuated NO bioavailability. This creates intensified $\dot{Q}O_2/\dot{V}O_2$ dysfunction in females with HF; however, this can potentially be countered with dietary supplementation of inorganic nitrate. Altogether, the present dissertation suggests that targeting NO bioavailability, particularly in female HF patients, could be a beneficial non-pharmaceutical therapeutic strategy.

Exploring the mechanisms of sexual dimorphism in oxygen delivery-to-utilization matching in skeletal muscle

by

Jesse Charles Craig

B.A., Washburn University, 2011
M.S., Kansas State University, 2015

A DISSERTATION

submitted in partial fulfillment of the requirements for the degree

DOCTOR OF PHILOSOPHY

Department of Kinesiology
College of Human Ecology

KANSAS STATE UNIVERSITY
Manhattan, Kansas

2018

Approved by:

Major Professor
David C. Poole

Copyright

Abstract

The onset of skeletal muscle contractions induces rapid and robust increases in metabolic rate ($\dot{V}O_2$) and blood flow ($\dot{Q}$) in order to supply the energetic demands of the muscle. In young healthy populations, these variables increase proportionally to maintain oxygen flux into the myocyte for both sexes. However, while the resultant changes in $\dot{V}O_2$ and $\dot{Q}$ conflate to establish adequate driving pressures of oxygen (PO_2), it appears that the underlying control processes express distinct sexual dimorphism. Estrogen is crucial for cardiovascular control for young women through its relationship with nitric oxide (NO) and results in lower blood pressure and risk of cardiovascular disease for women. However, in post-menopausal women and some disease states, such as heart failure (HF), these protections are lost due to reductions in estrogen and NO bioavailability which causes women to catch and surpass men in rates of hypertension and cardiovascular disease. The purpose of this dissertation is to explore the mechanisms responsible for establishing the oxygen delivery-to-utilization matching ($\dot{Q}O_2/\dot{V}O_2$) necessary for skeletal muscle contractions in health and disease.

In the first investigation (Chapter 1), we explored the effect of altered NO bioavailability on spinotrapezius muscle interstitial space PO_2 (PO_2*is*; determined by $\dot{Q}O_2/\dot{V}O_2$) of healthy male and female rats. We show that both sexes regulate PO_2*is* to similar levels at rest and during skeletal muscle contractions. However, modulating NO bioavailability exposes sex differences in this regulation with females having greater reliance on basal NO bioavailability and males having greater responsiveness to exogenous NO. In the second investigation (Chapter 2), we sought to determine whether measures of central and peripheral function in HF rats predicted exercise tolerance (as critical speed (CS)). We showed for the first time, that CS can be resolved in HF animals and that decrements in central cardiac (echocardiography) and peripheral skeletal muscle function (PO_2*is*) predicted CS. Building upon these findings, the third investigation (Chapter 3) aimed to determine if the sex differences in the control of PO_2*is* seen in healthy rats translated to greater deficits in HF for females. Furthermore, this investigation sought to determine if five days of dietary nitrate supplementation (an exogenous NO source) would raise PO_2*is* in HF rats, with a greater effect seen in females. We revealed that HF reduces PO_2*is* at rest and during skeletal muscle contractions and this negative effect is exacerbated for females. However, elevating NO bioavailability with dietary nitrate increases resting PO_2*is* and alters the

dynamic response during contractions with females potentially being more responsive than males.

The results herein reveal the importance of NO in the control of $\dot{Q}O_2/\dot{V}O_2$ in health. The onset of HF results in deleterious declines in exercise tolerance, which are mediated through reductions in central and peripheral function, due, in part, to attenuated NO bioavailability. This creates intensified $\dot{Q}O_2/\dot{V}O_2$ dysfunction in females with HF; however, this can potentially be countered with dietary supplementation of inorganic nitrate. Altogether, the present dissertation suggests that targeting NO bioavailability, particularly in female HF patients, could be a beneficial non-pharmaceutical therapeutic strategy.

Table of Contents

List of Figures

List of Tables

Dedication

This dissertation work is dedicated to my father, Jack E. Craig (1958-2014). Thank you for always listening and sharing your advice. I would not have been here without your push. Think of you every day. Miss you every day.

Love, your son.

Preface

Chapters 1 & 3 of this dissertation represent original research articles that have been published following or are currently in the peer-review process. Citations are listed below and these articles are reproduced here with the permission from the publishers.

Craig, J.C., T.D. Colburn, D.M. Hirai, M.J. Schettler, T.I. Musch, and D.C. Poole. Sex and nitric oxide bioavailability interact to modulate interstitial PO_2 in healthy rat skeletal muscle. *Journal of Applied Physiology.* 124: 1558-1566, 2018.

Craig, J.C., T.D. Colburn, D.M. Hirai, T.I. Musch, and D.C. Poole. Sexual dimorphism in the control of skeletal muscle interstitial PO_2 of heart failure rats: Effects of dietary nitrate supplementation. *Nitric Oxide*. In review.

Chapter 1 - Sex and nitric oxide bioavailability interact to modulate interstitial PO_2 in healthy rat skeletal muscle

Jesse C. Craig[1], Trenton D. Colburn[1], Daniel M. Hirai[1], Michael J. Schettler[2], Timothy I. Musch[1,2], and David C. Poole[1,2]

[1]Department of Kinesiology, Kansas State University, Manhattan, KS, USA

[2]Department of Anatomy and Physiology, Kansas State University, Manhattan, KS, USA

Summary

Pre-menopausal women express reduced blood pressure and risk of cardiovascular disease relative to age-matched men. This purportedly relates to elevated estrogen levels increasing nitric oxide synthase (NOS) activity and NO-mediated vasorelaxation. We tested the hypotheses that female rat skeletal muscle would: 1) evince a higher O_2 delivery-to-utilization ratio ($\dot{Q}O_2/\dot{V}O_2$) during contractions; and 2) express greater modulation of $\dot{Q}O_2/\dot{V}O_2$ with changes to NO bioavailability, compared to males. The spinotrapezius muscle of Sprague-Dawley rats (females = 8, males = 8) was surgically exposed and electrically-stimulated (180 s, 1 Hz, ~6 V). The Oxyphor G4 was injected into the muscle and phosphorescence quenching employed to determine the temporal profile of interstitial PO_2 (PO_2*is*, determined by $\dot{Q}O_2/\dot{V}O_2$). This was performed under three conditions: control (CON), 300 μM sodium nitroprusside (SNP; NO donor), and 1.5 mM L-arginine methyl ester (L-NAME; NOS blockade) superfusion. No sex differences were found for the PO_2*is* kinetics parameters in CON or L-NAME ($P > 0.05$), but females elicited a lower baseline following SNP (males: 42 ± 3 vs females: 36 ± 2 mmHg, $P < 0.05$). Females had a lower ΔPO_2*is* during contractions following SNP (males: 22 ± 3 vs females: 17 ± 2 mmHg, $P < 0.05$), but there were no sex differences for the temporal response to contractions ($P > 0.05$). The total NO effect (SNP minus L-NAME) on PO_2*is* was not different between sexes. However, the spread across both conditions was shifted to a lower absolute range for females (reduced SNP baseline and greater reduction following L-NAME). These data support that females have a greater reliance on basal NO bioavailability and males have a greater responsiveness to exogenous NO and less responsiveness to reduced endogenous NO.

Introduction

Women have lower incidence of hypertension and cardiovascular disease up to the onset of menopause, at which point they catch up to, or surpass, that of age-matched men (104). This phenomena has been attributed to the protective effect of estrogen on the cardiovascular system (91), which is linked to lower muscle sympathetic nerve activity (93, 103, 129), increased expression of endothelial (75, 156) and neuronal (43) nitric oxide synthases, and thus lower blood pressure (23, 73, 91). The functional effects of estrogen on cardiovascular and metabolic regulation in young, healthy subjects are less clear. While differences in blood pressure are commonly found between men and women (23, 73), whether this results in contrasting patterns of blood flow ($\dot{Q}$) distribution to skeletal muscle remains equivocal, with some investigations finding differences between the sexes (69, 110) and others not (51, 81, 87, 140). Rogers and Sheriff (125) showed that estrogen plays a critical role in the regulation of terminal aortic $\dot{Q}$ (*i.e.*, bulk $\dot{Q}$ to the hindlimb) during low- to moderate-intensity treadmill exercise in rats, but this effect was not necessarily linked to a sex difference. Fadel *et al.*, (43) found that estrogen replacement in healthy, ovariectomized rats attenuated the ovariectomy-induced reduction in femoral artery $\dot{Q}$ and vascular conductance during electrically-induced contractions with the effect being principally mediated through nitric oxide (NO) pathways. Work from our laboratory has recently found no differences in respiratory muscle $\dot{Q}$ between male and female rats during moderate- and near maximal-intensity treadmill exercise (133).

An important consideration when investigating sex differences is metabolic (*i.e.*, $\dot{V}O_2$) control, since $\dot{Q}$ is tightly related to $\dot{V}O_2$ across a range of exercise intensities (2). Males show greater maximal oxygen uptake ($\dot{V}O_2max$) compared to their female counterparts which is largely attributed to greater muscle mass, hemoglobin volume, and maximal cardiac output. Normal female hormonal fluctuations (*i.e.*, menstrual cycle) do not affect submaximal or maximal $\dot{V}O_2$ (32, 68), but oral contraceptive-induced supra-physiological levels of female sex hormones may reduce $\dot{V}O_2max$ (19, 78). Measurements of $\dot{Q}$ and $\dot{V}O_2$ are often taken at set time points or during steady-state exercise and may overlook potential sex differences in the transition from rest to exercise (*i.e.*, the dynamic response). Attempts to quantify and compare the dynamics of $\dot{Q}$ and $\dot{V}O_2$ following the onset of exercise in healthy women and men are limited

The measurement of the partial pressure of oxygen (PO_2) within skeletal muscles is a powerful tool that assesses $\dot{Q}$O-to-$\dot{V}O_2$ matching close to the site of O_2 usage with excellent spatial and temporal fidelity, particularly during the transition from rest to skeletal muscle contractions in healthy (22, 24, 58) and diseased (45, 56, 65) rats. Therefore, the purpose of the present investigation was to determine the role of sex and NO bioavailability on skeletal muscle $\dot{Q}$O-to-$\dot{V}O_2$ matching at rest and following the onset of submaximal muscle contractions. Specifically, we tested the hypotheses that female rats would: 1) elicit an elevated muscle O_2 delivery-to-utilization ratio (and thus higher interstitial PO_2) during contractions; and 2) demonstrate a greater responsiveness to altered NO bioavailability.

Materials and Methods

Sixteen young adult (~3-4 mo. old) age-matched Sprague-Dawley rats (Charles River Laboratories, Wilmington, MA) including 8 male (body wt: 384 ± 19 g) and 8 female (body wt: 283 ± 9 g) rats were maintained in accredited animal facilities at Kansas State University on a 12-h light-dark cycle with food and water provided *ad libitum* in isolated cages. All procedures were approved by the Institutional Animal Care and Use Committee of Kansas State University and conducted according to the National Research Council *Guide for the Care and Use of Laboratory Animals*. All experiments were conducted between 1-3 weeks of the animals' arrival to the facilities. This allowed sufficient time for the animals to acclimate to their new settings and ensured the groups remained age-matched.

Surgical Preparation

On the day of the experiment, rats were initially anesthetized with a 5% isoflurane-O_2 mixture and subsequently maintained on 2-3% isoflurane-O_2. Following the isolation of the carotid artery, a catheter (PE-10 connected to PE-50, Intra-Medic polyethylene tubing, Clay Adams Brand, Becton, Dickinson and Company, Sparks, MD) was inserted into the carotid artery for measurement of mean arterial pressure (MAP) and heart rate (HR). A second catheter was introduced into the caudal artery for the administration of pentobarbital sodium anesthesia and arterial blood sampling. Upon closing the incisions for the carotid and caudal catheters, rats were progressively transitioned to pentobarbital sodium anesthesia. Depth of anesthesia was continuously monitored via the toe pinch and blink reflexes; with additional anesthesia administered as necessary. Rats were placed on a heating pad to maintain a core temperature of ~38 ˚C (measured via rectal probe). Incisions were then made to expose the left spinotrapezius muscle with overlying skin and fascia reflected such that the integrity of the neural and vascular supply was maintained (4). Using 6-0 silk sutures, platinum iridium wire electrodes were secured to the rostral (cathode) and caudal (anode) regions of the muscle to facilitate electrically induced contractions. Surrounding exposed tissue was covered with Saran wrap (Dow Brands, Indianapolis, IN) to minimize the exposure of superfused solutions to bordering tissues and reduce tissue dehydration. Exposed muscle was superfused frequently with warmed (38 ˚C) Krebs-Henseleit bicarbonate buffered solution equilibrated with 5% CO_2-95% N_2. The spinotrapezius muscle was selected based on its mixed muscle fiber-type composition and citrate

synthase activity, which resembles the quadriceps muscle in humans (33, 79) and convenience with respect to minimally invasive exposure (4).

Experimental Protocol

Three separate contraction bouts were performed under control (CON), sodium nitroprusside (SNP; NO donor, 300 μM), and Nω nitro-L-arginine methyl ester (L-NAME; nonselective NO synthase (NOS) inhibitor, 1.5 mM) conditions. The initial two conditions (either CON or SNP) were randomly determined, while the final condition was always L-NAME. This was necessary due to the long half-life of L-NAME. The drugs were administered via superfusion (3 ml total volume) on the spinotrapezius over 180 s of continuous interstitial PO_2 (PO_2*is*) recording. The recording was extended for an additional 180 s to confirm that baseline PO_2*is* had stabilized prior to the onset of muscle contractions and for 180 s of muscle contractions. Contractions were evoked via electrical stimulation (1 Hz, 6-7 V, 2 ms pulse duration) with a Grass S88 Stimulator (Quincy, MA, USA). This contraction protocol increases spinotrapezius muscle blood flow four- to five-fold and metabolic rate six- to seven-fold without altering blood pH and is consistent with moderate intensity exercise (10, 58). Between contraction bouts, rats were given 20-30 min of recovery with regular superfusion of Krebs-Henseleit solution. Our laboratory has previously shown this duration of recovery elicits reproducible microvascular PO_2 (PO_2mv) (24, 56) responses. Upon completion of the protocol, rats were euthanized with intra-arterial potassium chloride overdose (1 ml/kg of 4M KCl).

Spinotrapezius Interstitial PO_2 Measurement

Phosphorescence quenching was used to measure PO_2*is* in the spinotrapezius at rest and during contractions using a frequency domain phosphorometer (PMOD 5000; Oxygen Enterprises, Philadelphia, PA, USA) as previously described (60). Briefly, the Oxyphor G4 (Pd-*meso*-tetra-(3,5-dicarboxyphenyl)-tetrabenzo-porphyrin) was injected locally (3-4 10 μL injections at 10 μM concentration) using a 29G needle with care taken to avoid damaging any visible vasculature. After injection, the spinotrapezius was covered with Saran wrap and given at least 20 min to allow the G4 to diffuse throughout the interstitial space. This Oxyphor is well-suited for use in biological tissues due to its inability to cross membranes and stability across physiological pH ranges (41); it is however, temperature sensitive and therefore spinotrapezius

temperature was measured using a non-contact infrared thermometer. Mean spinotrapezius temperature was 32.4 ± 0.2 °C, with no differences between sexes or change during contractions.

Phosphorescence quenching applies the Stern-Volmer relationship (41, 126), which describes the quantitative O_2 dependence of the phosphorescent probe G4 via the equation:

$$PO_2is = [(\tau_0/\tau) - 1]/(k_Q \cdot \tau_0)$$

where k_Q is the quenching constant and τ and τ_0 are the phosphorescence lifetimes at the ambient O_2 concentration and in the absence of O_2, respectively. For G4 in tissue at 32.5 °C, k_Q is 258 $mmHg^{-1} \cdot s^{-1}$ and τ_0 is 226 μs (41). Since muscle temperature does not appreciably change over the duration of the contraction protocol used herein, the phosphorescence lifetime is determined exclusively by the O_2 partial pressure. After injection of G4, the common end of the bifurcated light guide was positioned 3-4 mm above the dorsal surface of the exposed spinotrapezius. The phosphorometer modulates sinusoidal excitation frequencies between 100 Hz and 20 kHz and allows phosphorescence lifetime measurements from 10 μs to ~2.5 ms. PO_2is was measured continuously and recorded at 2 s intervals throughout the duration of the experimental protocol.

Analysis of Spinotrapezius Interstitial PO_2 Kinetics

The kinetics analyses of the PO_2is responses were conducted using 30 s of resting data and the 180 s contraction bout using a mono-exponential plus time delay model:

$$PO_2(t) = PO_{2(BL)} - \Delta_1PO_2 (1- e^{-(t - TD)/\tau})$$

or a mono-exponential plus time delay with a secondary component when necessary:

$$PO_2(t) = PO_{2(BL)} - \Delta_1PO_2 (1- e^{-(t - TD)/\tau}) + \Delta_2PO_2 (1- e^{-(t - TD_2)/\tau_2})$$

where $PO_2(t)$ represents the PO_2is at any point in time, $PO_{2(BL)}$ is the baseline before the onset of contractions, Δ_1PO_2 and Δ_2PO_2 are the primary and secondary amplitudes, TD and TD_2 are the time delays before the drop and secondary rise in PO_2, and τ and τ_2 are the time constants (*i.e.*, the time required to reach 63% of the amplitude) for the primary and secondary amplitudes. The mean response time (MRT) was calculated as the sum of the model derived TD and τ. When the secondary component model was necessary, the primary amplitude was constrained to not exceed the nadir value to maximize the accuracy of the primary response kinetics (see Figure 1 for example). The goodness of model fit was determined using the criteria: 1) the coefficient of determination; 2) sum of the squared residuals; 3) visual inspection and analysis of the model fits

to the data and the residuals; and 4) manual calculation of the time taken to reach 63% of the primary response (T_{63}) compared to the model-derived MRT. Since Δ_2PO_2 (*i.e.*, undershoot of PO_2) was often non-exponential in nature, Δ_2PO_2 was determined manually, when necessary, by calculating the difference between the steady-state PO_2 at the end of contractions minus the nadir value of PO_2 during contractions.

Central Hemodynamics and Blood Samples

MAP and HR were measured during the experiment via the right carotid artery catheter connected to a pressure transducer and Digi-med Blood Pressure Analyzer (model 400; Micro-Med, Louisville, KY). Approximately 0.4 ml of blood was sampled from the caudal artery catheter at the end of the experiment for the determination of arterial blood lactate concentration ($[La^-]$), pH, PCO_2, $\%O_2$ saturation, and hematocrit (Nova Stat Profile M; Nova Biomedical, Waltham, MA).

Statistical Analysis

All curve fitting and statistical analyses were performed using a commercially available software package (SigmaPlot 12.5, Systat Software, San Jose, CA, USA). Sex differences for rat descriptive variables, blood gases, and effects of superfusion on resting variables (i.e., ΔMAP, ΔHR, and $\Delta PO_{2(BL)}$) were compared using unpaired Student's t-tests. PO_2*is* kinetics parameters were compared among conditions using 2-way repeated measures ANOVA (sex x superfusion) with Tukey's *post hoc* tests as necessary. Goodness of model fit (i.e., fitting-derived MRT vs model-independent T_{63}) was compared using paired Student's t-tests with both sexes represented in each group. Pearson's product-moment correlations and linear regressions were used to determine relationships among variables. Data are presented as means ± standard deviation unless otherwise noted. Significance was accepted at $p < 0.05$.

Results

Male rats were heavier than their age-matched female counterparts (384 ± 55 vs 283 ± 25 g; $p < 0.001$) and spinotrapezius mass paralleled these differences (0.38 ± 0.04 vs 0.26 ± 0.03 g; $p < 0.001$). The spinotrapezius mass to body mass ratio was not different between sexes ($p = 0.61$). No sex differences were found for arterial [La^-] (1.7 ± 0.4 vs 1.2 ± 0.4 mM, $p = 0.12$), $\%O_2$ saturation (94 ± 3 vs 92 ± 4 %; $p = 0.25$), or hematocrit (34 ± 3 vs 34 ± 3 %; $p = 0.86$) for males and females, respectively. Males had lower arterial PCO_2 (34 ± 6 vs 44 ± 6 mmHg; $p = 0.01$) and higher pH (7.42 ± 0.04 vs 7.36 ± 0.02; $p < 0.01$), indicative of moderate hyperventilation. There were no sex differences for resting MAP (106 ± 12 vs 99 ± 14 mmHg; $p = 0.23$) or HR (371 ± 31 vs 365 ± 25 beats/min; $p = 0.76$) for males and females, respectively.

A representative PO_2*is* profile is presented in Figure 1-1 to highlight the modeling fit and signal-to-noise of the PO_2*is* measurement. Both sexes showed an exponential drop in PO_2*is* following the onset of contractions that led to a PO_2*is* 'undershoot' before reaching a steady-state PO_2*is* of 15.8 ± 2.8 and 13.1 ± 3.6 mmHg ($p = 0.22$) for males and females, respectively. There were no sex differences for PO_2*is* before or during contractions in the control condition (Figure 1-2, Table 1-1). The model-independent estimation of T_{63} did not differ from the model-derived MRT (16.5 ± 5.0 vs 16.5 ± 5.5 s; $p = 0.92$) supporting the robustness of the model fitting procedures.

The effects of SNP superfusion on resting PO_2*is* are shown in Figure 1-3 (left panel). Following SNP superfusion, both sexes demonstrated an increase of PO_2*is* but this was of lesser magnitude for the female rats ($p < 0.01$). There was no between-sex difference for ΔHR ($p = 0.95$; Table 1-2) although females showed a greater drop in MAP ($p = 0.04$; Table 1-2). Females expressed a lower post-superfusion baseline PO_2*is* than males ($p = 0.04$) and a smaller primary amplitude of PO_2*is* decrease during contractions ($p = 0.03$; Figure 1-4, Table 1-1). The PO_2*is* undershoot during contractions was reduced in both sexes compared to control and L-NAME (all $p < 0.001$; Figure 1-5) and was not different between the sexes ($p = 0.47$). SNP slowed PO_2*is* kinetics as evidenced by the increased MRT (driven by an increased τ) compared to control and L-NAME for both sexes (all $p < 0.05$) and was not different between the sexes ($p = 0.96$). The steady-state PO_2*is* at the end of contractions was increased following SNP compared to control

and L-NAME (all $p < 0.02$) and was not different between males and females (20.8 ± 4.7 vs 20.7 ± 4.2 mmHg; $p = 0.93$). The model-independent estimation of T_{63} was not different from the model-derived MRT (24.6 ± 12.6 vs 25.4 ± 14.1 s; $p = 0.34$).

L-NAME superfusion decreased resting PO_2is to a greater extent in females when compared to males ($p = 0.04$, Figure 1-3, right panel). The ΔMAP following L-NAME superfusion was not different between males and females ($p = 0.96$), but females showed a greater reduction in HR ($p = 0.04$; Table 1-2). Similar to the control condition, no differences between the sexes for PO_2is on-kinetics were found during contractions following L-NAME (Figure 1-4, Table 1-1) with a steady-state PO_2is of 13.1 ± 3.1 and 12.8 ± 6.1 mmHg ($p = 0.93$), for males and females, respectively. The model-independent estimation of T_{63} was not different from the model-derived MRT (13.3 ± 2.8 vs 13.5 ± 2.3 s; $p = 0.61$).

Discussion

The primary original findings of the present investigation show that skeletal muscle PO_2*is* (determined by the matching of $\dot{Q}$O-to-$\dot{V}O_2$) does not differ between females and males during muscle contractions under CON conditions; however, alterations in NO bioavailability (via SNP and L-NAME) expose differences in PO_2*is* regulation at rest and during contractions. Specifically, SNP elicited a smaller effect on PO_2*is* (*i.e.*, smaller increase) in female rats at rest and during contractions compared to males; while L-NAME showed a greater impact (*i.e.*, larger reduction) in females at rest compared to males. These results provide partial support for our hypothesis that females would exhibit a greater responsiveness to alterations in NO bioavailability and suggest that females might rely more on NO to maintain skeletal muscle $\dot{Q}$O-to-$\dot{V}O_2$ matching at rest as evidenced by the greater transient reduction in PO_2*is* expressed by females following L-NAME superfusion. Females may also have a lower 'capacity' to augment PO_2*is* in response to a NO donor due to a greater bioavailability (and thus role in basal regulation) of endogenous NO compared to males. Another explanation for the reduced responsiveness to SNP in females could relate to a ceiling effect caused by some anatomical difference in the vasculature or muscle. The total NO effect (SNP minus L-NAME; see Figure 3) was not different between the sexes, however, the relationship was shifted to a lower PO_2*is* range in the females. An understanding of these effects of NO bioavailability on PO_2*is* is important because this carrier-free space is considered to represent a substantial barrier to oxygen flux from the blood to the mitochondria (153) with PO_2*is* and alteration thereof potentially impacting metabolic control.

Female and Male PO_2*is* Similarities for Control

Revealing the (dis)similarities between females and males for O_2 delivery-to-utilization matching at the level of the skeletal muscle interstitial space is a potentially powerful means to inform and help resolve the conflicting findings of sex differences in $\dot{Q}$ and $\dot{V}O_2$. The present investigation revealed that during the CON condition male and female rats both regulated PO_2*is* at a similar level at rest and during contractions. This commonality of regulation between male (59) and female (13) rats is also apparent in the upstream PO_{2mv} compartment, despite a differing temporal response (i.e., TD, τ, MRT) and qualitative shape (i.e., undershoot amplitude) compared to the PO_2*is* compartment.

Controversy exists with respect to potential sex differences in the individual components of PO_2*is* (*i.e.*, $\dot{Q}O_2$ and $\dot{V}O_2$), particularly with regard to the regulation of active muscle $\dot{Q}$ (and $\dot{Q}O_2$) during exercise. Some studies have found that females have a greater exercising vasodilator response (and thus, higher $\dot{Q}$) than males (69, 110), others have found no differences (51, 81, 87, 124, 133, 140) across a range of exercise intensities and modalities. Males may elicit higher absolute muscle $\dot{Q}$ values during exercise, but those differences are abolished when $\dot{Q}$ is expressed relative to workload. The second determining variable of the PO_2*is*, $\dot{V}O_2$, is less contentious. The maximal $\dot{V}O_2$ in females is typically lower, in absolute terms, owing mainly to less lean muscle and lower achievable workloads. Examined at submaximal intensities, there does not appear to be any appreciable sex difference for pulmonary or limb $\dot{V}O_2$ (124, 139) when related to workload. Taken together, the aforementioned studies and this present investigation suggest that the cardiorespiratory system and metabolic apparatus are tuned to regulate muscle $\dot{Q}O$ and $\dot{V}O_2$ during normal operating conditions regardless of sex; however, the specific nature of that control might differ between the sexes (see *Female and Male (Dis)similarities Following SNP and L-NAME* below). The present investigation advances this understanding by directly measuring PO_2 at the site where the cardiorespiratory system and metabolic apparatus interact, in close proximity to the site of O_2 utilization.

Interestingly, a prominent undershoot in PO_2*is* was observed which approximated 60% of the primary amplitude in both sexes (undershoot observed in 100% of rats). This undershoot has been attributed to, and is exacerbated by, mismatched $\dot{Q}O$ and $\dot{V}O_2$ due to aging (11, 89), disease (12, 46, 65), and changes in NO availability (47, 58) seen in the upstream microvascular space (*i.e.*, PO_{2mv}). This study is the first to observe the undershoot phenomenon consistently in the muscle interstitial space in both healthy male and female rats. These data suggest that this undershoot phenomena is a normal response in the interstitial space. The interstitial space may exhibit unique PO_2 profiles because of the compartment's proximity to both the microvascular $\dot{Q}$ and intracellular myoglobin/mitochondria. The present investigation, and previous work from our laboratory (60), revealed a PO_2*is* that is substantially higher than the myoglobin PO_2 (2-5 mmHg (121)) and expected mitochondrial PO_2 (0-2 mmHg) during contractions. In this context, the PO_2*is* undershoot seen during contractions may be crucial for reestablishing the gradient

needed for O_2 flux into the intracellular compartment. That SNP attenuated and L-NAME augmented the undershoot (see *Female and Male (Dis)similarities Following SNP and L-NAME* below), supports that NO plays an important role for the establishment of adequate O_2 flux into the myocyte during contractions.

Female and Male PO_2*is* (Dis)similarities Following SNP and L-NAME

NO signaling is important within many physiological systems in the body and has the ability to modulate both components of PO_2 (i.e., $\dot{Q}O$ and $\dot{V}O_2$). As a powerful vasodilatory agent, NO can increase $\dot{Q}$ via relaxation of smooth muscle which increases vascular conductance (134). NO also modulates oxidative respiration within the mitochondria (17) which serves to reduce $\dot{V}O_2$. Increased NO bioavailability (SNP) should then increase $\dot{Q}$ and/or decrease $\dot{V}O_2$ while decreased NO bioavailability (L-NAME) would induce the converse. The expected outcome of SNP superfusion would be an increased PO_2 while L-NAME superfusion would decrease PO_2 (as seen in PO_2*mv* studies (47, 58)).

SNP increased the baseline PO_2*is* in both females and males to twice that of the pre-superfusion baselines with females achieving a post-superfusion PO_2*is* ~15% lower than the males ($PO_{2(BL)}$, Table 1-1) . Neither the absolute values or Δ for PO_2 were correlated with MAP or HR in either sex following SNP superfusion (data not shown, r^2: 0.05-0.2), suggesting that the differential response to SNP was not driven by differences in driving pressure or HR. Instead, these differences appear to be the result of direct effects of SNP on the peripheral vasculature and/or skeletal muscle. Previous work investigating the vascular reactivity response to SNP in humans found no sex differences in some studies (136, 154), but, in contrast, Kneale *et al*., (76) reported that females exhibited a reduced increase in forearm $\dot{Q}$ compared to males across a range of SNP doses. Unfortunately, those studies were not equipped to measure the metabolic consequences of SNP or the potential interaction it may have with the increased $\dot{Q}$. The results herein, when taken in consideration with Kneale *et al*., (76) and PO_2*mv* studies (47, 58), suggest that the smaller increase in PO_2*is* seen in the females at rest was driven by a attenuated increase in $\dot{Q}$ rather than a modulation of $\dot{V}O_2$ (due to the low metabolic rate of resting skeletal muscle).

The female PO_2*is* primary amplitude (Δ_1PO_2) with contractions was smaller than the males under SNP. However, the relative rate of change for PO_2*is* (represented by Δ_1PO_2/τ) was not different between females and males following SNP; which was also not different from CON or L-NAME for either sex. These results support that the muscle metabolic rate (*i.e.*, $\dot{V}O_2$) was not different between the sexes, if the rate of decrease in PO_2*is* is primarily driven by the intracellular metabolic apparatus and resulting O_2 flux into the cell. Although not unequivocal, $\dot{V}O_2$ kinetics have been shown to be independent of augmented $\dot{Q}$ in both healthy humans (54) and isolated muscle (53). Furthermore, since the model and muscle contractions used herein have supported this view (13), we argue for like metabolic profiles herein.

SNP reduced the incidence and amplitude of the PO_2*is* undershoot for both sexes compared to CON and L-NAME (Table 1-1 and Figure 1-5). The augmented $\dot{Q}$ induced by SNP increased the nadir PO_2*is* during contractions to values greater than the steady-state PO_2*is* achieved in CON and L-NAME, likely reflecting a $\dot{Q}$ in excess of the metabolic demand. Thus, the undershoot which may have been necessary to preserve the PO_2 gradient and O_2 flux in the CON condition was not observed following SNP. Another potential explanation for the reduction in the undershoot occurrence is that the excess $\dot{Q}$ mitigated any delay in the $\dot{Q}O_2$ matching to $\dot{V}O_2$. Whatever the case, observation of these data in Figure 5 suggests there may be a 'threshold' type effect in the interplay between the nadir and undershoot amplitudes. The undershoot amplitudes were reduced to zero once the nadir PO_2*is* was greater than ~15 mmHg. Further work is necessary to determine if this observation has physiological underpinnings or is a product of the experimental protocol. This novel observation supports the hypothesis that a functional barrier to O_2 flux exists between the interstitial and intracellular spaces (see Fem*ale and Male Similarities for Control* above).

Inhibition of NOS reveals that NO plays an important role in the control of resting skeletal muscle $\dot{Q}$ in both animals (88, 108, 117, 127, 150) and humans (84, 119, 128, 136, 151). It has also been shown that pre-menopausal women, and post-menopausal women treated with estrogen, exhibit a greater vasoconstrictor response to NOS inhibition compared to age-matched males (76, 84, 136) and post-menopausal women without estrogen treatment (84). In the present investigation, L-NAME superfusion reduced resting PO_2*is* to a greater extent in females versus

males (Figure 3, right panel), supporting the notion that the increased NOS-generated NO in females (43, 75, 156) leads to different regulation of $\dot{Q}$O-to-$\dot{V}O_2$ matching across sexes. However, at the onset of contractions (i.e., $PO_{2(BL)}$), neither sex evinced a lower PO_2*is* compared to the CON condition. The lack of an effect on resting PO_2*is* with NOS inhibition could be explained by the substantial microvascular to interstitial PO_2 gradient (60), which may serve to 'buffer' the reduction of PO_2*is* in the face of reduced PO_2*mv* (47). Similarly, there exists redundancy in the pathways that regulate $\dot{Q}$ (for review see (67)), which could act to offset the attenuation of PO_2*is* imposed by L-NAME. Despite the lack of an effect on the baseline PO_2 or the other parameters of the kinetics response, L-NAME increased the undershoot as a proportion of the primary amplitude. The undershoot in PO_2*is* that was observed to approximate 60% of the primary amplitude in CON was increased to approximately 84% by L-NAME, supporting the role of NO in establishing the PO_2 gradient necessary for facilitating myocyte O_2 flux.

Experimental Considerations

The estrus cycle of the female rats was not controlled for in the present study leaving the possibility that sex differences in the primary measurements were obfuscated by varying levels of estrogen present. However, had this indeed been the case, we would have expected greater variance within the female rat group compared to the males, but this scenario was not found in any of the primary measurements. Additionally, the proestrus phase occupies ~10 h of the typical rat 4-5 day cycle (149), which reduces the chances these rats were currently in the high estrogen phase. Future studies aiming to maximize the potential for sex hormone driven differences in PO_2*is* should target the ovulation/proestrus phase. Linear regression analyses were performed to explore the notion that the differences in body weight between the female and male rats could somehow have accounted for some of the (dis)similarities seen in the present investigation. However, body mass and spinotrapezius mass were not related to the primary variables. The most likely instance of this confounding effect is with the depth of anesthesia and resultant ventilatory pattern of the rats (reflected in arterial PCO_2 and pH). With regard to the differences in pH, we cannot exclude the potential effect this could have on the vasoreactivity of the microvessels (90).

Conclusions

The primary novel finding of the present investigation is that female and male rats regulate skeletal muscle interstitial space O_2 delivery-to-utilization matching (reflected as PO_2*is*) at a similar level under CON conditions. The ratio of $\dot{Q}$O-to-$\dot{V}O_2$ can be modulated by altering NO bioavailability, with SNP (NO donor) increasing and L-NAME (NOS blockade) decreasing the ratio. Interestingly, the relationship between resting PO_2*is* and NO bioavailability was altered based on the sex of the animal with females exhibiting a lower PO_2*is* range across the availability of NO while males evince a higher range. Shown herein for the first time in the interstitial space was the presence of a substantial PO_2 undershoot during CON that was expressed in all rats (regardless of sex), which suggests that the interstitial site is important for controlling blood-myocyte O_2 flux. The occurrence and amplitude of this PO_2*is* undershoot was shown to be reduced by a NO donor.

Table 1-1 Interstitial PO_2 Kinetics Parameters of the Spinotrapezius at Rest and During 180 s of Contractions Following Control, SNP, and L-NAME Superfusion

	Control		SNP		L-NAME	
	Male	**Female**	**Male**	**Female**	**Male**	**Female**
$PO_{2(BL)}$ (mmHg)	20.4 ± 2.5	18.2 ± 4.9	41.9 ± 9.5 *†‡	35.8 ± 6.6 †‡	15.9 ± 4.4	14.4 ± 4.6
Δ_1PO_2 (mmHg)	11.6 ± 2.2	12.0 ± 4.4	21.6 ± 7.1 *†‡	16.6 ± 4.2 †‡	10.4 ± 3.5	9.5 ± 2.8
τ (s)	9.2 ± 2.8	10.5 ± 4.0	23.5 ± 16.0 †‡	20.2 ± 15.5 ǂ	9.8 ± 2.5	9.9 ± 2.3
TD (s)	6.7 ± 3.0	6.4 ± 3.4	2.0 ± 1.7 *†	5.1 ± 3.9	3.3 ± 1.1 †	3.9 ± 1.6
MRT (s)	16.0 ± 4.2	17.0 ± 6.9	25.5 ± 15.5 †‡	25.3 ± 13.6 ǂ	13.1 ± 2.5	13.8 ± 2.1
Δ_2PO_2 (mmHg)	7.0 ± 2.9	7.0 ± 2.1	0.6 ± 1.6†‡	1.5 ± 3.1 †‡	7.6 ± 2.2	7.9 ± 3.5
Δ_1PO_2/τ (mmHg/s)	1.4 ± 0.8	1.2 ± 0.5	1.1 ± 0.5	1.1 ± 0.5	1.1 ± 0.6	1.0 ± 0.5

$PO_{2(BL)}$, baseline interstitial PO_2; Δ_1PO_2, PO_2 primary amplitude; τ, time constant; TD, time delay; MRT, mean response time; Δ_2PO_2, PO_2 undershoot during contractions. Values are means ± SD. *****, $p < 0.05$ vs female within superfusion. †, $p < 0.05$ vs control within sex. ǂ, $p < 0.05$ vs L-NAME within sex.

Table 1-2 Effect of SNP and L-NAME Superfusion on Resting Central Hemodynamics

	SNP		L-NAME	
	Male	**Female**	**Male**	**Female**
ΔMAP (mmHg)	-1 ± 1	-6 ± 2 *****	2 ± 3	1 ± 2
ΔHR (bpm)	26 ± 5	25 ± 4	3 ± 5	-9 ± 3 *****

Values are means ± SD. *****, $p < 0.05$ vs male within superfusion.

Figure 1-1 A representative interstitial PO_2 profile (closed circles) during 180 s of muscle contractions

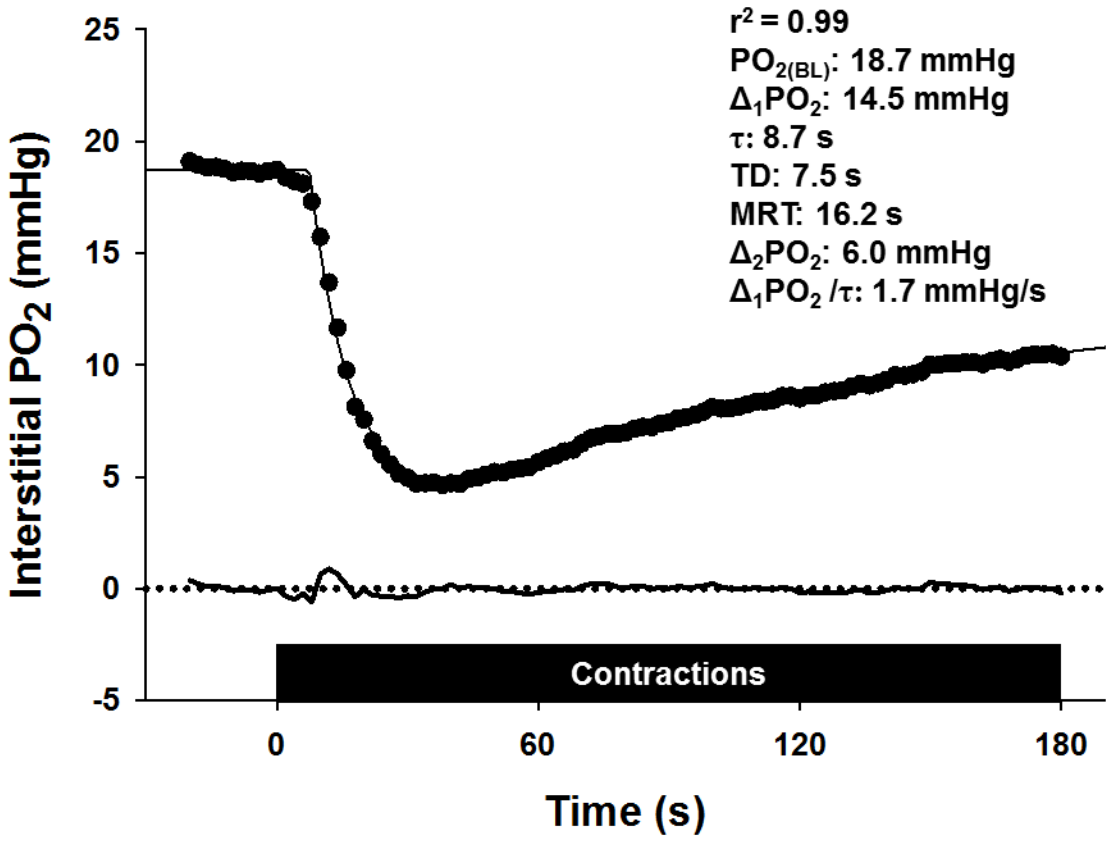

The solid line overlaid on the data represents the fit determined by the modeling procedure. Modeling was performed such that emphasis was put on the primary response of the PO_2 profile (see text for details). The bolded solid line below represents the residuals of the fit. Inset text reports kinetics parameters determined by this procedure.

Figure 1-2 Control condition group average spinotrapezius interstitial PO_2 temporal response during 180 s of muscle contractions

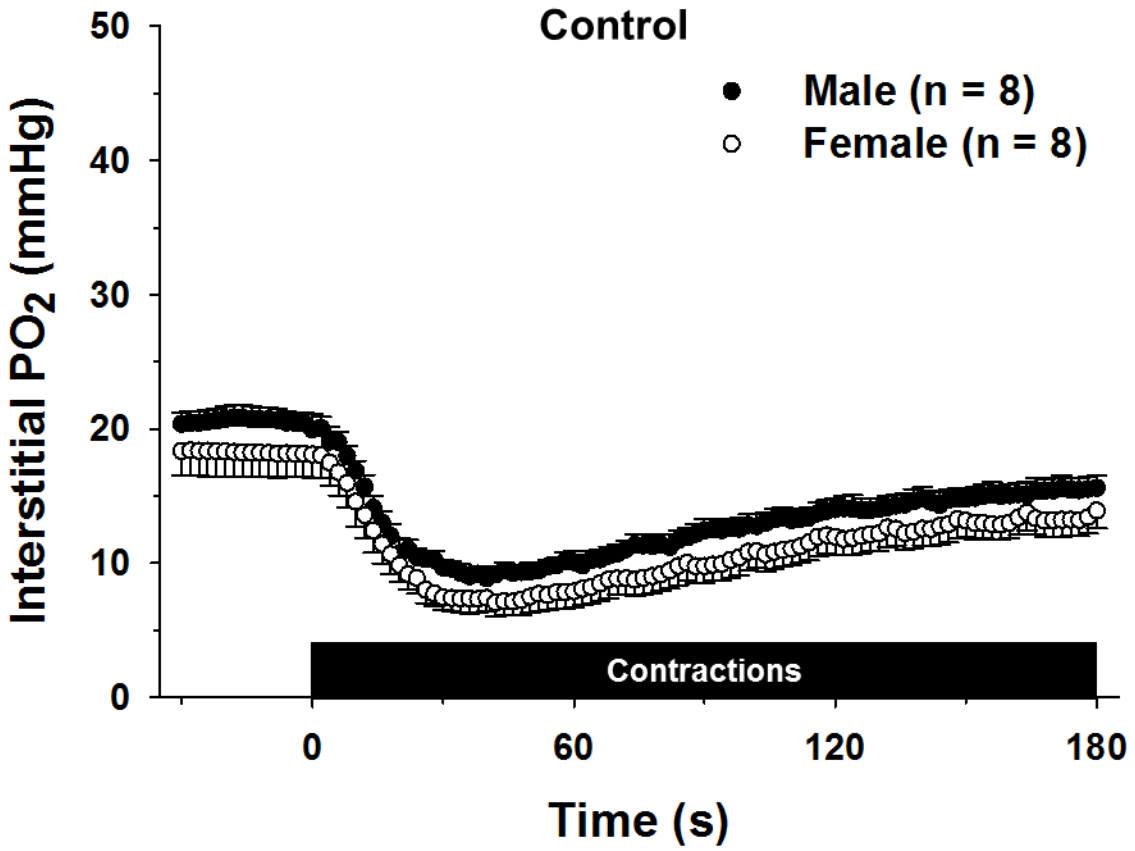

No differences were found between males (closed circles; n = 8) and females (open circles; n = 8) at rest or during contractions. Data are means ± SE.

Figure 1-3 Absolute change for resting spinotrapezius interstitial PO_2 following superfusion of sodium nitroprusside (SNP, 300 μM) and N^{ω} nitro-L-arginine methyl ester (L-NAME, 1.5 mM) for male (closed bars) and female (open bars) rats

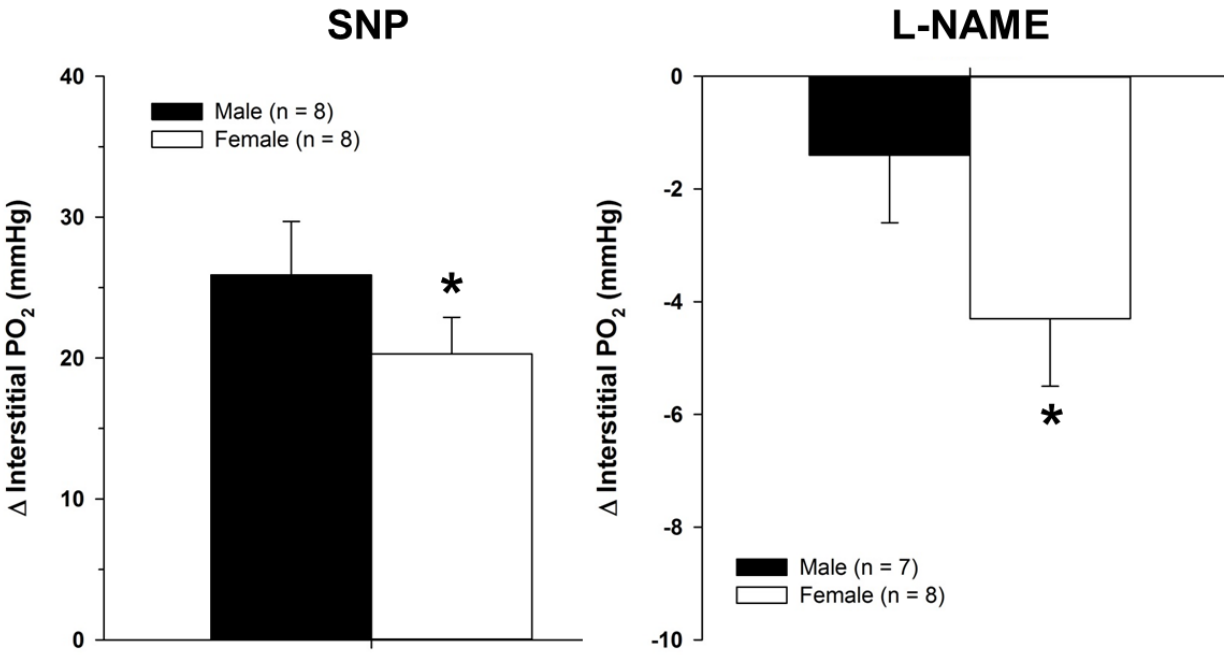

Δ PO_2 was calculated as the difference between 30 s of baseline PO_2 before superfusion and 30 s of PO_2 following the superfusion and stabilization period. Data are means ± SE. * significantly different from males ($p < 0.05$). All plots represent 8 animals per condition, except for male L-NAME which is 7 animals.

Figure 1-4 Group average spinotrapezius interstitial PO_2 temporal response during 180 s of muscle contractions for the SNP and L-NAME conditions

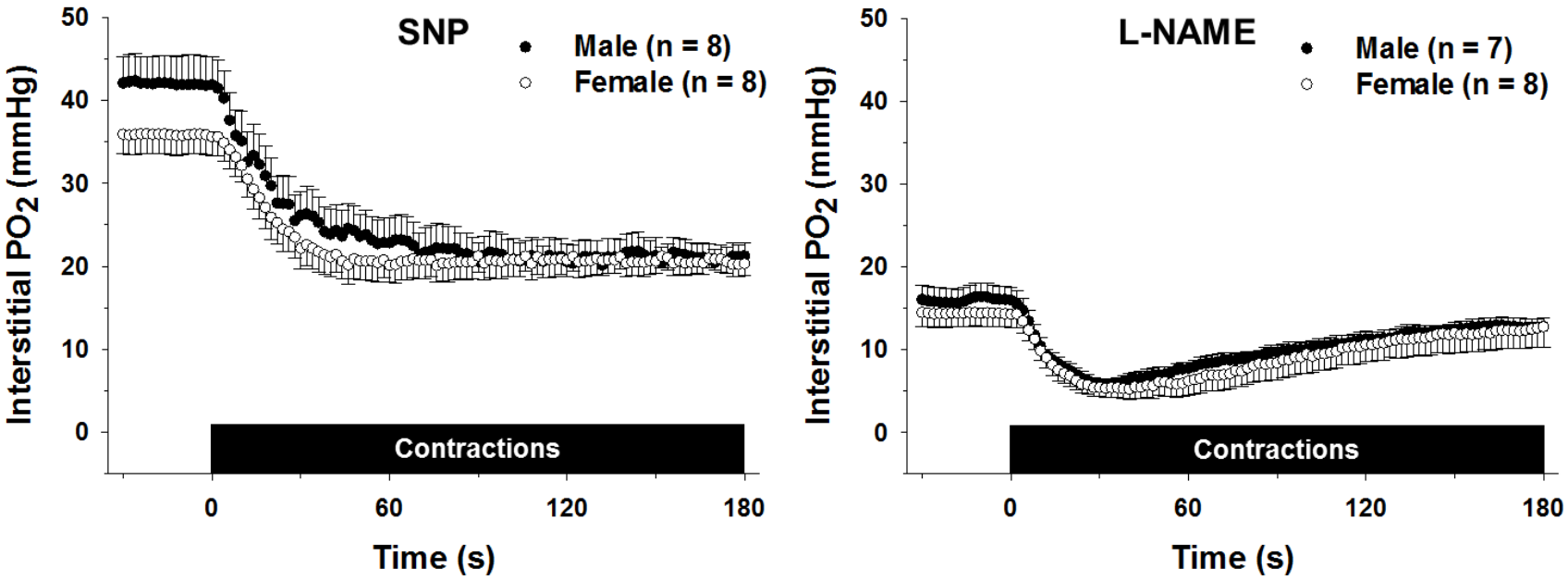

Left: SNP condition group average spinotrapezius interstitial PO_2 temporal response during 180 s of muscle contractions. Males (closed circles, n = 8) had a significantly greater baseline PO_2 than females (open circles, n = 8) following SNP superfusion. The Δ PO_2 during contractions was also greater in males (see text for details). Data are means ± SE. *Right*: L-NAME condition group average spinotrapezius interstitial PO_2 temporal response during 180 s of muscle contractions. No differences were found between males (closed circles; n = 7) and females (open circles; n = 8) at rest or during contractions, although the Δ PO_2 in response to L-NAME superfusion was greater in females (see Fig. 2). Data are means ± SE.

Figure 1-5 Female and male rat individual interstitial PO_2 (PO_2*is*) undershoots as a function of the PO_2*is* nadirs achieved during spinotrapezius contractions

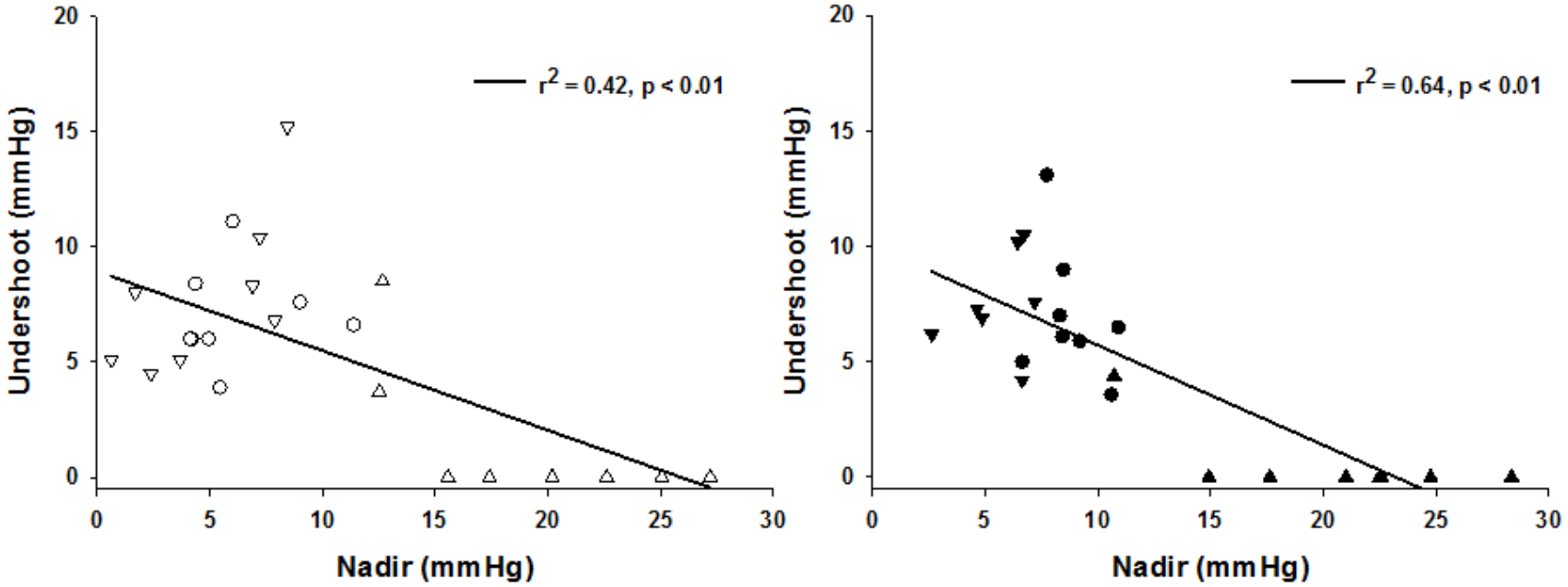

Left: Female rat individual interstitial PO_2 (PO_2*is*) undershoots as a function of the PO_2*is* nadirs achieved during spinotrapezius contractions. *Right*: Male rat individual PO_2*is* data. In both groups, SNP superfusion (triangles; n = 8 for both) significantly increased the PO_2*is* nadir and reduced the PO_2*is* undershoot compared to the control condition (circles; n = 8 for both) and L-NAME (inverted triangles; n = 8 for females, n = 7 for males). Linear regression revealed significant relationships for both female ($r^2 = 0.42$, $p < 0.01$) and male ($r^2 = 0.64$, $p < 0.01$) rats. Visual inspection of the data reveals that there may be a 'threshold' effect in the nadir PO_2*is* (see text for details).

Chapter 2 - Partitioning the central and peripheral contributions to the speed-duration relationship in heart failure rats

Jesse C. Craig[1], Trenton D. Colburn[1], Jacob T. Caldwell[1], Daniel M. Hirai[1], Ayaka Tabuchi[1], Dryden R. Baumfalk[1], Bradley J. Behnke[1], Carl J. Ade[1], Timothy I. Musch[1,2], David C. Poole[1,2]

[1]Department of Kinesiology, Kansas State University, Manhattan, KS, USA

[2]Department of Anatomy and Physiology, Kansas State University, Manhattan, KS, USA

Summary

A primary symptom of heart failure (HF) is exercise intolerance; however, the contribution of central and peripheral factors to this intolerance is unknown. The hyperbolic relationship between exercise intensity and time-to-exhaustion (speed-duration relationship) defines exercise tolerance but has been underutilized in HF. We tested the hypotheses that critical speed (CS), but not D′, would be reduced in HF; and that both central and peripheral functional measurements would correlate directly with CS. Multiple treadmill constant-speed runs-to-exhaustion were used to describe CS and D′ in control and HF rats. Central (left ventricular (LV)) function was determined via Doppler echocardiography (fractional shortening (FS)) and micromanometer-tipped catheters (LV end-diastolic pressure (LVEDP)). Peripheral O_2 delivery-to-utilization matching was determined via phosphorescence quenching (interstitial PO_2, PO_2*is*) in the soleus and white gastrocnemius during electrically-induced twitch contractions (1 Hz, 8 V). CS was lower in HF compared to control (38.3 ± 1.0 vs 44.1 ± 0.6 m/min, $p < 0.001$) but D′ was not different (HF: 70 ± 11, control: 62 ± 14 m; $p = 0.67$). HF reduced FS (23 ± 2 vs 48 ± 3%, $p < 0.001$) and increased LVEDP (16 ± 2 vs 6 ± 1 mmHg, $p < 0.001$) compared to control. HF reduced soleus PO_2*is* at rest and during contractions (both $p < 0.01$) but had no effect on white gastrocnemius PO_2*is* ($p > 0.05$). CS was correlated with FS ($r = 0.9$, $p < 0.001$) and soleus end-contraction PO_2*is* ($r = 0.75$, $p = 0.02$). We show in this model of moderate HF, decrements in central cardiac function and peripheral skeletal muscle vascular function correlate directly with impaired exercise tolerance (i.e., CS). This compromised exercise tolerance is likely due to reduced perfusive and diffusive O_2 delivery to oxidative muscles.

Introduction

The hyperbolic relationship between the power requirement and time to exhaustion for high intensity exercise defines exercise tolerance. This power- or speed-duration relationship is robust across a multitude of species in health and disease (for review see (113)). This relationship is defined by two parameters, the critical power (CP or critical speed, CS) and the curvature constant (W′ for power or D′ for speed). CP/CS represents the highest work output (or more appropriately metabolic rate (8)) which can be sustained primarily with aerobic energy production for a considerable duration. At work rates below CP/CS, steady-state values are obtained for pulmonary oxygen uptake ($\dot{V}O_2$) as well as blood and muscle lactate, pH, and phosphocreatine (116, 143). When the demands of the activity exceed CP/CS, these variables rapidly change to reach peak or nadir values that occur in close synchrony with exhaustion and the cessation of activity (116, 144). W′/D′ is mechanistically less well understood but represents a constant amount of work that can be performed above CP or CS. The size of W′ or D′ has been associated with concentrations of intramuscular lactate and phosphocreatine (143), the $\dot{V}O_2$ slow component amplitude (97, 145), the cross sectional area of the primary active muscle (94), and the accrual of peripheral fatigue (18). The parameters and predictions of exercise tolerance generated from this relationship hold across the spectrum of physical capacities, from sedentary and diseased populations to elite athletic performance.

A cardinal symptom of heart failure (HF) is exercise intolerance (114); however, the use of the speed-duration relationship remains underutilized in this population. To date, only one investigation has described CP in HF patients (92). These authors found that CP was reduced in HF compared to age-matched healthy controls and that $\dot{V}O_2$ and blood lactate attained steady-states below CP (92), in agreement with the findings in other populations (105, 106). However, this study was not designed to define the mechanistic determinants of the speed-duration relationship in HF (92). Although HF develops because of an initial insult to the heart, the disease is more appropriately described as a syndrome that coalesces to negative maladaptations across multiple physiological systems (for review see (115)). These maladaptations lead to reductions in perfusive oxygen delivery, reflected as reduced blood flow to active skeletal muscle (42, 102), occurring, in part, due to reduced cardiac output and dysfunctional vasocontrol in arterioles (35, 146). These perfusive O_2 delivery impairments appear to have the greatest

impact on the more oxidative fibers in HF (12, 25, 102). Importantly, this reduction in perfusive O_2 delivery occurs concomitantly with diffusive O_2 delivery decrements (42). The most compelling evidence for this diffusive limitation was the direct observation of skeletal muscle capillaries in HF rats, which revealed a reduction in the proportion of capillaries supporting continuous flow compared to control rats (74, 123). The speed-duration relationship can be used to examine the contribution of central and peripheral mechanisms to exercise intolerance in HF, which would provide important insight into the treatment options and outcomes for HF patients.

Therefore, the purpose of the present investigation was two-fold: 1) to establish the speed-duration relationship in an animal model of HF which is free from confounding prescription therapeutics; and 2) determine the central and peripheral mechanisms of the speed-duration relationship using a combination of non-invasive and invasive techniques not ethically or functionally available in human HF patients. We tested the following hypotheses: 1) CS (but not D′ as muscle morphology (34) and high energy phosphate (3) are typically unchanged in moderate HF) would be reduced in HF; 2) central and peripheral function measurements would express strong correlations with CS; and 3) the greatest peripheral dysfunction in HF would be found in highly oxidative muscle (soleus) compared to low-oxidative muscle (white gastrocnemius) and would be, at least in part, nitric oxide-mediated.

Materials and Methods

Ethical approval

Fifteen adult (4-5 mo. old) female Sprague-Dawley rats (Charles River Laboratories, Wilmington, MA) were maintained in accredited animal facilities at Kansas State University on a 12-h light-dark cycle with food and water provided *ad libitum* in isolated cages. All procedures were approved by the Institutional Animal Care and Use Committee of Kansas State University and conducted according to the National Research Council *Guide for the Care and Use of Laboratory Animals*. Rats were initially randomly assigned to control (n = 6) or HF (n = 9) groups.

Myocardial infarction protocol

Myocardial infarction (MI) was induced in HF rats (n = 9) by surgical ligation of the left main coronary artery as described previously (45, 100). Briefly, rats were initially anesthetized with a 5% isoflurane-O_2 mixture (Butler Animal Health Supply, Elk Grove Village, IL; Linweld, Dallas, TX) and maintained on an ~2% isoflurane-O_2 mixture and then intubated and mechanically ventilated with a rodent respirator (model 680, Harvard Instruments, Holliston, MA) for the duration of the surgical procedure. A left thoracotomy was performed to expose the heart through the fifth intercostal space and the left main coronary artery was ligated 1-2 mm distal to the edge of the left atrium with a 6-0 braided polyester suture. The thorax was then closed with 2-0 gut and the skin with 3-0 silk. Bupivacaine (1.5 mg/kg sc), ampicillin (50 mg/kg im), and buprenorphine (~0.03 mg/kg im) were administered to alleviate pain and reduce the risk of infection. Rats were monitored closely for ~8 h post-surgery for the development of arrhythmias and/or undue stress, with care administered as necessary following the removal from mechanical ventilation and anesthesia. At least 21 days of recovery were given to allow for complete remodeling of necrotic myocardial tissue and development of compensated HF (48, 100, 102). Control rats were maintained on site while the HF group underwent the MI protocol and recovery to maintain age-matched groups.

Treadmill acclimatization and determination of critical speed

All treadmill experiments were conducted on a custom-built motor-driven treadmill with the grade set to 5%. All rats completed an acclimatization phase across 6-10 days that consisted of daily 5 min runs. The initial runs were conducted at speeds of 20-25 m/min for the entire 5

min session. In the later runs, treadmill speed was increased to 30-50 m/min for the last ~1 min of the session to familiarize the rats with high speed running. This acclimatization protocol has been previously shown to not induce training adaptations (38, 101).

Following completion of the acclimatization phase, the speed-duration relationship was determined using the traditional multiple constant-speed method previously described (26, 27). Tests to exhaustion were performed at speeds eliciting exhaustion between 2 and 20 min. Each run began with an initial warm-up run at ~20 m/min for 2 min followed by ~1 min of quiet rest. The test was subsequently initiated with the treadmill speed being increased rapidly over a 10 s period to the required speed. Timing began when the investigator controlling the speed verified attainment of the desired speed. Rats were encouraged to run with bursts of air manually applied to the hindlimb whenever they drifted to the rear of the treadmill lane. Tests were terminated when rats were unable to maintain the required speed despite obvious exertion and encouragement. Termination of the test was determined by the same investigators, who were unaware of the exercise time, and exercise time was recorded to the nearest 0.1 s. Tests were determined to be successful when rats were unwilling or unable to right themselves for > 2 s when placed on their backs (i.e., lack of a righting reflex). The first run for all rats was performed at 60 m/min as this speed exceeds the critical speed of healthy rats (~45 m/min; (26, 27)), and subsequent runs were randomly assigned to fill out the desired range of times to exhaustion. Control rats were given at least 24 h and HF rats at least 48 h between tests to allow adequate recovery. When at least four successful constant-speed tests were completed, the parameters of the speed-duration relationship were determined by: 1) the hyperbolic speed-time model (time = D′ / (speed – CS)), where the asymptote of this curve is CS and the curvature constant is D′; and 2) the linear 1/time model (speed = D′ x 1/time + CS), where speed is plotted as a function of the inverse of time (s)-to-exhaustion, the intercept of the regression line is CS and the slope is D′ (26, 27, 113). Both models were used to ensure accuracy and robustness of CS estimation and displayed good agreement in both groups (see Figure 2-1 for representative fits).

Noninvasive and invasive determination of LV function and MI size

Transthoracic echocardiography was performed using a commercially available system (Logiq S8, GE Health Care, Milwaukee, WI, USA) with an 18 MHz linear transducer (L8-18i).

Rats were initially anesthetized with a 5% isoflurane-O_2 mixture then maintained on a ~1.5% isoflurane-O_2 mixture and placed on a heating pad (42 °C) to maintain core temperature. Standard two-dimensional and M-mode images from the mid-papillary level were obtained with frame rates > 50 frames s^{-1}. Ventricular dimensions and wall thicknesses were obtained from M-mode measurements for at least four consecutive cardiac cycles. All echocardiographic data were stored on the local hard drive and analyzed by an investigator using the manufacturer's dedicated software. Left ventricular (LV) dimensions were measured from M-mode measurements across at four consecutive cardiac cycles at end-systole (LVIDs) and end-diastole (LVIDd). Similarly, LV posterior wall (PW) thickness was measured at end-systole (PWs) and diastole (PWd). End-systole and end-diastole were defined as the time point of minimal and maximal dimensions respectively. Fractional shortening (FS) was calculated from the measures of LV chamber diameters: FS = [(LVIDd-LVIDs)/LVIDd] × 100. Left end-systolic (LVESv) and end-diastolic (LVEDv) volumes were calculated using the Teichholz formula: LV volume = (7.0 / 2.4 + LV dimension) × LV dimension^3). Stroke volume was calculated as: SV = LVEDv – LVESv. Ejection Fraction (EF) was calculated from the measures of LV volumes: EF = [(LVEDv-LVESv)/LVEDv] × 100. See Figure 2-2 for representative rat echocardiographic images pre- and post-MI. These measurements were performed on all rats prior to randomization into groups. The MI group had subsequent measurements 7- and 21-days post-infarction. All rats had a final echocardiographic assessment ~2 days after the determination of the speed-duration relationship (total time ~49-56 days post-infarction).

On the day of the terminal experiment (see interstitial PO_2 methods below), rats were anesthetized with the same isofurane-O_2 mixture and protocol described above. Following cannulation of the right carotid artery a micromanometer (2-french catheter-tip pressure manometer, Millar Instruments, Houston, TX) was advanced retrogradely into the LV to determine LV end diastolic pressure (LVEDP). These data were collected with a PowerLab/LabChart data acquisition system (AD Instruments); all data were displayed in real time and recorded for offline analysis. LVEDP was determined as the mean of 5 consecutive cardiac cycles. The LV MI surface area was measured post-mortem using planimetry and expressed as %LV endocardial surface area.

Surgical preparation for interstitial PO_2 measurement

Following LV function measurements, a catheter (PE-10 connected to PE-50, Intra-Medic polyethylene tubing, Clay Adams Brand, Becton, Dickinson and Company, Sparks, MD) was inserted into the carotid artery for measurement of mean arterial pressure (MAP) and heart rate (HR). A second catheter was introduced into the caudal artery for the administration of pentobarbital sodium anesthesia. Then the incisions for the carotid and caudal catheters were closed. Subsequently, while still under isoflurane anesthesia, an incision was made above the lateral malleolus of the left hindlimb and the skin and fascia were reflected to expose the biceps femoris. The distal portion of the biceps femoris was reflected (3-0 silk suture) to expose the soleus and white gastrocnemius muscles. Platinum iridium electrodes were attached (6-0 suture) to the proximal (cathode) and distal (anode) regions of the muscles in order to elicit electrically-induced muscle contractions. Rats were then progressively transitioned to pentobarbital sodium anesthesia ([50 mg/ml]) with depth of anesthesia continuously monitored via toe pinch and corneal sensitivity reflexes; with additional anesthesia administered as necessary (as 0.03-0.05 ml of [50 mg/ml] diluted in 0.3 ml of heparinized saline).

Rats were placed on a heating pad to maintain a core temperature of ~38 °C (measured via rectal probe, AD Instruments). Surrounding exposed tissues were covered with Saran Wrap (Dow Brands, Indianapolis, IN) to reduce tissue dehydration and minimize exposure of bordering tissues to superfused solutions. Exposed muscle was superfused frequently with warmed (38.5 °C) Krebs-Henseleit bicarbonate buffered solution equilibrated with 5% CO_2-95% N_2.

Experimental protocol

Two separate soleus contraction bouts were performed under control and N^{ω} nitro-L-arginine methyl ester (L-NAME; nonselective NO synthase (NOS) inhibitor, 1.5 mM) conditions. The L-NAME bout was always performed second due to the long half-life of L-NAME. Muscle interstitial PO_2 (PO_2*is*) was recorded for ~40 s at rest, during 180 s of electrically-induced muscle contractions (1 Hz, 7-8 V, 2 ms pulse duration) with a Grass S88 Stimulator (Quincy, MA), and for 180 s of passive recovery. L-NAME was administered via superfusion (3 ml total volume) on the soleus over 180 s of continuous PO_2*is* recording. The recording was extended an additional 180 s to confirm that baseline PO_2*is* had stabilized and the same contraction and recovery protocol was repeated. Between contraction bouts, rats were

given 20-30 min of recovery with regular superfusion of Krebs-Henseleit solution. Our laboratory has previously shown this duration of recovery elicits reproducible PO_2*is* responses (29). The same contraction protocols were then performed on the white gastrocnemius, however, L-NAME had no effect on the white gastrocnemius and those data were excluded from subsequent data analysis. MAP and HR were measured during the experiment via the right carotid artery catheter connected to a pressure transducer (AD Instruments), displayed in real time, and stored for offline analysis. Upon completion of the protocol, rats were euthanized with intra-arterial potassium chloride overdose (1 ml/kg of 4M KCl).

Interstitial PO_2 measurement

Phosphorescence quenching was used to measure PO_2*is* at rest and during contractions using a frequency domain phosphorometer (PMOD 5000; Oxygen Enterprises, Philadelphia, PA) as previously described (29, 60). Briefly, the Oxyphor G4 (Pd-*meso*-tetra-(3,5-dicarboxyphenyl)-tetrabenzo-porphyrin) was injected locally (2-3 10 μL injections at 10 μM concentration) using a 29G needle with care taken to avoid damaging any visible vasculature. After injection, the muscle was covered with Saran Wrap and given at least 20 min to allow the G4 to diffuse throughout the interstitial space. Since this oxyphor does not cross membranes and is stable across physiological pH ranges (41), it is well-suited for use in biological tissues. The oxyphor is temperature sensitive and muscle temperature was measured using a non-contact infrared thermometer. The mean exposed-muscle temperature was 30.1 ± 0.2 °C, with no differences between groups, muscles, or following contractions.

Phosphorescence quenching applies the Stern-Volmer relationship (41, 126), which describes the quantitative O_2 dependence of the phosphorescent probe G4 via the equation: PO_2*is* $= [(\tau_0/\tau) - 1]/(k_Q \cdot \tau_0)$, where k_Q is the quenching constant and τ and τ_0 are the phosphorescence lifetimes at the ambient O_2 concentration and in the absence of O_2, respectively. For G4 in tissue at ~30 °C, k_Q is ~258 $mmHg^{-1} \cdot s^{-1}$ and τ_0 is ~226 μs (41). Since muscle temperature does not appreciably change over the duration of the contraction protocol used herein, the phosphorescence lifetime is determined exclusively by the O_2 partial pressure. After injection of G4, the common end of the bifurcated light guide was positioned 3-4 mm above the surface of the exposed muscle. The phosphorometer modulates sinusoidal excitation frequencies between 100 Hz and 20 kHz and allows phosphorescence lifetime measurements from 10 μs to ~2.5 ms.

PO_2*is* was measured continuously and recorded at 2 s intervals throughout the duration of the experimental protocol. All PO_2*is* measurements were performed in a dark room with minimal extraneous light exposure.

Analysis of interstitial PO_2 kinetics

The kinetics analyses of the PO_2*is* responses were conducted using 20 s of resting data and the 180 s contraction bout using a mono-exponential plus time delay model:

$$PO_2\,(t) = PO_{2(BL)} - \Delta_1 PO_2\,(1 - e^{-(t - TD)/\tau})$$

or a mono-exponential plus time delay with a secondary component when necessary:

$$PO_2\,(t) = PO_{2(BL)} - \Delta_1 PO_2\,(1 - e^{-(t - TD)/\tau}) + \Delta_2 PO_2\,(1 - e^{-(t - TD_2)/\tau_2})$$

where PO_2 (*t*) represents the PO_2*is* at any point in time, $PO_{2(BL)}$ is the baseline before the onset of contractions and any appreciable change in PO_2*is*, $\Delta_1 PO_2$ and $\Delta_2 PO_2$ are the primary and secondary amplitudes, TD and TD_2 are the time delays before the fall and secondary rise in PO_2, and τ and τ_2 are the time constants (*i.e.*, the time required to reach 63% of the amplitude) for the primary and secondary amplitudes. The mean response time (MRT) was calculated as the sum of the model derived TD and τ. When the secondary component model was necessary, the primary amplitude was constrained to not exceed the nadir value to maximize the accuracy of the primary response kinetics (29). The goodness of model fit was determined using the criteria: 1) the coefficient of determination; 2) sum of the squared residuals; and 3) visual inspection and analysis of the model fits to the data and the residuals. Since $\Delta_2 PO_2$ (*i.e.*, undershoot of PO_2) was often non-exponential in nature, $\Delta_2 PO_2$ was determined manually, when necessary, by calculating the difference between the PO_2*is* at the end of contractions minus the nadir value of PO_2*is* during contractions.

Skeletal muscle citrate synthase activity

The soleus muscle, white portions of the gastrocnemius muscle, and plantaris muscle were used for determination of citrate synthase activity. This mitochondrial enzyme, is a marker of muscle oxidative capacity and was analyzed using adapted methods previously described in (40). In brief, 15 µl and 30 µl samples were diluted using 210 µl and 195 µl of tris buffer, respectively. In addition, 15 µl of acetyl coenzyme A (Cayman Chemical, Ann Arbor, MI), and 30 µl of DTNB (Thermo Fisher Scientific, Waltham, MA) were added to each sample. Samples were incubated in a spectrophotometer (accuSkan GO; Fisher Scientific, Hampton, NH) for 5

min at 30°C before readings. Following incubation, readings were collected with the spectrophotometer at 412 nm once per minute for 5 min followed by the addition of 30 µl of oxalacetic acid (Sigma-Aldrich, St. Louis, MO) to all samples and immediately analyzed again. Citrate synthase enzyme activity is reported as µmol/min/g wet weight of sample tissue.

Statistical analysis

All curve fitting and statistical analyses were performed using a commercially available software package (SigmaPlot 12.5, Systat Software, San Jose, CA). Differences between the hyperbolic and linear 1/time model estimates of CS and D′ were compared across all rats using paired t-tests. Group differences for rat descriptive variables, speed-duration parameters, and resting hemodynamics (i.e., MAP and HR) during the PO_2*is* experiment were compared using unpaired Student's t-tests. Normality was assured using the Shapiro-Wilk test. If either the normality or equal variance assumptions were violated, a Mann-Whitney Rank Sum test was used to compare the above variables. Serial LV function measurements for the HF group were compared across time using 1-way repeated measures ANOVA. Comparisons of LV function across groups (pre-infarction and post-CS) were compared using 2-way repeated measures ANOVA using one factor repetition. Control condition PO_2*is* kinetics parameters and skeletal muscle citrate synthase activity were compared among groups using 2-way repeated measures ANOVA (group x muscle). The effect of L-NAME superfusion on soleus PO_2*is* kinetics parameters was compared within the soleus groups using 2-way repeated measures ANOVA (group x condition). When significant differences were detected, this was verified using Tukey's honest significant difference *post hoc* tests. Pearson's product-moment correlations and linear regressions were used to determine relationships among variables. Data are presented as means ± standard error unless otherwise noted. Significance was accepted at $p < 0.05$.

Results

Nine of the original 15 rats successfully completed the protocol. Two control and two HF rats could not be motivated to run as required for the experimental protocol. An additional two HF rats died during the MI surgery. Since all rats did not complete the protocol, the statistical power achieved (0.78 – 1.0) has been reported for the primary variables. The body mass of the groups did not differ at the end of their final CS test (control: 338 ± 14, HF: 360 ± 15 g; $p = 0.33$).

Determination of CS and D′

The times to exhaustion, hyperbolic and linear 1/time model fits, and estimated CS are shown for two representative rats in Figure 2-1. The combined-group CS (hyperbolic: 40.7 ± 1.1, 1/time: 40.8 ± 1.1 m/min; $p = 0.83$), and D′ (hyperbolic: 68.0 ± 9.2, 1/time: 67.7 ± 8.9 m; $p = 0.92$) did not differ between the models used to estimate the parameter, so the best fit (based on r^2) was employed for all subsequent comparisons. CS was significantly lower in HF compared to control rats (38.3 ± 1.0 vs 44.1 ± 0.6 m/min; $p < 0.001$, power = 0.99) but D′ was not different (HF: 70 ± 11, control: 62 ± 14 m; $p = 0.67$). The individual rat speed-duration parameters from both model estimations are presented in Table 2-1.

LV function

The average MI size in the HF group was 32 ± 3% and LVEDP was nearly 3-fold higher than controls (HF: 16 ± 2, control: 6 ± 1 mmHg; $p < 0.01$). The individual rat LV characteristics and functional measurements following speed-duration testing are presented in Table 2-2. The LV of the HF group was significantly dilated (LVIDd, LVIDs, LVEDv, and LVESv; all $p < 0.001$, power > 0.8), the septal wall was hypertrophied (PWd and PWs; both $p < 0.02$, power = 0.78), and the LV contractile function was substantially reduced (FS and EF; both $p < 0.001$; power = 1.0) compared to control. Figure 2-3 displays the group mean FS across time during recovery and following CS determination (all other echo measurements expressed parallel directional changes and time courses). FS was not different between groups pre-MI ($p = 0.52$) and there was no effect of time in the control group ($p = 0.72$). HF FS was severely reduced by Post-7 ($p < 0.001$) with no further changes throughout the recovery period or following CS determination.

MI size was found to be highly correlated with the noninvasive (FS; $r = -0.96$, $p < 0.001$) and invasive (LVEDP; $r = 0.89$, $p = 0.001$) LV functional measurements (Figure 2-4: *Top* and *Middle*, respectively). FS and LVEDP were also highly correlated with each other ($r = -0.89$, $p = 0.002$, Figure 2-4: *Bottom*). FS was highly correlated with CS ($r = 0.9$, $p < 0.001$, Figure 2-5: *Top*) as was LVEDP ($r = -0.74$, $p = 0.02$, data not shown).

Soleus and white gastrocnemius PO_2*is*

Resting MAP was not different between groups (control: 93 ± 6, HF: 93 ± 3 mmHg; $p = 0.99$) but resting HR was greater for HF compared to control (359 ± 6 vs 320 ± 9 beats/min; $p < 0.01$). MAP and HR did not change appreciably during the contraction protocol. Kinetics parameter group means for the white gastrocnemius, soleus, and L-NAME treated soleus are presented in Table 2-3. The group PO_2*is* profiles are presented in Figure 2-6. There were no between-group differences for the white gastrocnemius; however, the white gastrocnemius operated at a much lower PO_2*is* compared to the soleus for both groups. In the soleus, HF rats expressed lower resting PO_2*is* and reduced amplitude (both, $p < 0.01$) compared to control rats. Despite the lower amplitude, the soleus nadir and end-exercise PO_2*is* was also reduced in the HF group (both, $p < 0.01$). L-NAME superfusion reduced soleus resting PO_2*is* in the control rats ($p = 0.02$) but had no effect on the HF group ($p = 0.87$, Figure 2-6: *Right*). Similarly, the nadir PO_2*is* was reduced following L-NAME for the control rats ($p < 0.01$) but had no effect on the HF group ($p = 0.73$). Baseline soleus PO_2*is* was negatively correlated with D′ ($r = -0.84$, $p < 0.01$, data not shown) and end-contraction soleus PO_2*is* was found to be highly correlated with CS ($r = 0.75$, $p = 0.02$, Figure 2-5: *Bottom*).

Skeletal muscle citrate synthase

No differences in citrate synthase activity were found between groups for the soleus (ratio of HF / control: 0.96; $p = 0.74$), plantaris (1.01; $p = 0.98$), or white gastrocnemius (1.11; $p = 0.36$).

Discussion

Resolution of the mechanistic bases for the exercise intolerance induced by HF is an important physiological goal that has major clinical implications. The principal original findings of the present investigation include determination of the effects of HF on the parameters of speed-duration relationship in an animal model of HF free from prescription therapeutics that would complicate interpretation in human HF patients. Specifically, HF reduced CS, which represents the highest level of activity sustainable through primarily oxidative pathways, while leaving D′, the energy stores parameter, unchanged. Indices of central cardiac and skeletal muscle function correlated strongly with CS likely due to their role in reducing perfusive and diffusive O_2 delivery to oxidative muscle fibers in this population. Importantly, the reduced CS occurred in the absence of impaired locomotory muscle oxidative enzyme capacity supporting an upstream (i.e., decreased PO_2*is*) basis for compromised exercise tolerance; at least in this model of moderate HF (approximating Class II-III HF). These findings provide support for the viability of this rat model of HF, with reduced ejection fraction, to evaluate targeted therapeutics intended to improve exercise tolerance and quality of life and potentially reduce morbidity and mortality in the human HF population.

The speed-duration relationship in heart failure

The present investigation revealed for the first time that the speed-duration relationship can be determined in HF rats and that CS is lowered while D′ is preserved compared to control. Although high intensity exercise is advocated for HF patients (98, 152), determination of the speed-duration relationship in human HF patients might meet with resistance from ethics review boards. Therefore, the rodent model of HF could prove to be a powerful tool to evaluate the effects of targeted interventions on physical activity tolerance in this population. Whereas maximal oxygen uptake ($\dot{V}O_{2max}$) is an excellent predictor of all-cause mortality (15) and heart transplant need (86), CS is a better indicator of physical activity tolerance and task-specific performance than $\dot{V}O_{2max}$ (1, 105, 106, 118). The single study to determine the speed-duration relationship in human HF patients did not report the effect of HF on D′ (92); however, it has been postulated that HF would reduce D′ (113) in a manner similar to chronic obstructive pulmonary disease (COPD) (105). When refitting the mean data from Mezzani and colleagues (92), the D′ parameter appears to be ~30% lower in the HF group compared to the controls. Since

the O_2 delivery impairments in HF primarily impact more oxidative fibers (12, 25, 102) and would intuitively reduce CS, we hypothesized that this population's increased reliance on more glycolytic fibers (52, 137) and preservation of muscle morphology in moderate HF (34) would result in a preserved D′. Further research is warranted to clarify this discrepancy, but it is important to consider that the HF rats in the present investigation were motivated to run until absolute exhaustion (reflected by the lack of a righting reflex) while the previously mentioned COPD (105) and HF (92) patients' exercise tolerances were likely symptom limited (e.g., exaggerated perception of effort induced by dyspnea). Had these patient populations indeed been symptom limited rather than fully expending D′, the resulting effect would be a reduced tolerance to exercise above CS (i.e., apparent reduction of D′).

Cardiac function in heart failure

Echocardiographic assessment of LV function following MI-induced HF is a valuable clinical and research tool in both humans (107, 111) and rats (6, 82, 132). We show herein that noninvasive and invasive assessments of LV function in HF are highly correlated with each other and, for the first time, strongly related to the performance parameter CS, which delineates the threshold of sustainable physical activity. Previous work suggests that there is no correlation between resting LV functional measurements and maximal exercise capacity (i.e., peak $\dot{V}O_2$) in HF during an incremental/ramp test (49, 57). One interpretation of this finding is that LV function is either a poor indicator of exercising LV function or is less important to exercise capacity than peripheral function during peak or maximal efforts. Resting LV function does, however, relate to submaximal sustained exercise performance (i.e., CS), which is more indicative of daily physical activity tolerance and ability in HF. Additional validation of the present findings in human HF patients is required, but the present data do provide a compelling argument as to the value of noninvasive LV functional measurements (e.g., echocardiography) to evaluate the effect of targeted interventions on HF patient exercise tolerance without the need for multiple, strenuous tests. Additionally, the present investigation confirms the earlier work of Litwin and colleagues (82), in that serial echocardiographic assessment of LV function in HF rats reveals a very rapid onset of LV dysfunction (7 days post MI) that is stable across multiple subsequent weeks (up to 8 weeks) of recovery and exercise testing.

Peripheral function in heart failure

The present investigation, to the best of our knowledge, is the first use of the phosphorescence quenching technique to measure PO_2 in the interstitial space of HF rats. We show herein, that resting PO_2*is* and the contraction-induced amplitude are reduced in HF rats compared to healthy controls but only in the oxidative soleus and not the glycolytic white gastrocnemius muscle. These differences were manifest despite a lack of change in central hemodynamic variables (i.e., HR and MAP) during contractions, supporting a peripheral vascular dysfunction locus. These findings are in agreement with the detrimental effects of HF on bulk blood flow (102) and the upstream microvascular PO_2 compartment (12, 37) previously identified in our laboratory. Thus, reduced perfusive and diffusive delivery of O_2 coalesces to lower the absolute PO_2*is* across the rest and exercise transition. This reduction in the driving pressure of O_2 across the sarcolemma will contribute to the increased reliance on non-oxidative energy production and earlier onset of exercise cessation evident in HF patients.

Interestingly, the soleus PO_2*is* kinetics response (i.e., MRT) was slowed for HF in the present investigation, in contrast to the speeding of the PO_2 profile in the microvascular space (12). This dissimilar temporal response could be due to differences in the regulation of PO_2 in these two compartments (29, 60) and/or the closer proximity to the myocyte/mitochondria of the interstitial space. Skeletal muscle mitochondrial oxidative capacity, indicated by citrate synthase activity, is not usually compromised at this level of HF (i.e., moderate (3, 12, 34, 37, 85) and the present data); and there is evidence of a skeletal muscle metabolic reserve in HF revealed using small muscle mass exercise (42). It must be noted, however, that this is not always the case as locomotory muscle citrate synthase activity levels are occasionally reduced in HF (34, 50, 131) but this effect is modest compared with severe HF (3, 34). The matching of O_2 delivery (i.e., blood flow) and utilization (i.e., $\dot{V}O_2$) determines PO_2, and changes to one or the other, or both, must have occurred to slow the temporal response for HF compared to control. Since there is no evidence of improved blood flow in HF, we hypothesize that altered intracellular metabolic control drove the temporal PO_2*is* changes observed herein. Two potential causes of this altered metabolic control are: 1) heterogeneous distribution of blood flow within the contracting muscle leading to inactive mitochondria potentially being over perfused while more active mitochondria were under perfused (see (123) for capillary functional deficits in HF); and/or 2) a relatively greater metabolic inertia in HF mitochondria compared to control.

Heart failure reduces smooth muscle NO bioavailability and blockade of NO synthase with L-NAME discriminates the physiological contribution of endogenous NO (46, 47). L-NAME superfusion had the greatest effect on resting and contracting soleus PO_2*is* in the control group and no appreciable effects on the absolute values of PO_2*is* for HF soleus or white gastrocnemius from either group. This coheres with previous work showing NOS inhibition via L-NAME had the greatest impact on more oxidative muscle fiber blood flow (62), and we now show for the first time that this projects into the interstitial space lowering PO_2*is* of the more oxidative soleus muscle in healthy rats. Our laboratory has previously shown that L-NAME has an attenuated effect on blood flow (63) and microvascular PO_2 (46) for HF rats. The results herein and our laboratory's previous work (46, 63) continue to demonstrate that a reduced nitric oxide bioavailability plays a fundamental role in HF O_2 delivery-to-utilization dysfunction.

Experimental considerations

Several limitations must be acknowledged when interpreting the data from the present investigation. Firstly, our sample size is small and could increase the chance of Type I errors, however our primary outcomes achieved adequate statistical power (0.8 – 1.0) for an alpha level of 0.05. Paired with the large effect sizes seen in this model of HF, we are confident that these observations are robust. Secondly, it is established that isoflurane anesthesia impacts cardiac function as measured with echocardiography (135). We contend that because the same level of isoflurane (~1.5%) was used for both groups in the present investigation, these effects should not confound interpretations of the underlying physiology. Finally, only young female rats were used and these data may not completely represent the effects of HF in males or in aged rats. Sexual dimorphism in young healthy rats is evident in vascular control, particularly when NO bioavailability is modulated (29). On the other hand, females are an underserved population in cardiovascular research and our findings provide an important first step to better understand physical activity tolerance in HF and the mechanistic bases of the speed-duration relationship in this disease. Additionally, the control group CS in the present investigation was near that reported in healthy male rats (~45 m/min (26, 27)), suggesting that there are no appreciable sex differences for CS within the control population.

Conclusions

We show for the first time that CS and D′ can be resolved in an animal model of HF whereby CS is reduced but D′ is not. Crucially, this HF model is free from prescription therapeutics that confounds interpretation of the mechanistic relationship between HF and CS or D′ in humans. We show that in this model of moderate HF (i.e. LVEDP < 20 mmHg), where skeletal muscle oxidative capacity is preserved, decrements in central cardiac function (determined via echocardiography) and peripheral skeletal muscle O_2 delivery-to-utilization function (determined via phosphorescence quenching) correlate directly with impaired exercise tolerance likely due to reduced perfusive and diffusive O_2 delivery to oxidative muscle fibers.

Table 2-1 Individual Speed-duration Relationship Parameters as Determined Using the Hyperbolic and 1/time Models for Control and Heart Failure Rats

		Hyperbolic			1/time			Best fit	
		CS (m/min)	D′ (m)	r^2	CS (m/min)	D′ (m)	r^2	CS (m/min)	D′ (m)
Con	**1**	41.3	107	0.989	42.9	93	0.991	42.9	93
	5	45.2	48	0.995	44.0	57	0.994	45.2	48
	9	45.0	29	0.994	44.6	31	0.977	45.0	29
	11	43.1	78	0.998	43.9	71	0.995	43.1	78
	Mean	43.7	66	0.994	43.9	63	0.989	44.1	62
	SE	0.9	17	0.002	0.4	13	0.004	0.6	14
HF	**3**	39.1	92	0.928	40.7	82	0.901	39.1	92
	6	40.9	101	0.994	39.2	119	0.978	40.9	101
	7	34.8	61	0.998	35.4	58	0.926	34.8	61
	13	38.0	50	0.999	38.2	48	0.996	38.0	50
	15	38.9	46	0.994	38.2	50	0.962	38.9	46
	Mean	38.3	70	0.98	38.3	71	0.95	38.3*****	70
	SE	1.0	11	0.01	0.9	13	0.02	1.0	11

Con, control; HF, heart failure; CS, critical speed; D′, curvature constant. *****, $p < 0.05$ vs Con.

Table 2-2 Doppler Echocardiographic Assessment of Left Ventricular Function Across Time for Control and Heart Failure Rats

	Pre		Post-7		Post-21		Post-CS	
	Con	**HF**	**Con**	**HF**	**Con**	**HF**	**Con**	**HF**
LVIDd (cm)	0.69 ± 0.02	0.66 ± 0.04	--	0.78 ± 0.03ǂ	--	0.85 ± 0.01ǂ	0.71 ± 0.04	0.85 ± 0.02*ǂ
LVIDs (cm)	0.35 ± 0.02	0.35 ± 0.03	--	0.59 ± 0.02ǂ	--	0.70 ± 0.05ǂ	0.37 ± 0.04	0.66 ± 0.03*ǂ
PWd (cm)	0.16 ± 0.02	0.20 ± 0.04	--	0.23 ± 0.03	--	0.19 ± 0.01	0.16 ± 0.01	0.25 ± 0.02*
PWs (cm)	0.28 ± 0.02	0.31 ± 0.03	--	0.30 ± 0.02	--	0.26 ± 0.04	0.27 ± 0.02	0.34 ± 0.02*
FS (%)	48.7 ± 1.4	46.9 ± 1.7	--	24.0 ± 1.6ǂ	--	18.0 ± 5.5ǂ	47.8 ± 2.7	22.6 ± 2.1*ǂ
LVEDv (ml)	0.75 ± 0.06	0.68 ± 0.1	--	1.05 ± 0.1ǂ	--	1.32 ± 0.04ǂ	0.83 ± 0.14	1.34 ± 0.1*ǂ
LVESv (ml)	0.12 ± 0.02	0.12 ± 0.02	--	0.49 ± 0.04ǂ	--	0.79 ± 0.17ǂ	0.14 ± 0.04	0.67 ± 0.09*ǂ
SV (ml)	0.63 ± 0.05	0.56 ± 0.08	--	0.56 ± 0.07	--	0.53 ± 0.14	0.68 ± 0.1	0.67 ± 0.05
EF (%)	84.8 ± 1.3	83.1 ± 1.6	--	53.1 ± 2.7ǂ	--	41.0 ± 11.3ǂ	83.6 ± 2.7	50.5 ± 3.6*ǂ

Con, control (n = 4); HF, heart failure (n = 5 for all except Post-21, n = 3); Pre, pre-infarction measurement; Post-7, 7-9 days post-infarction; Post-21, 21-23 days post-infarction; Post-CS, post speed-duration testing (49-56 days); LVIDd, Left ventricular end-diastolic diameter; LVIDs, LV end-systolic diameter; PWd, end-diastolic septal wall thickness; PWs, end-systolic septal wall thickness; FS, fractional shortening; LVEDv, LV end-diastolic volume; LVESv, LV end-systolic volume; SV, stroke volume; EF, ejection fraction. Data are means ± SE. *****, $P < 0.05$ vs Con within time; ǂ, $P < 0.05$ vs Pre within group.

Table 2-3 Interstitial PO_2 Kinetics Parameters of White Gastrocnemius and Soleus at Rest and During 180 s of Contractions for Control and Heart Failure Rats

	White Gastrocnemius		Soleus		Soleus + L-NAME	
	Con	**HF**	**Con**	**HF**	**Con**	**HF**
$PO_{2(BL)}$ (mmHg)	7.2 ± 1.5ǂ	7.0 ± 0.3ǂ	24.7 ± 2.1	16.1 ± 2.6*****	21.4 ± 0.4ǂ	15.9 ± 2.7*****
Δ_1PO_2 (mmHg)	5.0 ± 1.1ǂ	4.2 ± 0.6	13.5 ± 1.7	9.6 ± 2.3*****	12.6 ± 0.8	9.4 ± 1.9
τ (s)	16.6 ± 1.9	16.3 ± 2.1	12.7 ± 3.0	16.7 ± 3.2	13.4 ± 3.0	22.9 ± 1.9*****
TD (s)	5.9 ± 0.5ǂ	5.5 ± 0.9ǂ	13.1 ± 1.3	18.4 ± 1.6*****	9.5 ± 1.4ǂ	12.9 ± 1.7ǂ
MRT (s)	22.6 ± 2.4	21.9 ± 2.0ǂ	25.8 ± 2.0	35.1 ± 4.1*****	22.9 ± 3.9	35.7 ± 3.2*****
$PO_{2(Nadir)}$ (mmHg)	2.2 ± 0.4ǂ	2.7 ± 0.5ǂ	11.2 ± 1.9	6.5 ± 0.8*****	9.0 ± 1.1ǂ	8.8 ± 1.1
Δ_2PO_2 (mmHg)	1.1 ± 0.3ǂ	1.2 ± 0.5	3.2 ± 0.3	2.3 ± 0.2	3.3 ± 1.1	2.0 ± 0.4
$PO_{2(End)}$ (mmHg)	3.3 ± 0.4ǂ	3.9 ± 0.5ǂ	14.4 ± 2.1	8.7 ± 0.9*****	12.3 ± 1.1	8.8 ± 1.1*****

Con, control (n = 4); HF, heart failure (n = 5); $PO_{2(BL)}$, baseline interstitial PO_2; Δ_1PO_2, PO_2 primary amplitude; τ, time constant; TD, time delay; MRT, mean response time; $PO_{2(Nadir)}$, lowest PO_2 during contractions; Δ_2PO_2, PO_2 undershoot during contractions; $PO_{2(End)}$, PO_2 at the end of contractions. Values are means ± SE. *****, $p < 0.05$ vs Con within muscle. ǂ, $p < 0.05$ vs Soleus within group.

Figure 2-1 Representative speed-duration relationship modeling

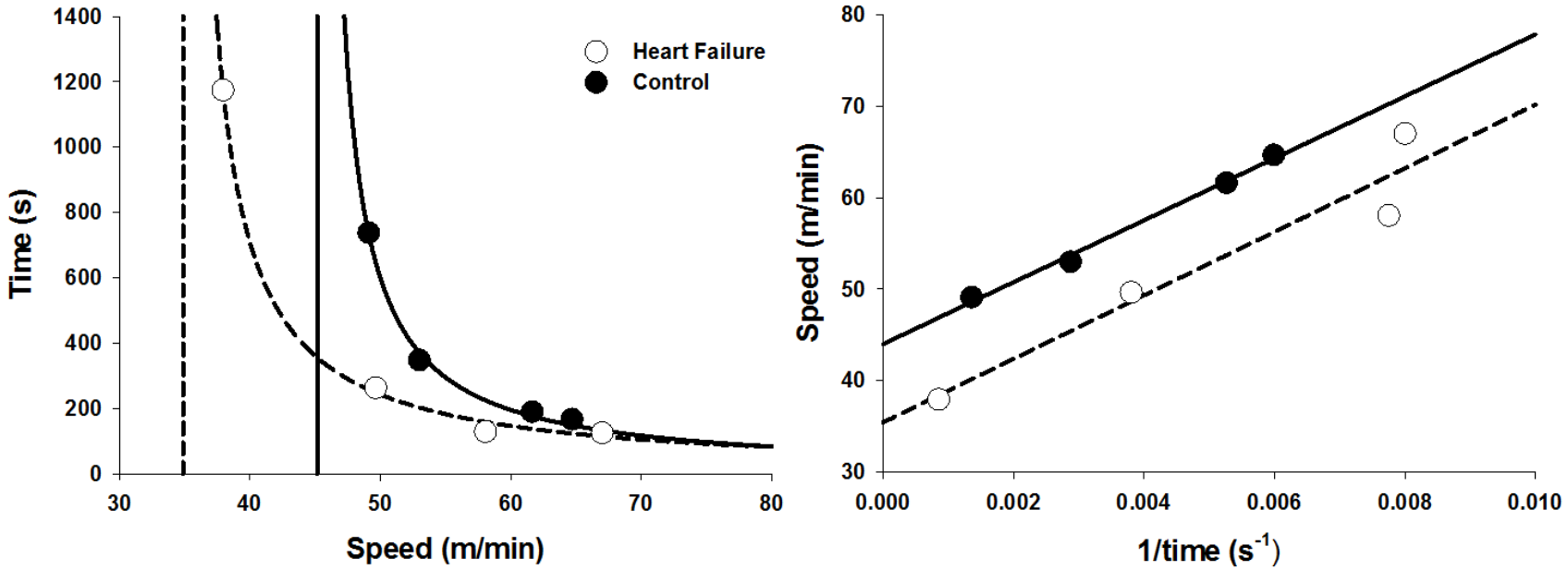

Both hyperbolic (*Left*) and 1/time (*Right*) models for a control (filled circles, Con 5) and heart failure (open circles, HF 7) rat are presented. There was good agreement of parameter estimation between models. Critical speed was drastically reduced (indicated by the leftward and downward shift for the hyperbolic and 1/time model, respectively) but D′ was not different (best appreciated from the parallel slopes in the right panel).

Figure 2-2 Echocardiographic assessment of left ventricular (LV) function

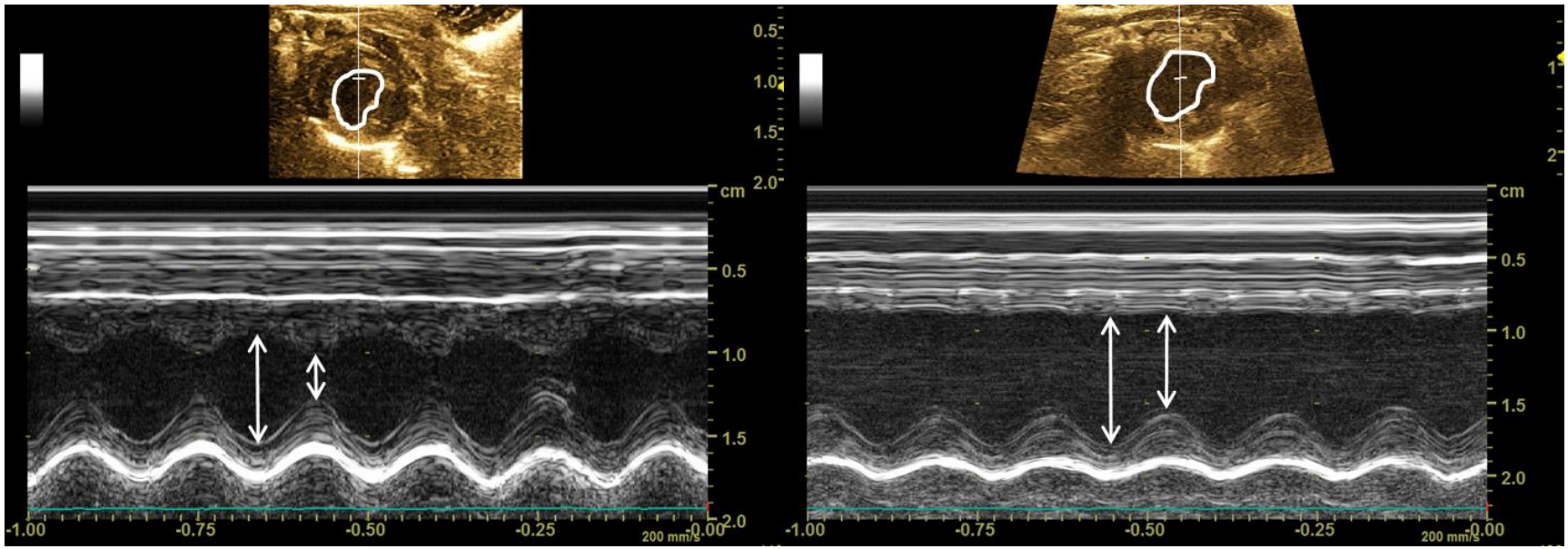

A representative rat pre-infarction (*Left*) and 7 days post-infarction (*Right*) is presented. Top portion: 2D image of LV used to guide M-mode imaging (bottom portion) at the level of the papillary muscle. Arrows demarcate LVIDd and LVIDs dimensions. M-mode imaging represents continuous measurement across 1 s for both images.

Figure 2-3 Group mean echocardiographic fractional shortening assessed across time

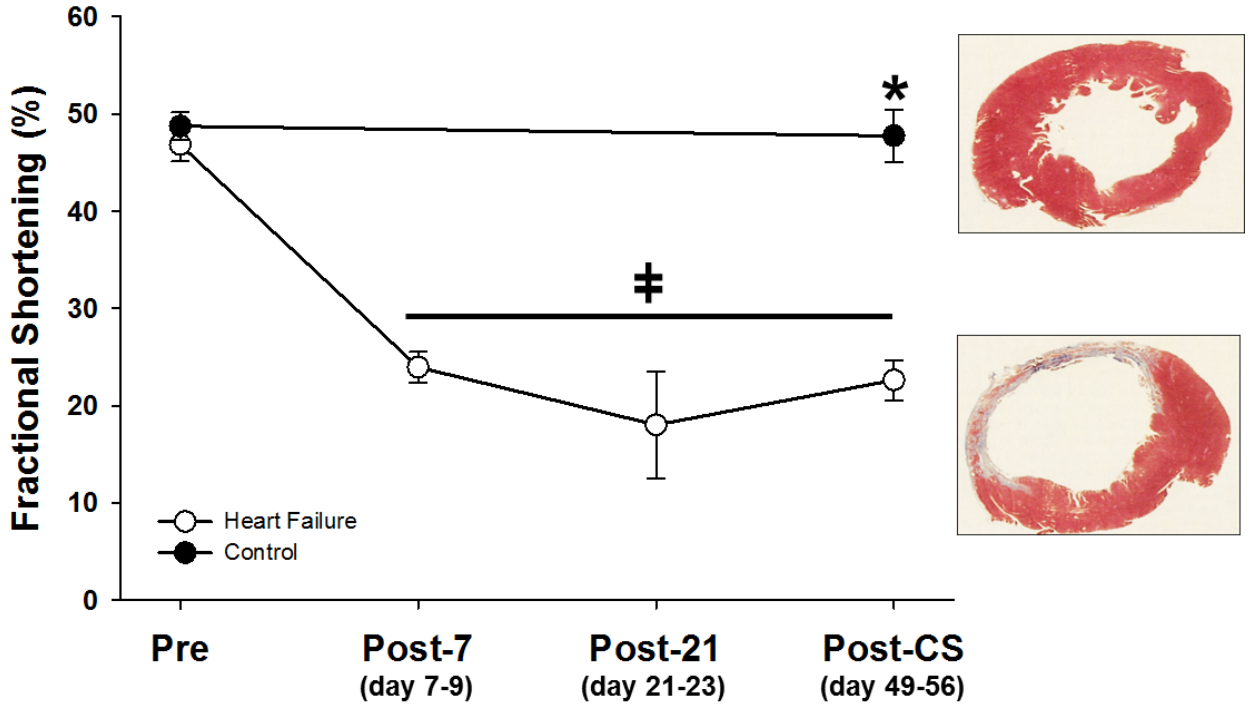

Both control (filled circles; n = 4) and heart failure (open circles; n = 5 for all except Post-21, n = 3) rats are represented. Inset images are transverse sections of healthy and infarcted left ventricles. Data are means ± SE. *, $p < 0.05$ vs heart failure within time; ǂ, $p < 0.05$ vs Pre within group.

Figure 2-4 Relationship between heart anatomical and functional variables

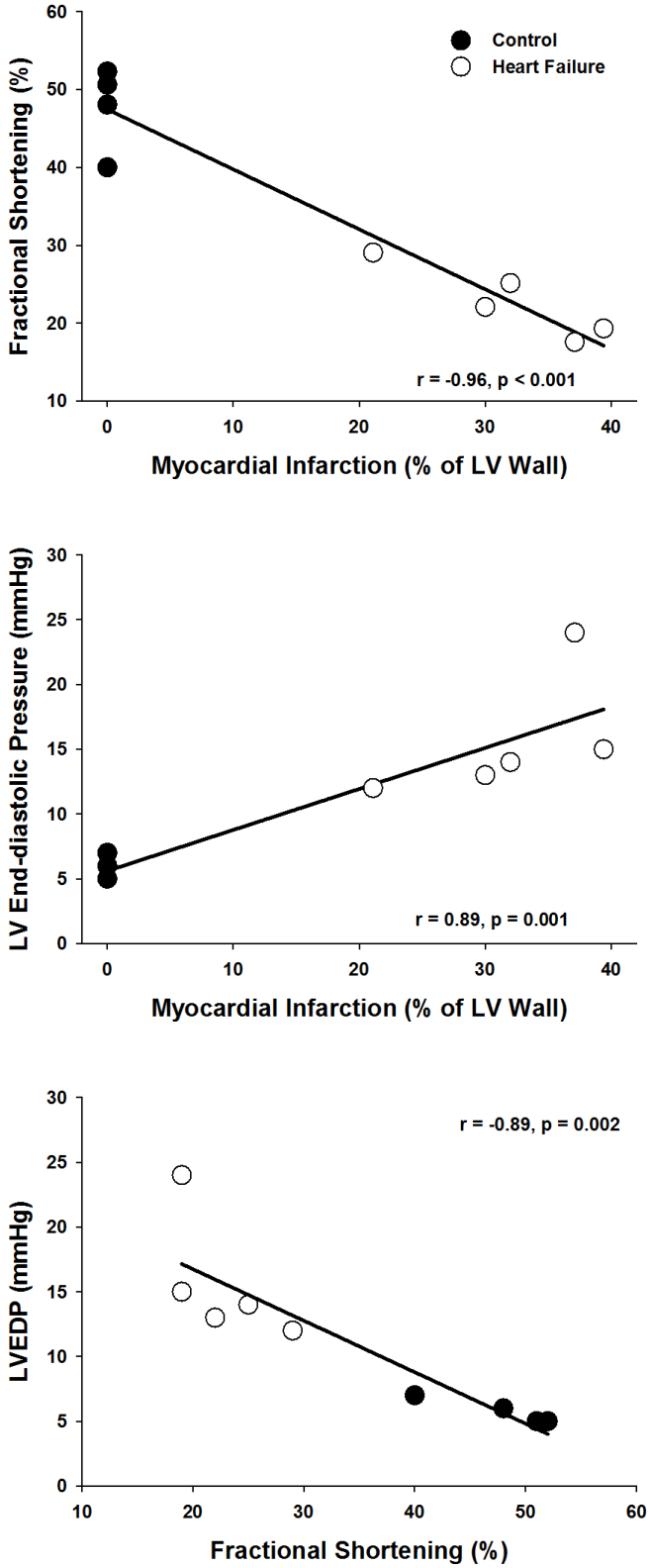

Top: fractional shortening (FS) as a function of myocardial infarction size.

Middle: left ventricular (LV) end-diastolic pressure (LVEDP) as a function of myocardial infarction size.

Bottom: correlation between FS and LVEDP. Heart failure (open circles) and control (filled circles) rats are represented in each figure.

Figure 2-5 Central and peripheral contribution to critical speed (CS)

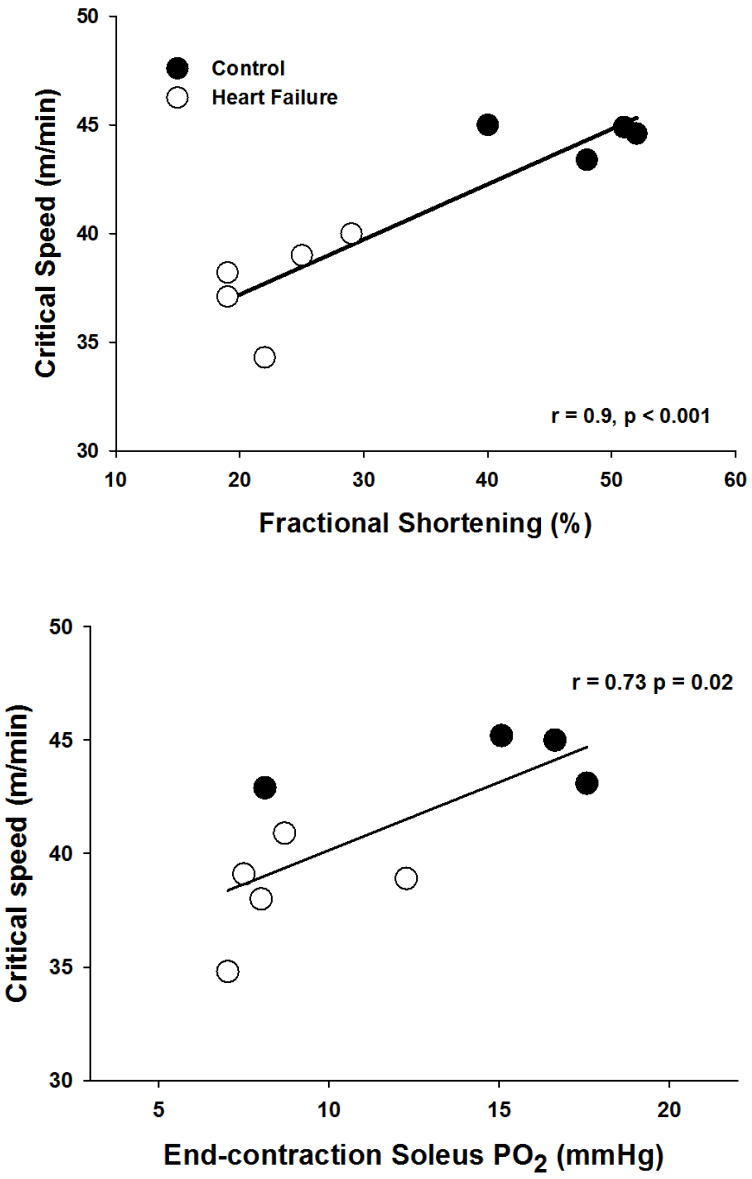

Top: CS as a function of fractional shortening.

Bottom: CS as a function of end-contraction soleus interstitial PO_2. Heart failure (open circles) and control (filled circles) rats are represented in each figure.

Figure 2-6 Group mean interstitial PO_2 (PO_2*is*) at rest and during contractions

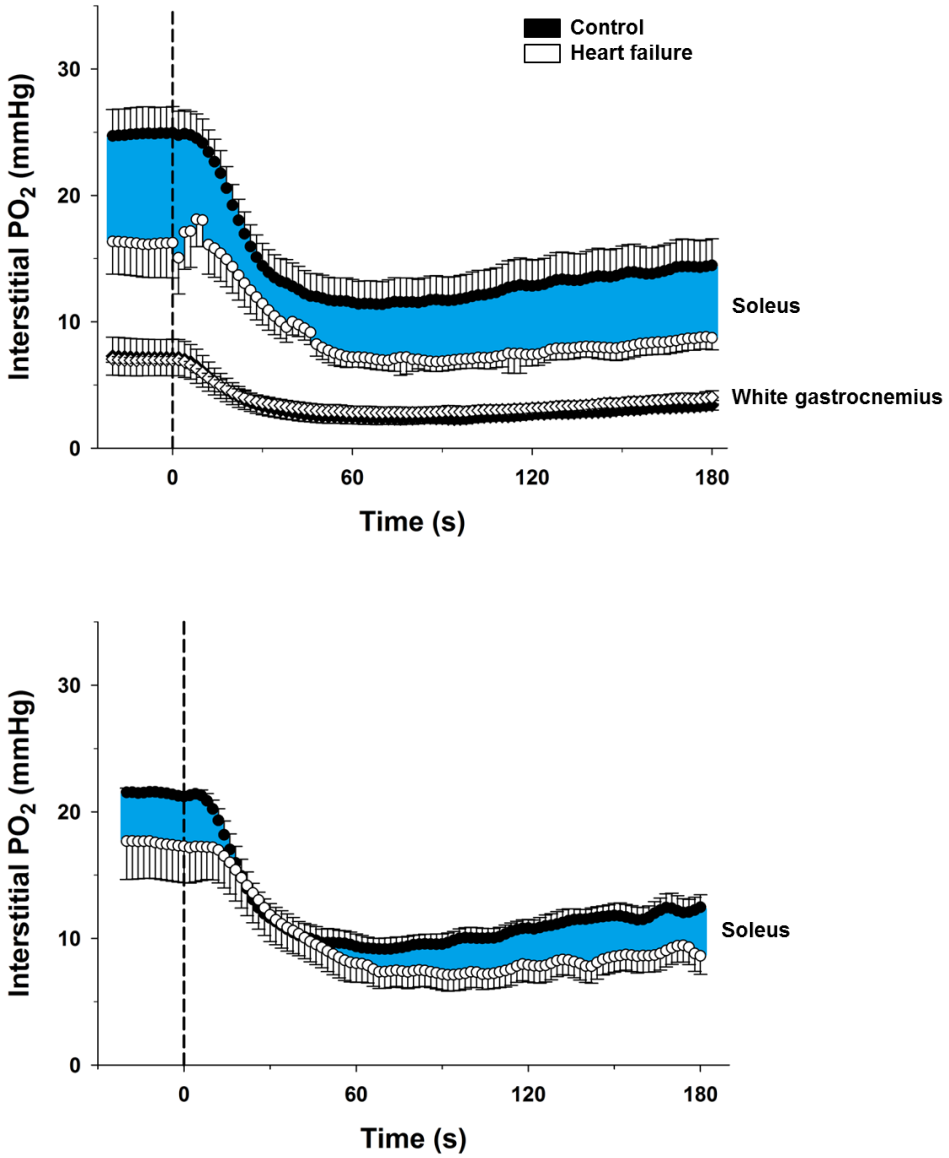

Electrically-induced twitch contractions were initiated at Time 0 (vertical dashed line).

Top: control condition PO_2*is* for both control (filled symbols; n = 4) and heart failure (open symbols; n = 5) rats in the soleus (circles) and white gastrocnemius (diamonds).

Bottom: N^{ω} nitro-L-arginine methyl ester (L-NAME) condition soleus PO_2*is* for control (filled circles) and heart failure (open circles) rats. Data are means ± SE. Shaded area highlights the difference between control and heart failure rats in the soleus PO_2*is* profile which was greatly reduced following L-NAME superfusion.

Chapter 3 - Sexual dimorphism in the control of skeletal muscle interstitial PO_2 of heart failure rats: Effects of dietary nitrate supplementation

Jesse C. Craig[1], Trenton D. Colburn[1], Daniel M. Hirai[1], Timothy I. Musch[1,2], and David C. Poole[1,2]

[1]Department of Kinesiology, Kansas State University, Manhattan, KS, USA

[2]Department of Anatomy and Physiology, Kansas State University, Manhattan, KS, USA

Summary

Sex differences in the mechanisms underlying cardiovascular pathophysiology of O_2 transport in heart failure (HF) remain to be explored. In HF, nitric oxide (NO) bioavailability is reduced and contributes to deficits in O_2 delivery-to-utilization matching. Females may rely more on NO for cardiovascular control in health and as such experience greater decrements in HF. We tested the hypotheses that HF would reduce skeletal muscle interstitial PO_2 (PO_2*is*; determined by O_2 delivery-to-utilization matching) for both sexes compared to healthy and females would express greater dysfunction compared to males. Furthermore, we tested the hypothesis that five days of dietary nitrate (Nitrate; 1mmol/kg/day) would increase NO bioavailability and raise PO_2*is* in HF rats, with a greater effect seen in females. Forty-two Sprague-Dawley rats were randomly assigned to healthy, HF, or HF + Nitrate groups (all, n = 14). Spinotrapezius PO_2*is* was measured via phosphorescence quenching during electrically-induced twitch contractions (1 Hz, ~6 V, 180 s). HF reduced resting PO_2*is* for both sexes compared to healthy ($p < 0.01$), and the reduction was greater in female (~30%) compared to male (~20%) HF ($p < 0.05$). Both HF sexes expressed reduced PO_2*is* amplitudes following the onset of muscle contractions compared to healthy ($p < 0.01$). In contrast, resting PO_2*is* was not different between healthy and HF + Nitrate rats or males and females within HF + Nitrate. Only male HF + Nitrate expressed a reduced PO_2*is* amplitude compared to healthy ($p < 0.05$). In this model of moderate HF, O_2 delivery-to-utilization matching is attenuated in a sex-specific manner and dietary nitrate supplementation serves to offset this reduction with potentially greater efficacy in female HF rats.

Introduction

Cardiovascular disease is the leading cause of death among men and women in the United States and upwards of 6.5 million individuals are adversely affected by heart failure (HF) each year (14). There are differences in the incidence, morbidity, and mortality of HF between women and men (7, 64) and these may be related to the role of estrogen in nitric oxide (NO) bioavailability and sensitivity (120, 148); however, the specific sex differences in the mechanisms underlying the cardiovascular physiology in HF have not been well delineated. HF begins with an initial insult to the heart that progresses to multiple organ system dysfunction and eventually develops into a syndrome which critically impacts the oxygen (O_2) transport system by reducing O_2 availability and increasing O_2 requirements. The O_2 transport dysfunction can be attributed to central (i.e., reduced heart function (160)) and peripheral (i.e., diminished vascular (36, 159), skeletal muscle and mitochondrial (80, 137) function) maladaptations. Experimental evidence shows that HF increases the reliance on glycolytic Type II muscles during exercise (63, 102, 137) and decreases NO bioavailability (46, 63) which, in collective, serves to exacerbate the metabolic stress induced by deficits to the O_2 transport system. The culmination of these impairments is reduced muscle function and exercise intolerance (112, 114), reduced quality of life, and ultimately death. Recently, our laboratory revealed NO-mediated sex differences in the control of skeletal muscle interstitial PO_2 (PO_2*is*) in healthy rats (29), which reflects the matching of O_2 delivery to utilization. This interstitial site contributes greatly to O_2 flux resistance (60) and is a critical component in establishing the driving pressure of O_2 across the sarcolemma into the mitochondria in order to sustain the energetic demands of muscle contractions (i.e., metabolic control). Since NO plays an important role in the cardioprotection seen in healthy females and in the etiology of HF, it is likely that a female model of HF would show substantially exaggerated PO_2*is* dysfunction; however, to date, this hypothesis has not been explored.

An ideal therapeutic intervention for patients with HF would target both aspects of the O_2 transport system by increasing O_2 delivery and reducing O_2 requirements during activity. Dietary nitrate supplementation (including beetroot juice) increases exercise performance in healthy individuals (5, 77, 142, 155). This effect is accomplished by lowering O_2 consumption ($\dot{V}O_2$) (5, 77), speeding $\dot{V}O_2$ kinetics (16, 28, 70), and increasing blood flow (i.e., bulk O_2 delivery (20, 44)) during submaximal exercise, all of which contribute to the enhanced exercise tolerance

found during severe intensity exercise (16, 70, 155). The precise mechanism(s) for these effects remain uncertain, but they are facilitated through the reduction of the dietary nitrate to nitrite in the mouth (83). Once absorbed into the circulatory system, nitrite is readily converted to NO in hypoxic (31, 141) and acidic (95) environments, which are present in the exercising muscle (particularly Type II fibers) and intensified by HF. These beneficial effects of dietary nitrate translate to patients with cardiovascular disease. To date, the diseases investigated include HF with preserved ejection fraction (HFpEF) (39, 157), ischemic HF with reduced ejection fraction (HFrEF) (i.e., myocardial infarction induced HF) (45, 61), non-ischemic dilated cardiomyopathy (with rEF) (21, 72), and peripheral arterial disease (71). Dietary nitrate increases the tolerance to exercise in some (39, 71, 72, 157), but not all (61) of these studies. Females were represented in few of these studies (21, 39, 72), and importantly, were entirely absent from investigations of myocardial infarction induced HF (45, 61).

Thus, the present investigation was designed to fill these gaps in our knowledge. For instance: 1) whether the sex differences seen in healthy skeletal muscle PO_2*is* translate to exaggerated pathology (exacerbated lowering of PO_2*is*) in female HF; 2) if sex affects the efficacy of dietary nitrate supplementation in a pre-clinical model of myocardial infarction-induced HF; and 3) the mechanisms which underlie the beneficial effects of dietary nitrate to potentially improve cardiovascular health, quality of life (157, 158), and reduce mortality in patients with HF. Specifically, we tested the following hypotheses: 1) HF would reduce PO_2*is* and impair the kinetics response to a greater extent in female HF rats; and 2) dietary nitrate supplementation would improve the PO_2*is* baseline and amplitude to a greater extent in female compared to male HF.

Materials and Methods

Ethical approval

Forty-two young adult (3-5 mo. old) Sprague-Dawley rats (Charles River Laboratories, Wilmington, MA) rats were maintained in accredited animal facilities at Kansas State University on a 12-h light-dark cycle with food and water provided *ad libitum* in isolated cages. All procedures were approved by the Institutional Animal Care and Use Committee of Kansas State University and conducted according to the National Research Council *Guide for the Care and Use of Laboratory Animals*. Equal numbers of male and female rats (n = 7 of each sex per group) were randomly assigned to healthy control, HF, or HF + Nitrate groups (n = 14 per group).

Myocardial infarction protocol

Myocardial infarction was induced in HF rats by surgical ligation of the left main coronary artery as described previously (45, 100). Rats were initially anesthetized with a 5% isoflurane-O_2 mixture (Butler Animal Health Supply, Elk Grove Village, IL; Linweld, Dallas, TX) and maintained on a ~2% isoflurane-O_2 mixture. The rats were then intubated and mechanically ventilated with a rodent respirator (model 680, Harvard Instruments, Holliston, MA) for the duration of the procedure. The heart was exposed via a left thoracotomy through the fifth intercostal space and the left main coronary artery was ligated 1-2 mm distal to the edge of the left atrium with a 6-0 braided polyester suture. The thorax was then closed with 2-0 gut and the skin with 3-0 silk. Bupivacaine (1.5 mg/kg sc), ampicillin (50 mg/kg im), and buprenorphine (~0.03 mg/kg im) were administered to alleviate pain and reduce the risk of infection. Rats were monitored for ~8 h post-surgery for the development of arrhythmias and/or other complications with care administered as necessary. At least 21 days of recovery were given to allow for complete remodeling of necrotic myocardial tissue and development of compensated HF (100, 102).

Dietary nitrate supplementation and measurement of plasma [nitrite]

HF rats randomly assigned to the dietary nitrate group (HF + Nitrate) received 5 days of nitrate-rich beetroot juice (1 mmol/kg/day; Beet it, James White Drinks, Ipswich UK) diluted into ~90 ml of water each night and consumption was verified in the morning. During the day, rats received water *ad libitum*. This dose represents a [nitrate] similar to that used in humans (5, 28, 142, 155) and crucially elevates plasma [nitrite] commensurately (44, 45) after accounting

for the increased metabolic rate of rats (99) and differences in the pathway of dietary nitrate (96) compared to humans. Plasma [nitrite] analysis was performed via chemiluminescence with a Sievers NO analyzer (NOA 280i, Sievers Instruments, Boulder, CO) using the techniques described previously (28, 45, 155) on small blood samples (~0.6 ml) drawn from the caudal artery. Within 5 min of the blood draw, these whole blood samples were spun at ≥ 1000 g in a 4 °C centrifuge for 5 min. Aliquots of the separated plasma (~0.3 ml) were pipetted into separate Eppendorf tubes and stored at -80 °C until later analysis.

Surgical Preparation

On the day of the experiment (described below), rats were anesthetized with a 5% isoflurane-O_2 mixture and then maintained on 2-3% isoflurane-O_2. The right carotid artery was isolated and a catheter (PE-10 connected to PE-50, Intra-Medic polyethylene tubing, Clay Adams Brand, Becton, Dickinson and Company, Sparks, MD) was inserted for measurement of mean arterial pressure (MAP) and heart rate (HR) collected with a PowerLab/LabChart data acquisition system (AD Instruments). Another catheter was inserted into the caudal artery for the administration of pentobarbital sodium anesthesia ([50 mg/ml]) and arterial blood sampling. After closing the catheter incisions, rats were progressively transitioned off of isoflurane to pentobarbital sodium anesthesia. Adequacy of anesthesia was monitored using toe pinch and corneal reflexes. Additional anesthesia was administered when necessary as 0.03-0.05 ml doses diluted in ~0.3 ml of heparinized saline. Rats were placed on a heating pad to maintain a core temperature of ~38 ˚C (measured via rectal probe). Incisions were then made to expose the left spinotrapezius muscle with overlying skin and fascia reflected as previously described (29, 60). Using 6-0 silk sutures, platinum iridium wire electrodes were secured to the rostral (cathode) and caudal (anode) portions of the muscle to facilitate electrically induced twitch contractions. Adjacent exposed tissue was covered with Saran wrap (Dow Brands, Indianapolis, IN) to reduce tissue dehydration. The exposed spinotrapezius was superfused frequently with warmed (38 ˚C) Krebs-Henseleit bicarbonate buffered solution equilibrated with 5% CO_2-95% N_2.

Experimental protocol

Twitch contractions of the spinotrapezius were electrically evoked (1 Hz, 6-7 V, 2 ms pulse duration) with a Grass S88 Stimulator (Quincy, MA, USA) for 180 s. This contraction protocol increases spinotrapezius muscle blood flow ~ 5-fold and metabolic rate ~7-fold without

altering blood pH and is consistent with moderate intensity exercise (10, 58) and elicits reproducible responses (29). Phosphorescence quenching was used to measure PO_2*is* in the spinotrapezius at rest and during contractions using a frequency domain phosphorometer (PMOD 5000; Oxygen Enterprises, Philadelphia, PA, USA) as previously described (29, 60). Briefly, the Oxyphor G4 (Pd-*meso*-tetra-(3,5-dicarboxyphenyl)-tetrabenzo-porphyrin) was injected locally (3-4 10 μL injections at 10 μM concentration) using a 29G needle with care taken to avoid damaging any visible vasculature. After injection, the spinotrapezius was covered with Saran wrap and given at least 20 min to allow the G4 to diffuse throughout the interstitial space. This Oxyphor is well-suited for use in biological tissues due to its inability to cross membranes and stability across physiological pH ranges (41); it is however, temperature sensitive and therefore spinotrapezius temperature was measured using a non-contact infrared thermometer. Mean spinotrapezius temperature was 32.1 ± 0.1 °C, with no differences between groups or change during contractions.

Phosphorescence quenching applies the Stern-Volmer relationship (41, 126), which describes the quantitative O_2 dependence of the phosphorescent probe G4 via the equation:

$$PO_{2is} = [(\tau_0/\tau) - 1]/(k_Q \cdot \tau_0)$$

where k_Q is the quenching constant and τ and τ_0 are the phosphorescence lifetimes at the ambient O_2 concentration and in the absence of O_2, respectively. For G4 in tissue at ~32.5 °C, k_Q is ~258 $mmHg^{-1} \cdot s^{-1}$ and τ_0 is ~226 μs (41). As muscle temperature does not appreciably change over the duration of the contraction protocol used herein, the phosphorescence lifetime is determined entirely by the O_2 partial pressure. After injection of G4, the common end of the bifurcated light guide was positioned 3-4 mm above the surface of the exposed muscle. PO_2*is* was measured continuously and recorded at 2 s intervals throughout the duration of the experimental protocol. All PO_2*is* measurements were performed in a dark room with minimal extraneous light exposure. Upon completion of the protocol, rats were euthanized with intra-arterial potassium chloride overdose (1 ml/kg of 4M KCl).

Analysis of interstitial PO_2 kinetics

The kinetics analyses of the PO_2*is* responses were conducted using 10 s of resting data and the 180 s contraction bout using a mono-exponential plus time delay model:

$$PO_2\,(t) = PO_{2(BL)} - \Delta_1 PO_2\,(1 - e^{-(t - TD)/\tau})$$

or a mono-exponential plus time delay with a secondary component when necessary:

$$PO_2\,(t) = PO_{2(BL)} - \Delta_1 PO_2\,(1 - e^{-(t - TD)/\tau}) + \Delta_2 PO_2\,(1 - e^{-(t - TD_2)/\tau_2})$$

where $PO_2\,(t)$ represents the PO_2*is* at any point in time, $PO_{2(BL)}$ is the baseline before the onset of contractions and any appreciable change in PO_{2is}, $\Delta_1 PO_2$ and $\Delta_2 PO_2$ are the primary and secondary amplitudes, TD and TD_2 are the time delays before the fall and secondary rise in PO_2, and τ and τ_2 are the time constants (*i.e.*, the time required to reach 63% of the amplitude) for the primary and secondary amplitudes. The mean response time (MRT) was calculated as the sum of the model derived TD and τ. When the secondary component model was necessary, the primary amplitude was constrained to not exceed the nadir value to maximize the accuracy of the primary response kinetics (29). The goodness of model fit was determined using the following criteria: 1) the coefficient of determination; 2) sum of the squared residuals; and 3) visual inspection and analysis of the model fits to the data and the residuals. Since $\Delta_2 PO_2$ (*i.e.*, undershoot of PO_2) was often non-exponential in nature, $\Delta_2 PO_2$ was determined manually by calculating the difference between the PO_{2is} at the end of contractions minus the nadir value of PO_{2is} during contractions.

Heart failure classification

On the day of the terminal experiment described above additional procedures were performed on the HF groups to describe the level of HF achieved by the myocardial infarction. Following cannulation of the right carotid artery, a micromanometer (2-french catheter-tip pressure manometer, Millar Instruments, Houston, TX) was advanced retrogradely into the left ventricle (LV) to determine LV end-diastolic pressure (LVEDP). These data were recorded with the same PowerLab/LabChart data acquisition system (AD Instruments). LVEDP was determined as the mean of 5 consecutive cardiac cycles. The LV infarction surface area was measured post-mortem using planimetry and expressed as %LV endocardial surface area.

Statistical analysis

All curve fitting and statistical analyses were performed using a commercially available software package (SigmaPlot 12.5, Systat Software, San Jose, CA). Differences between healthy, HF, and HF + Nitrate descriptive variables, hemodynamics (i.e., HR and MAP), and PO_2*is*

kinetics parameters were compared for sex and group differences using 2-way ANOVA. Differences between HF and HF + Nitrate for HF morphological and descriptive variables were compared for sex and group differences using 2-way ANOVA. Tukey's *post hoc* tests were used for multiple comparisons when significant differences were detected. Data are presented as means ± standard error. Significance was accepted at $p < 0.05$.

Results

Male rats were heavier than their female counterparts for all groups as expected (all $p < 0.001$; Table 3-1). There were no sex or group differences for resting HR and MAP (all $p > 0.05$; Table 3-1). Neither HR nor MAP changed appreciably during the contraction protocol (both $p > 0.05$, data not shown). The level of HF was not different between control and treatment groups (i.e., moderate HF; Table 3-2) and there were no differences between sexes for any morphological indices of HF (all $p > 0.05$) except for the lung mass to body mass ratio which was greater in females compared to males ($p < 0.05$).

Group mean PO_2is profiles at rest and during contractions are presented in Figure 3-1. There were no sex differences between healthy male and female rats, with the exception of females expressing a lower PO_2is nadir ($p < 0.05$, Table 3-3). HF reduced resting PO_2is for both sexes compared to healthy ($p < 0.01$, Table 3-3), but the reduction was greater in female compared to male HF rats ($p = 0.04$). Both sexes in HF expressed reduced PO_2is amplitudes following the onset of muscle contractions compared to healthy rats ($p < 0.01$) with no sex differences ($p = 0.3$). Female HF rats evidenced a reduced PO_2is undershoot and end-exercise PO_2is compared to healthy females (both $p < 0.02$) and HF males ($p = 0.02$ and $p = 0.001$, respectively). The difference between female and male rat PO_2is for all groups is shown in Figure 3-2.

Both sexes in the HF + Nitrate groups expressed elevated plasma [nitrite] compared to the HF groups (both, $p < 0.001$) with no differences between the sexes in either case (HF females: 56 ± 8; HF males: 45 ± 7; HF + Nitrate females: 156 ± 23; HF + Nitrate males: 165 ± 20 nM). Group mean PO_2is profiles for HF + Nitrate rats are presented in Figure 3 and the kinetics parameters are presented in Table 3-3. Nitrate supplementation resulted in resting PO_2is that were not different from healthy for female ($p = 0.51$) or male ($p = 0.39$) HF + Nitrate rats and there was no sex difference between female and male HF + Nitrate rats ($p = 0.59$). The male HF + Nitrate PO_2is amplitude was lower than healthy males ($p = 0.03$) but female HF + Nitrate was not different from healthy females ($p = 0.14$). The female HF + Nitrate MRT was significantly longer compared to male HF + Nitrate ($p = 0.02$), but neither were different from healthy (both $p > 0.05$). Female HF + Nitrate rats showed a reduced PO_2is undershoot and end-

exercise PO_2*is* compared to healthy females (both $p < 0.02$) and HF + Nitrate males ($p = 0.03$ and $p = 0.002$, respectively).

Discussion

Determining the mechanistic bases for exercise intolerance and the sexual (dis)similarities in HF patients carries important clinical implications. The primary original findings of the present investigation show that skeletal muscle PO_2*is* is reduced significantly at rest in both male and female HF rats, and this reduction is amplified in the females. Moreover, during contractions sex differences in PO_2*is* regulation are evident as female HF rats expressed a lower PO_2*is* nadir, undershoot, and end-exercise level compared to HF males. This indicates that females potentially see a greater decrement in peripheral O_2 delivery to utilization matching following myocardial infarction induced HF. These findings are important because this carrier-free space provides a substantial barrier to O_2 flux from the vascular space to the sarcolemma, and ultimately the mitochondria, potentially impacting metabolic control to a greater extent in female HF patients. Additionally, we show herein, for the first time, that 5 days of dietary nitrate (via beetroot juice) supplementation substantially improves O_2 delivery to utilization matching in the interstitial space of HF rats and that females may see a greater effect compared to males. These findings support the effectiveness of this therapeutic strategy to potentially improve quality of life and reduce morbidity and mortality in the human HF population.

Spinotrapezius Interstitial PO_2 in Heart Failure

We show herein for the first time, that the resting PO_2*is*, which is determined by the matching of O_2 delivery to utilization, is reduced in HF compared to healthy rats without differences in resting HR or MAP. The primary locus of this reduction is thought to be attenuated perfusive and diffusive O_2 delivery in the periphery since there were no obvious differences in central hemodynamics and skeletal muscle $\dot{V}O_2$ is very low at rest. Although not ubiquitous (particularly in the human upper limb (9, 130)), reduced resting peripheral blood flow has been shown in both human (66, 138) and animal (74, 102, 123) models of HF. Importantly, the impact of this reduced perfusive O_2 delivery is compounded by impaired diffusive O_2 delivery (42, 74, 123), likely due to heterogeneous capillary red cell hemodynamics (i.e., reduced red cell flux and velocity, and reduced proportion of capillaries supporting continuous flow) (74, 123). These attenuations in O_2 delivery would lead naturally to mismatched O_2 delivery-to-utilization despite the very low skeletal muscle $\dot{V}O_2$. This reduced resting PO_2*is* contrasts

importantly with microvascular PO_2 (PO_2*mv*, (12, 37)), in that PO_2*mv* is reduced in severe but not the moderate HF investigated herein. Although we were not able to explicitly test what caused this difference in the present investigation, one hypothesis is that PO_2*mv* is more effectively buffered from the reduced O_2 delivery across capillaries which may indicate that the PO_2*is* measurement is more sensitive to upstream dysfunction.

Interestingly, the primary response amplitude (Δ_1PO_2) during contractions was reduced in the HF groups compared to healthy controls. At the onset of muscle contractions, both O_2 delivery and utilization increase to meet the elevated energetic demands of the skeletal muscle. With respect to the healthy rats, the decreased Δ_1PO_2 in HF rats must be caused by either an increased O_2 delivery or a reduced utilization. Since increased blood flow has not been found in this population, it is more likely that reduced O_2 utilization lead to the differences seen herein. The oxidative capacity of HF rats (as indicated by citrate synthase activity) is often preserved at this level of HF (12, 34, 37), which suggests that the aforementioned mechanisms that lead to attenuated diffusive O_2 delivery (74, 123) may have also contributed to limiting muscle O_2 utilization. A potential explanation for this could be that the mitochondria which were more actively increasing oxidative phosphorylation were relatively more under perfused compared to the less active mitochondria. Additionally, since HF is often accompanied by fluid retention (i.e., tissue edema) the interstitial space could see an increased volume which would serve to impede O_2 flux into the myocyte. The methodology necessary to test these hypotheses are currently unavailable; however, evidence suggests that NO plays an important role in the regulation of both vascular O_2 delivery and spatial O_2 utilization within the cell (109, 147), indicating that the reduced NO bioavailability present in this disease is a primary cause of this dysfunction.

Sex Differences in the Control of Interstitial PO_2

Although in HF both sexes expressed a reduced $PO_{2(BL)}$ compared to healthy rats, the female group saw a greater reduction (~30% vs. ~20%) compared to males at equivalent levels of HF. As discussed above, this reduction in resting PO_2*is* is likely attributable to attenuated O_2 delivery. The contribution of NO to resting O_2 delivery has been pharmacologically dissected in both humans (119, 128, 136) and animals (88, 108, 150) with females showing a greater effect of endogenous NO inhibition compared to males (29, 76, 84, 136). The increased reliance on NO in

health for females paired with the reduced NO bioavailability induced by HF (46, 63) creates the potential for greater dysfunction in female HF patients (Hypothesis 1). To the best of our knowledge, the present investigation is the first to show sex specific effects of HF on skeletal muscle O_2 delivery to utilization matching, whereby HF induces greater decrements to PO_2*is* in female HF compared to male HF.

There was no difference between the sexes for Δ_1PO_2 in HF, but the undershoot (Δ_2PO_2) and end contraction PO_2*is* values were lower in the female HF group compared to both male HF and healthy females. This finding could be indicative of an increased fractional oxygen extraction in female HF, which agrees with the observation in human HF patients that exercising whole body O_2 utilization may be attenuated but the contracting/recruited muscle venous effluent PO_2 may be even lower than in healthy subjects (42). However, a more likely explanation is that an attenuated increase in O_2 delivery for the female HF rats resulted in the lower PO_2*is* baseline and end-exercise values. This profile has profound consequences with regard to metabolic control since PO_2*is* represents the driving pressure of the O_2 cascade across the sarcolemma into the mitochondria. These reductions are small in the absolute sense (~4 mmHg), but if they lead to deleterious changes of the intracellular PO_2, they result in altered metabolism and augmented production and accumulation of fatigue-inducing metabolites (55, 122). Substantiating these findings in an ovariectomized and/or aged model of HF would be ideal to discriminate whether the chronic reduction in NO bioavailability had a greater effect in the females of the present investigation due to their relative youth and/or the presence of estrogen. Nonetheless, these findings provide an important first step in our understanding of sex differences in the manifestation of HF and underscore the need for additional studies that include both sexes.

Effect of Dietary Nitrate on Interstitial PO_2 in Heart Failure

The reduced spinotrapezius PO_2*is* seen at rest in HF rats herein was not evident following 5 days of dietary nitrate supplementation. As discussed earlier, the presumable mechanism for this increase is improved O_2 delivery. Exercising blood flow (i.e., perfusive O_2 delivery) can be increased following dietary nitrate supplementation in healthy (44), older (20), and diseased (45) populations; however, resting blood flow appears to be unchanged (20, 28, 44, 45) supporting that this improved O_2 delivery was likely facilitated through diffusive rather than perfusive

mechanisms. In agreement with this notion, preliminary work from our laboratory revealed an increased proportion of skeletal muscle capillaries supporting continuous flow at rest in HF rats (i.e., increased diffusive O_2 transport capacity) following the same supplemental protocol used herein (30). This improved diffusive O_2 transport appears to have attenuated any O_2 utilization limitation, at least in the female HF rats, as their Δ_1PO_2 was no longer reduced compared to female healthy rats. It was recently revealed that dietary nitrate supplementation can increase local muscle O_2 extraction without altering bulk O_2 delivery in a human exercise model that mimics O_2 delivery limitations (28). An important finding of the present investigation is that dietary nitrate supplementation in HF rats revealed a significant slowing of the PO_2*is* kinetics (i.e., increased MRT) for the female HF rats compared to the male HF rats (but not the healthy female group, $p = 0.09$). An increased MRT is traditionally thought to reflect better matching of O_2 delivery to utilization for PO_2*mv* (10, 37) and is mechanistically explained by the observed increase of exercising blood flow following dietary nitrate supplementation in healthy and HF rats (44, 45). The combination of the greater relative increase in resting PO_2*is*, increased Δ_1PO_2, and slowed MRT in the female HF rats suggests that dietary nitrate supplementation is more efficacious in this population compared to males. Notwithstanding these effects, that the female HF end contraction PO_2 was still lower than males after dietary nitrate supplementation, while indicating greater fractional O_2 extraction, may also reflect lowered intramyocyte PO_2 with attendant pernicious consequences. An important next step would be to evaluate whether the sexual dimorphism seen herein translates to differential muscle function in a HF population. Muscle contractile function (as maximal knee extension efforts) was improved following dietary nitrate in a mixed population of HF patients during maximal effort contractions (21); however, that study was not designed to detect potential sex differences in the outcomes. Furthermore, the present investigation's findings are more indicative of moderate, rhythmic exercise where O_2 delivery plays an important role in sustained effort unlike the previously discussed maximal efforts where O_2 delivery is more vital for recovery between contractions (21).

Experimental Considerations

The primary limitation of the present study was the lack of control for the female rat estrus cycle (or ovariectomy), which precludes the differentiation between the effects of biological sex or sex hormones. Additionally, because we did not directly measure either O_2

delivery (as blood flow) or utilization (as metabolic rate) we can only hypothesize what drove the observed changes in the PO_2*is* using previously reported findings. We made efforts to not over interpret the present findings if data were not available from previous studies that directly measured O_2 delivery or utilization in HF and following dietary nitrate supplementation. Finally, we did not measure a performance outcome, such as muscle force production or endurance, so we are unable to explicitly state whether the observed effects would affect physical activity in these populations. However, we argue that the differential effects of HF and HF + Nitrate argues strongly for the need to include both sexes in cardiovascular research, particularly in populations which may have compromised NO bioavailability such as HF.

Conclusions

The primary novel finding of the present investigation is that myocardial infarction-induced HF reveals sexual dimorphism in the control of interstitial space O_2 delivery-to-utilization matching (indicated as PO_2*is*) in rats. Specifically, HF in female rats induces greater reductions in resting PO_2*is* compared to both healthy females and HF males, likely through peripheral vascular dysfunction mechanisms. Both sexes of HF rats expressed reduced PO_2*is* amplitudes during contractions compared to their healthy controls indicating reduced capacity to increase O_2 utilization. Following five days of dietary nitrate supplementation (as beetroot juice), resting PO_2*is* was improved in both HF sexes such that the values were not different from healthy controls. Interestingly, during contractions female HF rats no longer expressed reduced PO_2*is* amplitudes compared to healthy females while male HF rats remained lower than healthy males. Taken together, these findings indicate that, in this model of moderate HF, O_2 delivery-to-utilization matching is attenuated in a sex specific manner and dietary nitrate supplementation serves to offset this reduction with potentially greater efficacy in female HF rats during the early transient from rest to contractions.

Table 3-1 Healthy and Heart Failure Rat Body Weight and Resting Hemodynamics

	Healthy		Heart Failure		Heart Failure + Nitrate	
	Male	**Female**	**Male**	**Female**	**Male**	**Female**
Body weight (g)	373 ± 18	287 ± 10 *****	523 ± 11 †	337 ± 21 ***†**	506 ± 18 †	316 ± 8 *****
HR (beats/min)	395 ± 12	381 ± 18	364 ± 17	372 ± 9	362 ± 9	385 ± 11
MAP (mmHg)	107 ± 5	100 ± 6	100 ± 6	96 ± 4	101 ± 4	103 ± 5

HR, heart rate; MAP, mean arterial pressure. Values are means ± SE. *****, $p < 0.05$ vs male within group.

†, $p < 0.05$ vs healthy within sex.

Table 3-2 Morphological and Hemodynamic Characteristics of Heart Failure Groups

	Heart Failure		Heart Failure + Nitrate	
	Male	**Female**	**Male**	**Female**
Infarct size (%)	30 ± 2	33 ± 5	27 ± 3	31 ± 4
LVEDP (mmHg)	17 ± 1	16 ± 3	20 ± 4	15 ± 2
LV/Body mass (mg/g)	2.0 ± 0.1	1.9 ± 0.1	1.9 ± 0.1	2.0 ± 0.1
RV/Body mass (mg/g)	0.6 ± 0.1	0.6 ± 0.1	0.6 ± 0.1	0.6 ± 0.1
Lung/Body mass (mg/g)	3.6 ± 0.1	4.3 ± 0.2 *	3.8 ± 0.3	4.6 ± 0.3 *

HF, heart failure; LVEDP, left ventricular end-diastolic pressure; LV, left ventricle; RV, right ventricle. Data are means ± SE. All groups, $n = 7$. *, $p < 0.05$ vs male within group.

Table 3-3 Interstitial PO_2 Kinetics Parameters of the Spinotrapezius at Rest and During 180 s of Twitch Contractions

	Healthy		Heart Failure		Heart Failure + Nitrate	
	Male	**Female**	**Male**	**Female**	**Male**	**Female**
$PO_{2(BL)}$ (mmHg)	21.0 ± 0.7	19.2 ± 1.4	16.6 ± 2.2 †	13.7 ± 1.4 *†	17.8 ± 1.4	16.5 ± 2.3
Δ_1PO_2 (mmHg)	11.9 ± 0.8	12.9 ± 1.4	8.8 ± 1.4 †	7.6 ± 0.9 †	8.1 ± 1.1 †	9.7 ± 1.3
τ (s)	9 ± 1	11 ± 2	10 ± 2	11 ± 2	7 ± 1	14 ± 2 *
TD (s)	7 ± 1	7 ± 1	7 ± 2	10 ± 1	9 ± 1	9 ± 2
MRT (s)	16 ± 2	17 ± 3	17 ± 3	21 ± 2	16 ± 2	23 ± 2 *
$\Delta PO_2/\tau$ (mmHg/s)	1.5 ± 0.3	1.3 ± 0.2	1.0 ± 0.1 †	0.8 ± 0.2 †	1.4 ± 0.3	0.8 ± 0.2 *
$PO_{2(Nadir)}$ (mmHg)	9.1 ± 0.5	6.3 ± 1.1 *	7.7 ± 1.3	6.1 ± 0.9	9.8 ± 1.4	6.9 ± 1.5 *
Δ_2PO_2 (mmHg)	7.3 ± 1.1	7.4 ± 0.7	6.8 ± 1.6	4.3 ± 0.9 *†	5.1 ± 0.7	2.3 ± 0.2 *†
$PO_{2(End)}$ (mmHg)	16.0 ± 0.9	13.9 ± 1.3	14.5 ± 1.3	10.4 ± 1.0 *†	14.9 ± 1.6	9.2 ± 1.4 *†

$PO_{2(BL)}$, baseline interstitial PO_2; Δ_1PO_2, PO_2 primary amplitude; τ, time constant; TD, time delay; MRT, mean response time; Δ_2PO_2, PO_2 undershoot during contractions. All groups are n = 7. Values are means ± SE. *, $p < 0.05$ vs male within group. †, $p < 0.05$ vs healthy within sex.

Figure 3-1 Group average spinotrapezius interstitial PO_2 (PO_2*is*) at rest and during electrically-induced twitch contractions

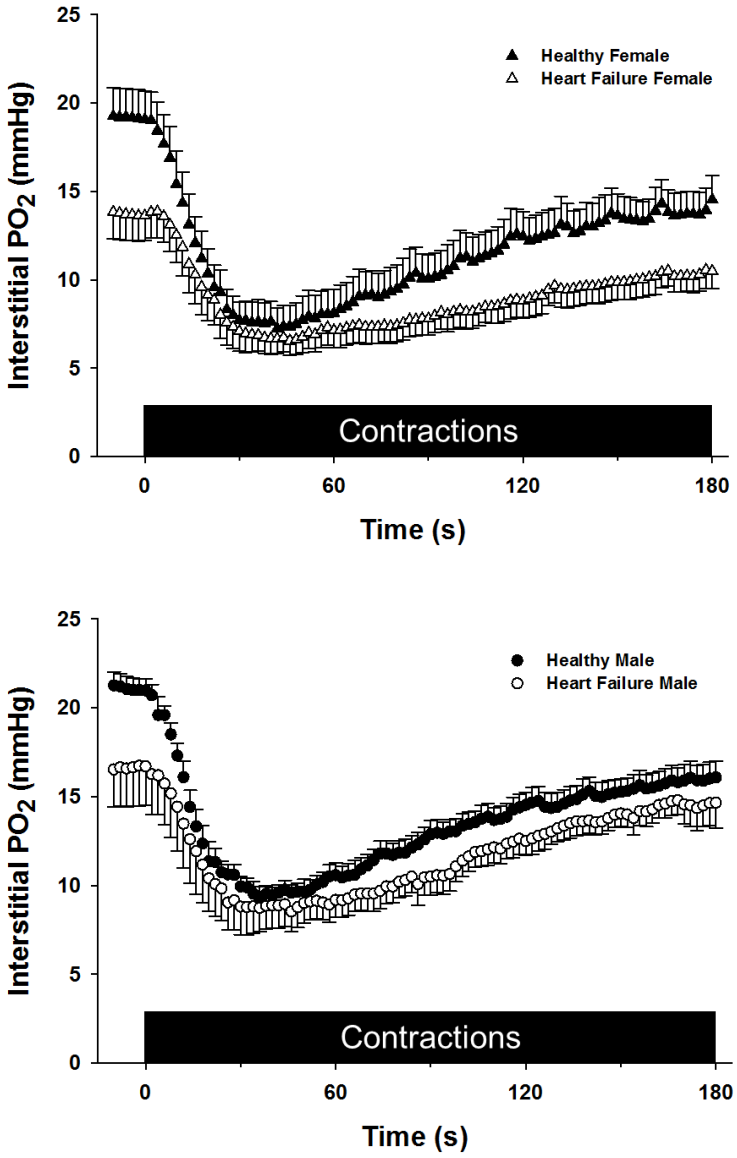

Top: Healthy females (filled triangles) and HF females (open triangles).

Bottom: Healthy male (filled circles) and HF males (open circles).

There were no differences between healthy female and male rats. HF reduced resting PO_2*is* in both sexes, and the decrease in resting PO_2*is* was greater in HF females compared to HF males. All data are means ± SE. All groups, n = 7.

Figure 3-2 Differences between Female and Male PO_2*is* at rest and during electrically-induced twitch contractions

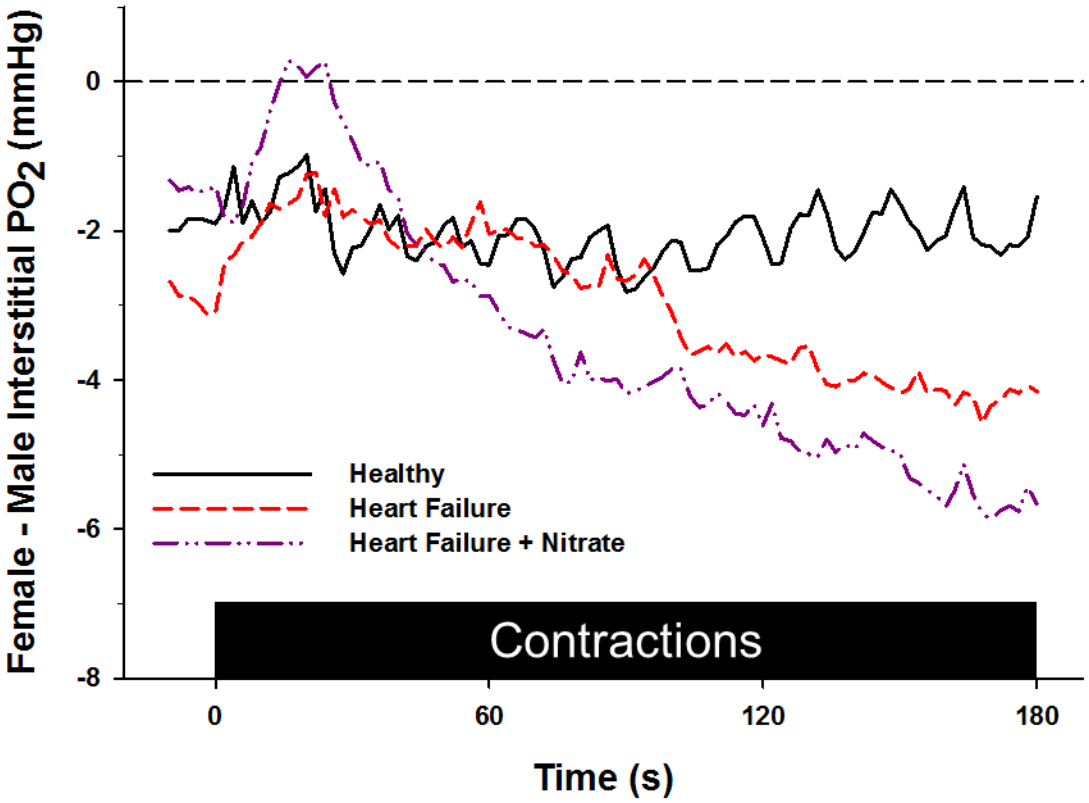

Healthy (solid black line), HF (dashed red line), and HF + Nitrate (dash-dotted purple line) groups are represented. In the Healthy rats, a small, but not significant, difference was present and remained constant across both rest and contractions. HF resulted in a significant difference for resting PO_2*is* between the sexes that was transiently worsened as contractions continued. Dietary nitrate supplementation in HF rats initially removed the sex difference in resting PO_2*is*, however, the sex differences were reestablished as muscle contractions continued (i.e., beyond 60 s).

Figure 3-3 Group average spinotrapezius interstitial PO_2 (PO_2*is*) at rest and during electrically-induced twitch contractions following 5 days of dietary nitrate supplementation (1 mmol/kg/day)

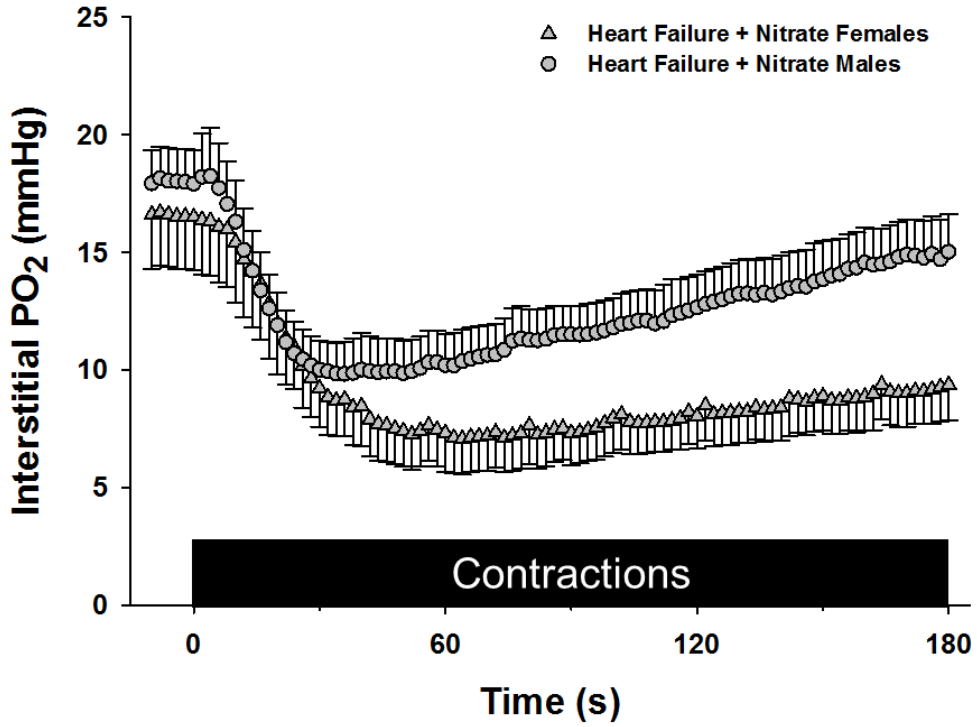

Data represent both females (triangles) and males (circles). Dietary nitrate supplementation increased resting PO_2*is* to values that were not different from Healthy rats and attenuated the sex difference present between the HF groups at rest. All data are means ± SE. Both groups, n = 7.

References

1. **Ade CJ, Broxterman RM, Craig JC, Schlup SJ, Wilcox SL, and Barstow TJ**. Relationship between simulated extravehicular activity tasks and measurements of physical performance. *Respir Physiol Neurobiol* 203: 19-27, 2014.

2. **Andersen P, and Saltin B**. Maximal perfusion of skeletal muscle in man. *J Physiol* 366: 233-249, 1985.

3. **Arnolda L, Brosnan J, Rajagopalan B, and Radda GK**. Skeletal-Muscle Metabolism in Heart-Failure in Rats. *American Journal of Physiology* 261: H434-H442, 1991.

4. **Bailey JK, Kindig CA, Behnke BJ, Musch TI, Schmid-Schoenbein GW, and Poole DC**. Spinotrapezius muscle microcirculatory function: effects of surgical exteriorization. *Am J Physiol Heart Circ Physiol* 279: H3131-3137, 2000.

5. **Bailey SJ, Winyard P, Vanhatalo A, Blackwell JR, Dimenna FJ, Wilkerson DP, Tarr J, Benjamin N, and Jones AM**. Dietary nitrate supplementation reduces the O_2 cost of low-intensity exercise and enhances tolerance to high-intensity exercise in humans. *J Appl Physiol (1985)* 107: 1144-1155, 2009.

6. **Baily RG, Lehman JC, Gubin SS, and Musch TI**. Non-invasive assessment of ventricular damage in rats with myocardial infarction. *Cardiovasc Res* 27: 851-855, 1993.

7. **Baker L, Meldrum KK, Wang M, Sankula R, Vanam R, Raiesdana A, Tsai B, Hile K, Brown JW, and Meldrum DR**. The role of estrogen in cardiovascular disease. *J Surg Res* 115: 325-344, 2003.

8. **Barker T, Poole DC, Noble ML, and Barstow TJ**. Human critical power-oxygen uptake relationship at different pedalling frequencies. *Experimental Physiology* 91: 621-632, 2006.

9. **Barrett-O'Keefe Z, Lee JF, Berbert A, Witman MA, Nativi-Nicolau J, Stehlik J, Richardson RS, and Wray DW**. Hemodynamic responses to small muscle mass exercise in heart failure patients with reduced ejection fraction. *Am J Physiol Heart Circ Physiol* 307: H1512-1520, 2014.

10. **Behnke BJ, Barstow TJ, Kindig CA, McDonough P, Musch TI, and Poole DC**. Dynamics of oxygen uptake following exercise onset in rat skeletal muscle. *Respir Physiol Neurobiol* 133: 229-239, 2002.

11. **Behnke BJ, Delp MD, Dougherty PJ, Musch TI, and Poole DC**. Effects of aging on microvascular oxygen pressures in rat skeletal muscle. *Respir Physiol Neurobiol* 146: 259-268, 2005.

12. **Behnke BJ, Delp MD, McDonough P, Spier SA, Poole DC, and Musch TI**. Effects of chronic heart failure on microvascular oxygen exchange dynamics in muscles of contrasting fiber type. *Cardiovascular Research* 61: 325-332, 2004.

13. **Behnke BJ, Kindig CA, Musch TI, Koga S, and Poole DC**. Dynamics of microvascular oxygen pressure across the rest-exercise transition in rat skeletal muscle. *Respir Physiol* 126: 53-63, 2001.

14. **Benjamin EJ, Blaha MJ, Chiuve SE, Cushman M, Das SR, Deo R, de Ferranti SD, Floyd J, Fornage M, Gillespie C, Isasi CR, Jimenez MC, Jordan LC, Judd SE, Lackland D, Lichtman JH, Lisabeth L, Liu S, Longenecker CT, Mackey RH, Matsushita K, Mozaffarian D, Mussolino ME, Nasir K, Neumar RW, Palaniappan L, Pandey DK, Thiagarajan RR, Reeves MJ, Ritchey M, Rodriguez CJ, Roth GA, Rosamond WD, Sasson C, Towfighi A, Tsao CW, Turner MB, Virani SS, Voeks JH, Willey JZ, Wilkins JT, Wu JH, Alger HM, Wong SS, Muntner P, American Heart Association Statistics C, and Stroke Statistics S**. Heart Disease and Stroke Statistics-2017 Update: A Report From the American Heart Association. *Circulation* 135: e146-e603, 2017.

15. **Blair SN, Kohl HW, Paffenbarger RS, Clark DG, Cooper KH, and Gibbons LW**. Physical-Fitness and All-Cause Mortality - a Prospective-Study of Healthy-Men and Women. *Jama-J Am Med Assoc* 262: 2395-2401, 1989.

16. **Breese BC, McNarry MA, Marwood S, Blackwell JR, Bailey SJ, and Jones AM**. Beetroot juice supplementation speeds O_2 uptake kinetics and improves exercise tolerance during severe-intensity exercise initiated from an elevated metabolic rate. *Am J Physiol Regul Integr Comp Physiol* 305: R1441-1450, 2013.

17. **Brown GC**. Nitric oxide and mitochondrial respiration. *Biochim Biophys Acta* 1411: 351-369, 1999.

18. **Broxterman RM, Craig JC, Smith JR, Wilcox SL, Jia C, Warren S, and Barstow TJ**. Influence of blood flow occlusion on the development of peripheral and central fatigue during small muscle mass handgrip exercise. *J Physiol* 593: 4043-4054, 2015.

19. **Casazza GA, Suh SH, Miller BF, Navazio FM, and Brooks GA**. Effects of oral contraceptives on peak exercise capacity. *J Appl Physiol (1985)* 93: 1698-1702, 2002.

20. **Casey DP, Treichler DP, Ganger CTt, Schneider AC, and Ueda K**. Acute dietary nitrate supplementation enhances compensatory vasodilation during hypoxic exercise in older adults. *J Appl Physiol (1985)* 118: 178-186, 2015.

21. **Coggan AR, Leibowitz JL, Spearie CA, Kadkhodayan A, Thomas DP, Ramamurthy S, Mahmood K, Park S, Waller S, Farmer M, and Peterson LR**. Acute Dietary Nitrate Intake Improves Muscle Contractile Function in Patients With Heart Failure: A Double-Blind, Placebo-Controlled, Randomized Trial. *Circ Heart Fail* 8: 914-920, 2015.

22. **Colburn TD, Ferguson SK, Holdsworth CT, Craig JC, Musch TI, and Poole DC**. Effect of sodium nitrite on local control of contracting skeletal muscle microvascular oxygen pressure in healthy rats. *J Appl Physiol (1985)* 122: 153-160, 2017.

23. **Convertino VA**. Gender differences in autonomic functions associated with blood pressure regulation. *Am J Physiol* 275: R1909-1920, 1998.

24. **Copp SW, Ferreira LF, Herspring KF, Hirai DM, Snyder BS, Poole DC, and Musch TI**. The effects of antioxidants on microvascular oxygenation and blood flow in skeletal muscle of young rats. *Exp Physiol* 94: 961-971, 2009.

25. **Copp SW, Hirai DM, Ferreira LF, Poole DC, and Musch TI**. Progressive chronic heart failure slows the recovery of microvascular O_2 pressures after contractions in the rat spinotrapezius muscle. *Am J Physiol Heart Circ Physiol* 299: H1755-1761, 2010.

26. **Copp SW, Hirai DM, Musch TI, and Poole DC**. Critical speed in the rat: implications for hindlimb muscle blood flow distribution and fibre recruitment. *J Physiol* 588: 5077-5087, 2010.

27. **Copp SW, Holdsworth CT, Ferguson SK, Hirai DM, Poole DC, and Musch TI**. Muscle fibre-type dependence of neuronal nitric oxide synthase-mediated vascular control in the rat during high speed treadmill running. *J Physiol* 591: 2885-2896, 2013.

28. **Craig JC, Broxterman RM, Smith JR, Allen JD, and Barstow TJ**. Effect of dietary nitrate supplementation on conduit artery blood flow, muscle oxygenation, and metabolic rate during handgrip exercise. *J Appl Physiol (1985)* 2018.

29. **Craig JC, Colburn TD, Hirai DM, Schettler MJ, Musch TI, and Poole DC**. Sex and nitric oxide bioavailability interact to modulate interstitial PO_2 in healthy rat skeletal muscle. *J Appl Physiol (1985)* 124: 1558-1566, 2018.

30. **Craig JC, Ferguson SK, Holdsworth CT, Colburn TD, Musch TI, and Poole DC**. Beetroot Supplementation Improves Microvascular Hemodynamics and Diffusive Oxygen Transport in Chronic Heart Failure Rats. *Med Sci Sports Exerc* 48: 669-669, 2016.

31. **Crawford JH, Isbell TS, Huang Z, Shiva S, Chacko BK, Schechter AN, Darley-Usmar VM, Kerby JD, Lang JD, Jr., Kraus D, Ho C, Gladwin MT, and Patel RP**. Hypoxia, red blood cells, and nitrite regulate NO-dependent hypoxic vasodilation. *Blood* 107: 566-574, 2006.

32. **Dean TM, Perreault L, Mazzeo RS, and Horton TJ**. No effect of menstrual cycle phase on lactate threshold. *J Appl Physiol (1985)* 95: 2537-2543, 2003.

33. **Delp MD, and Duan C**. Composition and size of type I, IIA, IID/X, and IIB fibers and citrate synthase activity of rat muscle. *J Appl Physiol (1985)* 80: 261-270, 1996.

34. **Delp MD, Duan C, Mattson JP, and Musch TI**. Changes in skeletal muscle biochemistry and histology relative to fiber type in rats with heart failure. *J Appl Physiol (1985)* 83: 1291-1299, 1997.

35. **Didion SP, Carmines PK, Ikenaga H, and Mayhan WG**. Enhanced constrictor responses of skeletal muscle arterioles during chronic myocardial infarction. *Am J Physiol-Heart C* 273: H1502-H1508, 1997.

36. **Didion SP, and Mayhan WG**. Effect of chronic myocardial infarction on in vivo reactivity of skeletal muscle arterioles. *Am J Physiol* 272: H2403-2408, 1997.

37. **Diederich ER, Behnke BJ, McDonough P, Kindig CA, Barstow TJ, Poole DC, and Musch TI**. Dynamics of microvascular oxygen partial pressure in contracting skeletal muscle of rats with chronic heart failure. *Cardiovasc Res* 56: 479-486, 2002.

38. **Dudley GA, Abraham WM, and Terjung RL**. Influence of exercise intensity and duration on biochemical adaptations in skeletal muscle. *J Appl Physiol Respir Environ Exerc Physiol* 53: 844-850, 1982.

39. **Eggebeen J, Kim-Shapiro DB, Haykowsky M, Morgan TM, Basu S, Brubaker P, Rejeski J, and Kitzman DW**. One Week of Daily Dosing With Beetroot Juice Improves Submaximal Endurance and Blood Pressure in Older Patients With Heart Failure and Preserved Ejection Fraction. *JACC Heart Fail* 4: 428-437, 2016.

40. **Esau PJ, Gittemeier EM, Opoku-Acheampong AB, Rollins KS, Baumfalk DR, Poole DC, Musch TI, Behnke BJ, and Copp SW**. Prostate cancer reduces endurance exercise capacity in association with reductions in cardiac and skeletal muscle mass in the rat. *Am J Cancer Res* 7: 2566-2576, 2017.

41. **Esipova TV, Karagodov A, Miller J, Wilson DF, Busch TM, and Vinogradov SA**. Two new "protected" oxyphors for biological oximetry: properties and application in tumor imaging. *Anal Chem* 83: 8756-8765, 2011.

42. **Esposito F, Mathieu-Costello O, Shabetai R, Wagner PD, and Richardson RS**. Limited maximal exercise capacity in patients with chronic heart failure: partitioning the contributors. *J Am Coll Cardiol* 55: 1945-1954, 2010.

43. **Fadel PJ, Zhao W, and Thomas GD**. Impaired vasomodulation is associated with reduced neuronal nitric oxide synthase in skeletal muscle of ovariectomized rats. *J Physiol* 549: 243-253, 2003.

44. **Ferguson SK, Hirai DM, Copp SW, Holdsworth CT, Allen JD, Jones AM, Musch TI, and Poole DC**. Impact of dietary nitrate supplementation via beetroot juice on exercising muscle vascular control in rats. *J Physiol* 591: 547-557, 2013.

45. **Ferguson SK, Holdsworth CT, Colburn TD, Wright JL, Craig JC, Fees A, Jones AM, Allen JD, Musch TI, and Poole DC**. Dietary nitrate supplementation: impact on skeletal muscle vascular control in exercising rats with chronic heart failure. *J Appl Physiol (1985)* 121: 661-669, 2016.

46. **Ferreira LF, Hageman KS, Hahn SA, Williams J, Padilla DJ, Poole DC, and Musch TI**. Muscle microvascular oxygenation in chronic heart failure: role of nitric oxide availability. *Acta Physiol (Oxf)* 188: 3-13, 2006.

47. **Ferreira LF, Padilla DJ, Williams J, Hageman KS, Musch TI, and Poole DC**. Effects of altered nitric oxide availability on rat muscle microvascular oxygenation during contractions. *Acta Physiol (Oxf)* 186: 223-232, 2006.

48. **Fishbein MC, Maclean D, and Maroko PR**. Experimental myocardial infarction in the rat: qualitative and quantitative changes during pathologic evolution. *Am J Pathol* 90: 57-70, 1978.

49. **Franciosa JA, Park M, and Levine TB**. Lack of correlation between exercise capacity and indexes of resting left ventricular performance in heart failure. *Am J Cardiol* 47: 33-39, 1981.

50. **Garnier A, Fortin D, Delomenie C, Momken I, Veksler V, and Ventura-Clapier R**. Depressed mitochondrial transcription factors and oxidative capacity in rat failing cardiac and skeletal muscles. *J Physiol* 551: 491-501, 2003.

51. **Gonzales JU, Thompson BC, Thistlethwaite JR, Harper AJ, and Scheuermann BW**. Forearm blood flow follows work rate during submaximal dynamic forearm exercise independent of sex. *J Appl Physiol (1985)* 103: 1950-1957, 2007.

52. **Gosker HR, van Mameren H, van Dijk PJ, Engelen MP, van der Vusse GJ, Wouters EF, and Schols AM**. Skeletal muscle fibre-type shifting and metabolic profile in patients with chronic obstructive pulmonary disease. *Eur Respir J* 19: 617-625, 2002.

53. **Grassi B, Gladden LB, Samaja M, Stary CM, and Hogan MC**. Faster adjustment of O_2 delivery does not affect $V(O_2)$ on-kinetics in isolated in situ canine muscle. *J Appl Physiol (1985)* 85: 1394-1403, 1998.

54. **Grassi B, Poole DC, Richardson RS, Knight DR, Erickson BK, and Wagner PD**. Muscle O_2 uptake kinetics in humans: implications for metabolic control. *J Appl Physiol (1985)* 80: 988-998, 1996.

55. **Haseler LJ, Richardson RS, Videen JS, and Hogan MC**. Phosphocreatine hydrolysis during submaximal exercise: the effect of FIO_2. *J Appl Physiol (1985)* 85: 1457-1463, 1998.

56. **Herspring KF, Ferreira LF, Copp SW, Snyder BS, Poole DC, and Musch TI**. Effects of antioxidants on contracting spinotrapezius muscle microvascular oxygenation and blood flow in aged rats. *J Appl Physiol (1985)* 105: 1889-1896, 2008.

57. **Higginbotham MB, Morris KG, Conn EH, Coleman RE, and Cobb FR**. Determinants of variable exercise performance among patients with severe left ventricular dysfunction. *Am J Cardiol* 51: 52-60, 1983.

58. **Hirai DM, Copp SW, Ferguson SK, Holdsworth CT, Musch TI, and Poole DC**. The NO donor sodium nitroprusside: evaluation of skeletal muscle vascular and metabolic dysfunction. *Microvasc Res* 85: 104-111, 2013.

59. **Hirai DM, Copp SW, Schwagerl PJ, Musch TI, and Poole DC**. Acute effects of hydrogen peroxide on skeletal muscle microvascular oxygenation from rest to contractions. *J Appl Physiol (1985)* 110: 1290-1298, 2011.

60. **Hirai DM, Craig JC, Colburn TD, Eshima H, Kano Y, Sexton WL, Musch TI, and Poole DC**. Skeletal muscle microvascular and interstitial PO_2 from rest to contractions. *J Physiol* 596: 869-883, 2018.

61. **Hirai DM, Zelt JT, Jones JH, Castanhas LG, Bentley RF, Earle W, Staples P, Tschakovsky ME, McCans J, O'Donnell DE, and Neder JA**. Dietary nitrate supplementation and exercise tolerance in patients with heart failure with reduced ejection fraction. *Am J Physiol Regul Integr Comp Physiol* 312: R13-R22, 2017.

62. **Hirai T, Visneski MD, Kearns KJ, Zelis R, and Musch TI**. Effects of NO synthase inhibition on the muscular blood flow response to treadmill exercise in rats. *J Appl Physiol (1985)* 77: 1288-1293, 1994.

63. **Hirai T, Zelis R, and Musch TI**. Effects of nitric oxide synthase inhibition on the muscle blood flow response to exercise in rats with heart failure. *Cardiovasc Res* 30: 469-476, 1995.

64. **Ho KK, Anderson KM, Kannel WB, Grossman W, and Levy D**. Survival after the onset of congestive heart failure in Framingham Heart Study subjects. *Circulation* 88: 107-115, 1993.

65. **Holdsworth CT, Ferguson SK, Colburn TD, Fees AJ, Craig JC, Hirai DM, Poole DC, and Musch TI**. Vascular K_{ATP} channels mitigate severe muscle O_2 delivery-utilization mismatch during contractions in chronic heart failure rats. *Respir Physiol Neurobiol* 238: 33-40, 2017.

66. **Isnard R, Lechat P, Kalotka H, Chikr H, Fitoussi S, Salloum J, Golmard JL, Thomas D, and Komajda M**. Muscular blood flow response to submaximal leg exercise in normal subjects and in patients with heart failure. *J Appl Physiol (1985)* 81: 2571-2579, 1996.

67. **Joyner MJ, and Casey DP**. Regulation of increased blood flow (hyperemia) to muscles during exercise: a hierarchy of competing physiological needs. *Physiol Rev* 95: 549-601, 2015.

68. **Jurkowski JE, Jones NL, Toews CJ, and Sutton JR**. Effects of menstrual cycle on blood lactate, O_2 delivery, and performance during exercise. *J Appl Physiol Respir Environ Exerc Physiol* 51: 1493-1499, 1981.

69. **Kellawan JM, Johansson RE, Harrell JW, Sebranek JJ, Walker BJ, Eldridge MW, and Schrage WG**. Exercise vasodilation is greater in women: contributions of nitric oxide synthase and cyclooxygenase. *Eur J Appl Physiol* 115: 1735-1746, 2015.

70. **Kelly J, Fulford J, Vanhatalo A, Blackwell JR, French O, Bailey SJ, Gilchrist M, Winyard PG, and Jones AM**. Effects of short-term dietary nitrate supplementation on blood pressure, O_2 uptake kinetics, and muscle and cognitive function in older adults. *Am J Physiol Regul Integr Comp Physiol* 304: R73-83, 2013.

71. **Kenjale AA, Ham KL, Stabler T, Robbins JL, Johnson JL, Vanbruggen M, Privette G, Yim E, Kraus WE, and Allen JD**. Dietary nitrate supplementation enhances exercise performance in peripheral arterial disease. *J Appl Physiol (1985)* 110: 1582-1591, 2011.

72. **Kerley CP, O'Neill JO, Reddy Bijjam V, Blaine C, James PE, and Cormican L**. Dietary nitrate increases exercise tolerance in patients with non-ischemic, dilated cardiomyopathy-a double-blind, randomized, placebo-controlled, crossover trial. *J Heart Lung Transplant* 35: 922-926, 2016.

73. **Kim A, Deo SH, Vianna LC, Balanos GM, Hartwich D, Fisher JP, and Fadel PJ**. Sex differences in carotid baroreflex control of arterial blood pressure in humans: relative contribution of cardiac output and total vascular conductance. *Am J Physiol Heart Circ Physiol* 301: H2454-2465, 2011.

74. **Kindig CA, Musch TI, Basaraba RJ, and Poole DC**. Impaired capillary hemodynamics in skeletal muscle of rats in chronic heart failure. *J Appl Physiol (1985)* 87: 652-660, 1999.

75. **Kleinert H, Wallerath T, Euchenhofer C, Ihrig-Biedert I, Li H, and Forstermann U**. Estrogens increase transcription of the human endothelial NO synthase gene: analysis of the transcription factors involved. *Hypertension* 31: 582-588, 1998.

76. **Kneale BJ, Chowienczyk PJ, Brett SE, Coltart DJ, and Ritter JM**. Gender differences in sensitivity to adrenergic agonists of forearm resistance vasculature. *J Am Coll Cardiol* 36: 1233-1238, 2000.

77. **Larsen FJ, Weitzberg E, Lundberg JO, and Ekblom B**. Effects of dietary nitrate on oxygen cost during exercise. *Acta Physiol (Oxf)* 191: 59-66, 2007.

78. **Lebrun CM, Petit MA, McKenzie DC, Taunton JE, and Prior JC**. Decreased maximal aerobic capacity with use of a triphasic oral contraceptive in highly active women: a randomised controlled trial. *Br J Sports Med* 37: 315-320, 2003.

79. **Leek BT, Mudaliar SR, Henry R, Mathieu-Costello O, and Richardson RS**. Effect of acute exercise on citrate synthase activity in untrained and trained human skeletal muscle. *Am J Physiol Regul Integr Comp Physiol* 280: R441-447, 2001.

80. **Lesnefsky EJ, Moghaddas S, Tandler B, Kerner J, and Hoppel CL**. Mitochondrial dysfunction in cardiac disease: ischemia--reperfusion, aging, and heart failure. *J Mol Cell Cardiol* 33: 1065-1089, 2001.

81. **Limberg JK, Eldridge MW, Proctor LT, Sebranek JJ, and Schrage WG**. Alpha-adrenergic control of blood flow during exercise: effect of sex and menstrual phase. *J Appl Physiol (1985)* 109: 1360-1368, 2010.

82. **Litwin SE, Katz SE, Morgan JP, and Douglas PS**. Serial echocardiographic assessment of left ventricular geometry and function after large myocardial infarction in the rat. *Circulation* 89: 345-354, 1994.

83. **Lundberg JO, Weitzberg E, and Gladwin MT**. The nitrate-nitrite-nitric oxide pathway in physiology and therapeutics. *Nat Rev Drug Discov* 7: 156-167, 2008.

84. **Majmudar NG, Robson SC, and Ford GA**. Effects of the menopause, gender, and estrogen replacement therapy on vascular nitric oxide activity. *J Clin Endocrinol Metab* 85: 1577-1583, 2000.

85. **Mancini DM, Coyle E, Coggan A, Beltz J, Ferraro N, Montain S, and Wilson JR**. Contribution of intrinsic skeletal muscle changes to ^{31}P NMR skeletal muscle metabolic abnormalities in patients with chronic heart failure. *Circulation* 80: 1338-1346, 1989.

86. **Mancini DM, Eisen H, Kussmaul W, Mull R, Edmunds LH, Jr., and Wilson JR**. Value of peak exercise oxygen consumption for optimal timing of cardiac transplantation in ambulatory patients with heart failure. *Circulation* 83: 778-786, 1991.

87. **Martin WH, 3rd, Ogawa T, Kohrt WM, Malley MT, Korte E, Kieffer PS, and Schechtman KB**. Effects of aging, gender, and physical training on peripheral vascular function. *Circulation* 84: 654-664, 1991.

88. **McAllister RM**. Endothelium-dependent vasodilation in different rat hindlimb skeletal muscles. *J Appl Physiol (1985)* 94: 1777-1784, 2003.

89. **McCullough DJ, Davis RT, 3rd, Dominguez JM, 2nd, Stabley JN, Bruells CS, and Behnke BJ**. Effects of aging and exercise training on spinotrapezius muscle microvascular PO_2 dynamics and vasomotor control. *J Appl Physiol (1985)* 110: 695-704, 2011.

90. **McGillivray-Anderson KM, and Faber JE**. Effect of acidosis on contraction of microvascular smooth muscle by alpha 1- and alpha 2-adrenoceptors. Implications for neural and metabolic regulation. *Circ Res* 66: 1643-1657, 1990.

91. **Mendelsohn ME, and Karas RH**. The protective effects of estrogen on the cardiovascular system. *N Engl J Med* 340: 1801-1811, 1999.

92. **Mezzani A, Corra U, Giordano A, Colombo S, Psaroudaki M, and Giannuzzi P**. Upper Intensity Limit for Prolonged Aerobic Exercise in Chronic Heart Failure. *Medicine and science in sports and exercise* 42: 633-639, 2010.

93. **Minson CT, Halliwill JR, Young TM, and Joyner MJ**. Influence of the menstrual cycle on sympathetic activity, baroreflex sensitivity, and vascular transduction in young women. *Circulation* 101: 862-868, 2000.

94. **Miura A, Endo M, Sato H, Sato H, Barstow TJ, and Fukuba Y**. Relationship between the curvature constant parameter of the power-duration curve and muscle cross-sectional area of the thigh for cycle ergometry in humans. *European Journal of Applied Physiology* 87: 238-244, 2002.

95. **Modin A, Bjorne H, Herulf M, Alving K, Weitzberg E, and Lundberg JO**. Nitrite-derived nitric oxide: a possible mediator of 'acidic-metabolic' vasodilation. *Acta Physiol Scand* 171: 9-16, 2001.

96. **Montenegro MF, Sundqvist ML, Nihlen C, Hezel M, Carlstrom M, Weitzberg E, and Lundberg JO**. Profound differences between humans and rodents in the ability to concentrate salivary nitrate: Implications for translational research. *Redox Biol* 10: 206-210, 2016.

97. **Murgatroyd SR, Ferguson C, Ward SA, Whipp BJ, and Rossiter HB**. Pulmonary O_2 uptake kinetics as a determinant of high-intensity exercise tolerance in humans. *J Appl Physiol (1985)* 110: 1598-1606, 2011.

98. **Musch TI**. Effects of sprint training on maximal stroke volume of rats with a chronic myocardial infarction. *J Appl Physiol (1985)* 72: 1437-1443, 1992.

99. **Musch TI, Bruno A, Bradford GE, Vayonis A, and Moore RL**. Measurements of metabolic rate in rats: a comparison of techniques. *J Appl Physiol (1985)* 65: 964-970, 1988.

100. **Musch TI, Moore RL, Leathers DJ, Bruno A, and Zelis R**. Endurance training in rats with chronic heart failure induced by myocardial infarction. *Circulation* 74: 431-441, 1986.

101. **Musch TI, Moore RL, Smaldone PG, Riedy M, and Zelis R**. Cardiac adaptations to endurance training in rats with a chronic myocardial infarction. *J Appl Physiol (1985)* 66: 712-719, 1989.

102. **Musch TI, and Terrell JA**. Skeletal muscle blood flow abnormalities in rats with a chronic myocardial infarction: rest and exercise. *Am J Physiol* 262: H411-419, 1992.

103. **Narkiewicz K, Phillips BG, Kato M, Hering D, Bieniaszewski L, and Somers VK**. Gender-selective interaction between aging, blood pressure, and sympathetic nerve activity. *Hypertension* 45: 522-525, 2005.

104. **NCHS**. In: *Health, United States, 2009: With Special Feature on Medical Technology*. Hyattsville (MD): 2010.

105. **Neder JA, Jones PW, Nery LE, and Whipp BJ**. Determinants of the exercise endurance capacity in patients with chronic obstructive pulmonary disease - The power-duration relationship. *Am J Resp Crit Care* 162: 497-504, 2000.

106. **Neder JA, Jones PW, Nery LE, and Whipp BJ**. The effect of age on the power/duration relationship and the intensity-domain limits in sedentary men. *European Journal of Applied Physiology* 82: 326-332, 2000.

107. **Nishimura RA, Tajik AJ, Shub C, Miller FA, Jr., Ilstrup DM, and Harrison CE**. Role of two-dimensional echocardiography in the prediction of in-hospital complications after acute myocardial infarction. *J Am Coll Cardiol* 4: 1080-1087, 1984.

108. **O'Leary DS, Dunlap RC, and Glover KW**. Role of endothelium-derived relaxing factor in hindlimb reactive and active hyperemia in conscious dogs. *Am J Physiol* 266: R1213-1219, 1994.

109. **Palacios-Callender M, Hollis V, Mitchison M, Frakich N, Unitt D, and Moncada S**. Cytochrome c oxidase regulates endogenous nitric oxide availability in respiring cells: A possible explanation for hypoxic vasodilation. *P Natl Acad Sci USA* 104: 18508-18513, 2007.

110. **Parker BA, Smithmyer SL, Pelberg JA, Mishkin AD, Herr MD, and Proctor DN**. Sex differences in leg vasodilation during graded knee extensor exercise in young adults. *J Appl Physiol (1985)* 103: 1583-1591, 2007.

111. **Picard MH, Wilkins GT, Ray PA, and Weyman AE**. Natural history of left ventricular size and function after acute myocardial infarction. Assessment and prediction by echocardiographic endocardial surface mapping. *Circulation* 82: 484-494, 1990.

112. **Piepoli MF, Guazzi M, Boriani G, Cicoira M, Corra U, Dalla Libera L, Emdin M, Mele D, Passino C, Vescovo G, Vigorito C, Villani GQ, Agostoni P, Working Group 'Exercise Physiology SC, and Cardiac Rehabilitation ISoC**. Exercise intolerance in chronic heart failure: mechanisms and therapies. Part I. *Eur J Cardiovasc Prev Rehabil* 17: 637-642, 2010.

113. **Poole DC, Burnley M, Vanhatalo A, Rossiter HB, and Jones AM**. Critical Power: An Important Fatigue Threshold in Exercise Physiology. *Medicine and science in sports and exercise* 48: 2320-2334, 2016.

114. **Poole DC, Hirai DM, Copp SW, and Musch TI**. Muscle oxygen transport and utilization in heart failure: implications for exercise (in)tolerance. *Am J Physiol Heart Circ Physiol* 302: H1050-1063, 2012.

115. **Poole DC, Richardson RS, Haykowsky MJ, Hirai DM, and Musch TI**. Exercise limitations in heart failure with reduced and preserved ejection fraction. *J Appl Physiol (1985)* 124: 208-224, 2018.

116. **Poole DC, Ward SA, Gardner GW, and Whipp BJ**. Metabolic and respiratory profile of the upper limit for prolonged exercise in man. *Ergonomics* 31: 1265-1279, 1988.

117. **Poucher SM**. The effect of NG-nitro-L-arginine methyl ester upon hindlimb blood flow responses to muscle contraction in the anaesthetized cat. *Exp Physiol* 80: 237-247, 1995.

118. **Puente-Maestu L, SantaCruz A, Vargas T, Martinez-Abad Y, and Whipp BJ**. Effects of training on the tolerance to high-intensity exercise in patients with severe COPD. *Respiration* 70: 367-370, 2003.

119. **Radegran G, and Saltin B**. Nitric oxide in the regulation of vasomotor tone in human skeletal muscle. *Am J Physiol* 276: H1951-1960, 1999.

120. **Rahimian R, Laher I, Dube G, and van Breemen C**. Estrogen and selective estrogen receptor modulator LY117018 enhance release of nitric oxide in rat aorta. *J Pharmacol Exp Ther* 283: 116-122, 1997.

121. **Richardson RS, Noyszewski EA, Kendrick KF, Leigh JS, and Wagner PD**. Myoglobin O2 desaturation during exercise. Evidence of limited O_2 transport. *J Clin Invest* 96: 1916-1926, 1995.

122. **Richardson RS, Noyszewski EA, Leigh JS, and Wagner PD**. Lactate efflux from exercising human skeletal muscle: role of intracellular PO_2. *J Appl Physiol (1985)* 85: 627-634, 1998.

123. **Richardson TE, Kindig CA, Musch TI, and Poole DC**. Effects of chronic heart failure on skeletal muscle capillary hemodynamics at rest and during contractions. *J Appl Physiol (1985)* 95: 1055-1062, 2003.

124. **Roepstorff C, Steffensen CH, Madsen M, Stallknecht B, Kanstrup IL, Richter EA, and Kiens B**. Gender differences in substrate utilization during submaximal exercise in endurance-trained subjects. *Am J Physiol Endocrinol Metab* 282: E435-447, 2002.

125. **Rogers J, and Sheriff DD**. Role of estrogen in nitric oxide- and prostaglandin-dependent modulation of vascular conductance during treadmill locomotion in rats. *J Appl Physiol (1985)* 97: 756-763, 2004.

126. **Rumsey WL, Vanderkooi JM, and Wilson DF**. Imaging of phosphorescence: a novel method for measuring oxygen distribution in perfused tissue. *Science* 241: 1649-1651, 1988.

127. **Shen W, Xu X, Ochoa M, Zhao G, Bernstein RD, Forfia P, and Hintze TH**. Endogenous nitric oxide in the control of skeletal muscle oxygen extraction during exercise. *Acta Physiol Scand* 168: 675-686, 2000.

128. **Shoemaker JK, Halliwill JR, Hughson RL, and Joyner MJ**. Contributions of acetylcholine and nitric oxide to forearm blood flow at exercise onset and recovery. *Am J Physiol* 273: H2388-2395, 1997.

129. **Shoemaker JK, Hogeman CS, Khan M, Kimmerly DS, and Sinoway LI**. Gender affects sympathetic and hemodynamic response to postural stress. *Am J Physiol Heart Circ Physiol* 281: H2028-2035, 2001.

130. **Shoemaker JK, Naylor HL, Hogeman CS, and Sinoway LI**. Blood flow dynamics in heart failure. *Circulation* 99: 3002-3008, 1999.

131. **Simonini A, Long CS, Dudley GA, Yue P, McElhinny J, and Massie BM**. Heart failure in rats causes changes in skeletal muscle morphology and gene expression that are not explained by reduced activity. *Circ Res* 79: 128-136, 1996.

132. **Sjaastad I, Sejersted OM, Ilebekk A, and Bjornerheim R**. Echocardiographic criteria for detection of postinfarction congestive heart failure in rats. *J Appl Physiol (1985)* 89: 1445-1454, 2000.

133. **Smith JR, Hageman KS, Harms CA, Poole DC, and Musch TI**. Respiratory muscle blood flow during exercise: Effects of sex and ovarian cycle. *J Appl Physiol (1985)* 122: 918-924, 2017.

134. **Stamler JS, and Meissner G**. Physiology of nitric oxide in skeletal muscle. *Physiol Rev* 81: 209-237, 2001.

135. **Stein AB, Tiwari S, Thomas P, Hunt G, Levent C, Stoddard MF, Tang XL, Bolli R, and Dawn B**. Effects of anesthesia on echocardiographic assessment of left ventricular structure and function in rats. *Basic Res Cardiol* 102: 28-41, 2007.

136. **Steinberg HO, Paradisi G, Cronin J, Crowde K, Hempfling A, Hook G, and Baron AD**. Type II diabetes abrogates sex differences in endothelial function in premenopausal women. *Circulation* 101: 2040-2046, 2000.

137. **Sullivan MJ, Green HJ, and Cobb FR**. Skeletal muscle biochemistry and histology in ambulatory patients with long-term heart failure. *Circulation* 81: 518-527, 1990.

138. **Sullivan MJ, Knight JD, Higginbotham MB, and Cobb FR**. Relation between central and peripheral hemodynamics during exercise in patients with chronic heart failure. Muscle blood flow is reduced with maintenance of arterial perfusion pressure. *Circulation* 80: 769-781, 1989.

139. **Tarnopolsky LJ, MacDougall JD, Atkinson SA, Tarnopolsky MA, and Sutton JR**. Gender differences in substrate for endurance exercise. *J Appl Physiol (1985)* 68: 302-308, 1990.

140. **Thompson BC, Fadia T, Pincivero DM, and Scheuermann BW**. Forearm blood flow responses to fatiguing isometric contractions in women and men. *Am J Physiol Heart Circ Physiol* 293: H805-812, 2007.

141. **Totzeck M, Hendgen-Cotta UB, Luedike P, Berenbrink M, Klare JP, Steinhoff HJ, Semmler D, Shiva S, Williams D, Kipar A, Gladwin MT, Schrader J, Kelm M, Cossins AR, and Rassaf T**. Nitrite regulates hypoxic vasodilation via myoglobin-dependent nitric oxide generation. *Circulation* 126: 325-334, 2012.

142. **Vanhatalo A, Bailey SJ, Blackwell JR, DiMenna FJ, Pavey TG, Wilkerson DP, Benjamin N, Winyard PG, and Jones AM**. Acute and chronic effects of dietary nitrate supplementation on blood pressure and the physiological responses to moderate-intensity and incremental exercise. *Am J Physiol Regul Integr Comp Physiol* 299: R1121-1131, 2010.

143. **Vanhatalo A, Black MI, DiMenna FJ, Blackwell JR, Schmidt JF, Thompson C, Wylie LJ, Mohr M, Bangsbo J, Krustrup P, and Jones AM**. The mechanistic bases of the power-time relationship: muscle metabolic responses and relationships to muscle fibre type. *J Physiol-London* 594: 4407-4423, 2016.

144. **Vanhatalo A, Fulford J, DiMenna FJ, and Jones AM**. Influence of hyperoxia on muscle metabolic responses and the power-duration relationship during severe-intensity exercise in humans: a ^{31}P magnetic resonance spectroscopy study. *Experimental Physiology* 95: 528-540, 2010.

145. **Vanhatalo A, Poole DC, DiMenna FJ, Bailey SJ, and Jones AM**. Muscle fiber recruitment and the slow component of O_2 uptake: constant work rate vs. all-out sprint exercise. *Am J Physiol-Reg I* 300: R700-R707, 2011.

146. **Varin R, Mulder P, Richard V, Tamion F, Devaux C, Henry JP, Lallemand F, Lerebours G, and Thuillez C**. Exercise improves flow-mediated vasodilatation of skeletal muscle arteries in rats with chronic heart failure - Role of nitric oxide, prostanoids, and oxidant stress. *Circulation* 99: 2951-2957, 1999.

147. **Victor VM, Nunez C, D'Ocon P, Taylor CT, Esplugues JV, and Moncada S**. Regulation of Oxygen Distribution in Tissues by Endothelial Nitric Oxide. *Circulation Research* 104: 1178-U1121, 2009.

148. **Wang D, Wang C, Wu X, Zheng W, Sandberg K, Ji H, Welch WJ, and Wilcox CS**. Endothelial dysfunction and enhanced contractility in microvessels from ovariectomized rats: roles of oxidative stress and perivascular adipose tissue. *Hypertension* 63: 1063-1069, 2014.

149. **Westwood FR**. The female rat reproductive cycle: a practical histological guide to staging. *Toxicol Pathol* 36: 375-384, 2008.

150. **White DG, Drew GM, Gurden JM, Penny DM, Roach AG, and Watts IS**. The effect of NG-nitro-L-arginine methyl ester upon basal blood flow and endothelium-dependent vasodilatation in the dog hindlimb. *Br J Pharmacol* 108: 763-768, 1993.

151. **Wilson JR, and Kapoor S**. Contribution of endothelium-derived relaxing factor to exercise-induced vasodilation in humans. *J Appl Physiol (1985)* 75: 2740-2744, 1993.

152. **Wisloff U, Stoylen A, Loennechen JP, Bruvold M, Rognmo O, Haram PM, Tjonna AE, Helgerud J, Slordahl SA, Lee SJ, Videm V, Bye A, Smith GL, Najjar SM, Ellingsen O, and Skjaerpe T**. Superior cardiovascular effect of aerobic interval training versus moderate continuous training in heart failure patients: a randomized study. *Circulation* 115: 3086-3094, 2007.

153. **Wittenberg BA, and Wittenberg JB**. Oxygen pressure gradients in isolated cardiac myocytes. *J Biol Chem* 260: 6548-6554, 1985.

154. **Wolzt M, Schmetterer L, Rheinberger A, Salomon A, Unfried C, Breiteneder H, Ehringer H, Eichler HG, and Fercher AF**. Comparison of non-invasive methods for the assessment of haemodynamic drug effects in healthy male and female volunteers: sex differences in cardiovascular responsiveness. *Br J Clin Pharmacol* 39: 347-359, 1995.

155. **Wylie LJ, Kelly J, Bailey SJ, Blackwell JR, Skiba PF, Winyard PG, Jeukendrup AE, Vanhatalo A, and Jones AM**. Beetroot juice and exercise: pharmacodynamic and dose-response relationships. *J Appl Physiol (1985)* 115: 325-336, 2013.

156. **Yang S, Bae L, and Zhang L**. Estrogen increases eNOS and NOx release in human coronary artery endothelium. *J Cardiovasc Pharmacol* 36: 242-247, 2000.

157. **Zamani P, Rawat D, Shiva-Kumar P, Geraci S, Bhuva R, Konda P, Doulias PT, Ischiropoulos H, Townsend RR, Margulies KB, Cappola TP, Poole DC, and Chirinos JA**. Effect of inorganic nitrate on exercise capacity in heart failure with preserved ejection fraction. *Circulation* 131: 371-380; discussion 380, 2015.

158. **Zamani P, Tan V, Soto-Calderon H, Beraun M, Brandimarto JA, Trieu L, Varakantam S, Doulias PT, Townsend RR, Chittams J, Margulies KB, Cappola TP, Poole**

DC, Ischiropoulos H, and Chirinos JA. Pharmacokinetics and Pharmacodynamics of Inorganic Nitrate in Heart Failure With Preserved Ejection Fraction. *Circ Res* 120: 1151-1161, 2017.

159. **Zelis R, and Flaim SF**. Alterations in vasomotor tone in congestive heart failure. *Prog Cardiovasc Dis* 24: 437-459, 1982.

160. **Zelis R, Flaim SF, Liedtke AJ, and Nellis SH**. Cardiocirculatory dynamics in the normal and failing heart. *Annu Rev Physiol* 43: 455-476, 1981.

Appendix A - Curriculum Vitae

JESSE C. CRAIG
Curriculum Vitae

Kansas State University
Department of Kinesiology
920 Denison Ave., Manhattan, Kansas 66506
Tel. 785-532-6765

EDUCATION

2015	M.S.	Kansas State University	Kinesiology
2011	B.A.	Washburn University	Kinesiology

HONORS AND AWARDS

2017	Doctoral Student Award, Dept. of Kinesiology, Kansas State University
2016	Clarenburg Research Fellow, Dept. of Anatomy & Physiology, Kansas State University
2015	Masters Scholar Award, American Kinesiology Association
2014	Distinguished Masters Student Scholarship Award, Dept. of Kinesiology, Kansas State University
2013-2018	Graduate Student Council Travel Award, Kansas State University

EXTRAMURAL FUNDING

Grants and Fellowships

2018 -	National Institutes of Health (NIH) Ruth L. Kirschstein National Research Service Award (NRSA) Institutional Training Grant (T32). National Heart, Lung, and Blood Institute. Awarded: 2T32HL007576-31.
2017	American Heart Association Pre-doctoral Research Fellowship. Not funded.

RESEARCH EXPERIENCE

Kansas State University

2015 - Clarenburg Research Laboratory (Mentors: David C. Poole, Ph.D. and Timothy I. Musch, Ph.D.)
2012 - 2015 Human Exercise Physiology Laboratory (Mentor: Thomas J. Barstow, Ph.D.)

TEACHING EXPERIENCE

Kansas State University, Department of Kinesiology

Physiology of Exercise Laboratory (2013 - 2018)
Bio-Behavioral Bases of Physical Activity Laboratory (2013 - 2014)
Multicultural Academic Program Success (MAPS) Bridge Program (2014 - 2017)
Anatomy and Physiology Laboratory (2014 - 2018)
Nutrition and Exercise Lecture (2015)
Cardiorespiratory/Comparative Physiology in Health and Disease (2016 - 2018)

DEPARTMENTAL SERVICE

Kansas State University

Committee Work

Kinesiology Student Advisory Board, graduate student representative
Assistant Professor Search Committee, Kinesiology

Coordinator

2015 - 2017 Physiology of Exercise Laboratory Coordinator

SERVICE TO PROFESSION

Reviewer

Journal of Applied Physiology
European Journal of Applied Physiology
Medicine & Science in Sports & Exercise

PROFESSIONAL SOCIETIES

American Physiological Society
American College of Sports Medicine
Central States Chapter of the American College of Sports Medicine

PUBLICATIONS

Refereed Journal Articles

1. Broxterman, R.M., C.J. Ade, S.L. Wilcox, S.J. Schlup, **J.C. Craig**, and T.J. Barstow. Influence of duty cycle on the power-duration relationship: Observations and potential mechanisms. *Respiratory Physiology & Neurobiology.* 192: 102-111, 2014.

2. Ade, C.J., R.M. Broxterman, **J.C. Craig**, S.J. Schlup, S.L. Wilcox, and T.J. Barstow. Relationship between simulated extravehicular activity tasks and measurements of physical performance. *Respiratory Physiology & Neurobiology.* 203: 19-27, 2014.

3. Broxterman, R.M., C.J. Ade, **J.C. Craig**, S.L. Wilcox, S.J. Schlup, and T.J. Barstow. The relationship between critical speed and the respiratory compensation point: coincidence or equivalence. *European Journal of Sport Science*. 15: 631-639, 2015.

4. Broxterman, R.M. C.J. Ade, **J.C. Craig**, S.L. Wilcox, S.J. Schlup, and T.J. Barstow. Influence of blood flow occlusion on muscle oxygenation characteristics and the parameters of the power-duration relationship. *Journal of Applied Physiology*.118: 880-889, 2015.

5. **Craig, J.C.**, R.M. Broxterman, and T.J. Barstow. Considerations for identifying the boundaries of sustainable performance. *Medicine & Science in Sports & Exercise*. 47: 1997, 2015.

6. Ade, C.J., R.M. Broxterman, **J.C. Craig**, and T.J. Barstow. Upper body aerobic exercise as a possible predictor of lower body performance. *Aerospace Medicine and Human Performance*. 86: 599-605, 2015.

7. Ade, C.J., R.M. Broxterman, **J.C. Craig**, S.J. Schlup, S.L. Wilcox, and T.J. Barstow. Standardized exercise tests and simulated terrestrial mission task performance. *Aerospace Medicine and Human Performance*. 86: 982-989, 2015.

8. Broxterman, R.M., **J.C. Craig**, J.R. Smith, S.L. Wilcox, C. Jia, S. Warren, and T.J. Barstow. Influence of blood flow occlusion on the development of peripheral and central fatigue during small muscle mass handgrip exercise. *The Journal of Physiology*. 593: 4043-4054, 2015.

9. Broxterman, R.M., **J.C. Craig**, C.J. Ade, S.L. Wilcox, and T.J. Barstow. The effect of resting blood flow occlusion on exercise tolerance and W'. *American Journal of Physiology – Regulatory, Integrative and Comparative Physiology*. 309: R684-R691, 2015.

10. Ade, C.J., R.M. Broxterman, **J.C. Craig**, S.J. Schlup, S.L. Wilcox, S. Warren, P. Kuehl, D. Gude, C. Jia, and T.J. Barstow. Prediction of lunar- and martian-based intra- and site-to-site task performance. *Aerospace Medicine and Human Performance*. 87: 367-374, 2016.

11. Noel, J.A., R.M. Broxterman, G.M. McCoy, **J.C. Craig**, K.J. Phelps, D.D. Burnett, M.A. Vaughn, T.J. Barstow, T.G. O'Quinn, J.C. Woodworth, J.M. DeRouchey, and J.M. Gonzalez. Use of electromyography to detect muscle exhaustion in finishing barrows fed ractopamine-HCl. *Journal of Animal Science*. 94: 2344-2356, 2016.

12. Broxterman, R.M., P.F. Skiba, **J.C. Craig**, S.L. Wilcox, C.J. Ade, and T.J. Barstow. W' expenditure and reconstitution during constant power exercise: mechanistic insight into the determinants of W'. *Physiological Reports*. 4: e12856, 2016.

13. Ferguson, S.K., C.T. Holdsworth, T.D. Colburn, J. Wright, **J.C. Craig**, A.J. Fees, A.M. Jones, J.D. Allen, T.I. Musch, and D.C. Poole. Dietary nitrate supplementation: Impact on skeletal muscle vascular control in exercising rats with chronic heart failure. *Journal of Applied Physiology*. 121: 661-669, 2016.

14. Colburn, T.D., S.K. Ferguson, C.T. Holdsworth, **J.C. Craig**, T.I. Musch, and D.C. Poole. Effect of sodium nitrite on local control of contracting skeletal muscle microvascular oxygen pressure in healthy rats. *Journal of Applied Physiology*. 122: 153-160, 2017.

15. Holdsworth, C.T., S.K. Ferguson, T.D. Colburn, A.J. Fees, **J.C. Craig**, D.M. Hirai, D.C. Poole, and T.I. Musch. Vascular K_{ATP} channels mitigate severe muscle O_2 delivery-utilization mismatch during contractions in chronic heart failure rats. *Respiratory Physiology and Neurobiology*. 238: 33-40, 2017.

16. Billinger, S.A., **J.C. Craig**, S. Kwapezeski, J.F. Sisante, E.D. Vidoni, R. Maletsky, and D.C. Poole. Dynamics of middle cerebral artery blood flow velocity during moderate intensity exercise. *Journal of Applied Physiology*. 122: 1125-1133, 2017.

17. **Craig, J.C.**, R.M. Broxterman, S.L. Wilcox, C. Chen, and T.J. Barstow. Influence of adipose tissue thickness, muscle site, and sex on near-infrared spectroscopy derived total-[hemoglobin + myoglobin]. *Journal of Applied Physiology*. 123: 1571-1578, 2017.

18. Hirai, D.M., **J.C. Craig**, T.D. Colburn, H. Eshima, Y. Kano, W.L. Sexton, T.I. Musch, and D.C. Poole. Skeletal muscle microvascular and interstitial PO_2 from rest to contractions. *The Journal of Physiology*. 596: 869-883, 2018.

19. **Craig, J.C.**, T.D. Colburn, D.M. Hirai, M.J. Schettler, T.I. Musch, and D.C. Poole. Sex and nitric oxide bioavailability interact to modulate interstitial PO_2 in healthy rat skeletal muscle. *Journal of Applied Physiology*. 124: 1558-1566, 2018.

Accepted for Publication

20. **Craig, J.C.**, R.M. Broxterman, J.R. Smith, J.D. Allen, and T.J. Barstow. Effect of dietary nitrate supplementation on conduit artery blood flow, muscle oxygenation, and metabolic rate during handgrip exercise. *Journal of Applied Physiology*. Accepted. DOI: 10.1152/japplphysiol.00772.2017

21. Ward*, J.L., **J.C. Craig***, Y. Liu, E.D. Vidoni, R. Maletsky, D.C. Poole, and S.A. Billinger. Effect of healthy aging and sex on middle cerebral artery blood velocity dynamics during moderate intensity exercise. *American Journal of Physiology – Heart and Circulatory Physiology*. Accepted. DOI: 10.1152/ajpheart.00129.2018

22. Broxterman, R.M., **J.C. Craig**, and R.S. Richardson. The respiratory compensation point/deoxy-BP are not valid surrogates for critical power/maximal lactate steady-state. *Medicine & Science in Sports & Exercise*. Accepted. DOI: 10.1249/MSS.0000000000001699

Manuscripts in Review

23. **Craig, J.C.**, T.D. Colburn, D.M. Hirai, T.I. Musch, and D.C. Poole. Sexual dimorphism in the control of skeletal muscle interstitial PO_2 of heart failure rats: Effects of dietary nitrate supplementation. *Nitric Oxide*. In review.

24. Hirai, D.M., T.D. Colburn, **J.C. Craig**, K. Hotta, Y. Kano, T.I. Musch, and D.C. Poole. Skeletal muscle interstitial O_2 pressures: Bridging the gap between the capillary and myocyte. *Microcirculation*. In review.

25. Caldwell, J.T., S.L. Sutterfield, H.K. Post, **J.C. Craig**, S.W. Copp, and C.J. Ade. Impact of acute dietary nitrate supplementation during exercise in hypertensive women. *Medicine & Science in Sports & Exercise*. In review.

26. Caldwell, J.T., S.L. Sutterfield, **J.C. Craig**, D.R. Baumfauk, S.W. Copp, and C.J. Ade. Vasoconstrictor responsiveness in post-menopausal hypertensive women. *Medicine & Science in Sports & Exercise*. In review.

27. Witte E., Y. Lui, J.L. Ward, E.D. Vidoni, K.S. Kempf, A. Whitaker, **J.C. Craig**, D.C. Poole, and S.A. Billinger. Exercise intensity and middle cerebral artery dynamics in humans. *Frontiers in Physiology*. In review.

Manuscripts in Preparation

28. **Craig, J.C.**, T.D. Colburn, J.T. Caldwell, D.M. Hirai, A. Tabuchi, D.R. Baumfalk, B.J. Behnke, C.J. Ade, T.I. Musch, and D.C. Poole. Partitioning the central and peripheral contributions to the speed-duration relationship in heart failure rats. In preparation.

29. Tabuchi, A., **J.C. Craig**, D.M. Hirai, T.D. Colburn, Y. Kano, D.C. Poole, and T.I. Musch. Systemic NOS inhibition reduces muscle oxygenation more in intact females than male rats. In preparation.

30. Colburn, T.D., C.T. Holdsworth, **J.C. Craig**, D.M. Hirai, T.I. Musch, D.C. Poole, and M.J. Kenney. ATP-sensitive K^+ channel inhibition via Glibenclamide does not increase lumbar or renal sympathetic nerve discharge in healthy rats. In preparation.

Book Chapters

1. **Craig, J.C.**, A. Vanhatalo, M. Burnley, A.M. Jones, and D.C. Poole. Critical power: Possibly the most important fatigue threshold in exercise physiology. In *Muscle and Exercise Physiology*, 2018. Edited by Jerzy A. Zoladz. Academic Press.

Conference Abstracts

1. **Craig J.C.**, C.J. Ade, R.M. Broxterman, S.L. Wilcox, S.J. Schlup, Y. Mendoza, L. Chavez, and T.J. Barstow. The Relationship Between Critical Speed and the Respiratory Compensation Point. American College of Sports Medicine, Indianapolis, IN, 2013.

2. Wilcox S.L., R.M. Broxterman, C.J. Ade, S.J. Schlup, **J.C. Craig**, L. Chavez, Y. Mendoza, and T.J. Barstow. The Relationship Between Physiologic Parameters In Upper Versus Lower Body Exercise. American College of Sports Medicine, Indianapolis, IN, 2013.

3. Schlup S.J., C.J. Ade, R.M. Broxterman, S.L. Wilcox, **J.C. Craig**, and T.J. Barstow. Kinetics of Leg and Capillary Blood Flow Response to Knee Extension Exercise. American College of Sports Medicine, Indianapolis, IN, 2013.

4. Ade C.J., R.M. Broxterman, S.J. Schlup, S.L. Wilcox, **J.C. Craig**, J. Bernard, and T.J. Barstow. Effects of Retrograde Shear on the Kinetics of Blood Flow to Hand Grip Exercise. American College of Sports Medicine, Indianapolis, IN, 2013.

5. Broxterman, R.M., C.J. Ade, S.L. Wilcox, **J.C. Craig**, and T.J. Barstow. Lunar and Mars Simulated Extravehicular Activity (EVA) Evoked Physiological Responses. Experimental Biology, San Diego, CA, 2014.

6. **Craig J.C.**, R.M. Broxterman, and T.J. Barstow. Influence of Adipose Tissue Thickness (ATT) On NIRS-derived Total [Hb + Mb] At Four Sites. American College of Sports Medicine, Orlando, FL, 2014.

7. Broxterman R.M., C.J. Ade, **J.C. Craig**, S.L. Wilcox, and T.J. Barstow. Muscle Oxygenation Characteristics Within the Contraction-Relaxation Cycle for Handgrip Exercise. American College of Sports Medicine, Orlando, FL, 2014.

8. **Craig J.C.**, R.M. Broxterman, and T.J. Barstow. Effect of Beetroot Juice Supplementation on Conduit Artery and Microvascular Hemodynamics During Small Muscle Mass Handgrip Exercise. Experimental Biology, Boston, MA, 2015.

9. Broxterman R.M., S.L. Wilcox, **J.C. Craig**, C. Jia, S. Warren, and T.J. Barstow. Influence of Ischemia on Peripheral and Central Fatigue During Handgrip Exercise. Experimental Biology, Boston, MA, 2015.

10. **Craig J.C.**, R.M. Broxterman, and T.J. Barstow. Beetroot Supplementation and Small Muscle Mass Handgrip Exercise: Effect on Central and Peripheral Fatigue. American College of Sports Medicine, San Diego, CA, 2015.

11. Broxterman R.M., C.J Ade, **J.C. Craig**, S.L. Wilcox, P.F. Skiba, and T.J. Barstow. Modeling the Utilization and Reconstitution of W' Within the Contraction-relaxation Cycle for Handgrip Exercise. American College of Sports Medicine, San Diego, CA, 2015.

12. **Craig J.C.**, S.K. Ferguson, C.T. Holdsworth, T.D. Colburn, T.I. Musch, and D.C. Poole. Beetroot Supplementation Improves Microvascular Hemodynamics and Diffusive Oxygen Transport in Chronic Heart Failure Rats. American College of Sports Medicine, Boston, MA, 2016.

13. Hammer S.M., **J.C. Craig**, R.M. Broxterman, and T.J. Barstow. Oxygen Utilization During the Contraction-Relaxation Cycle of Intermittent Forearm Exercise. American College of Sports Medicine, Boston, MA, 2016.

14. **Craig J.C.**, M.J. Schettler, T.D. Colburn, D.M. Hirai, D.C. Poole, and T.I. Musch. No Sex Differences in Muscle O_2 Delivery-to-Utilization Matching Before or During Contractions in Rats. American College of Sports Medicine, Denver, CO, 2017.

15. Colburn T.D., **J.C. Craig**, D.M. Hirai, K.S. Hageman, T.I. Musch, and D.C. Poole. NOS Blockade Reveals No Sex Difference in O_2 Delivery-to-Utilization Matching in Rats During Contractions. American College of Sports Medicine, Denver, CO, 2017.

16. **Craig J.C.**, T.D. Colburn, D.M. Hirai, D.C. Poole, and T.I. Musch. Dietary Nitrate Supplementation via Beetroot Juice Improves Muscle O_2 Delivery and Utilization Matching in Heart Failure Rats. Experimental Biology, Chicago, IL, 2017.

17. Colburn T.D., C.T. Holdsworth, **J.C. Craig**, D.M. Hirai, S. Montgomery, M.J. Kenney, T.I. Musch, and D.C. Poole. ATP-sensitive K^+ Channel Inhibition via Glibenclamide Does Not Increase Lumbar or Renal Sympathetic Nerve Discharge in Healthy Rats. Experimental Biology, Chicago, IL, 2017.

18. Hirai D.M., T.D. Colburn, **J.C. Craig**, T.I. Musch, and D.C. Poole. Dynamics of Skeletal Muscle Microvascular and Interstitial PO_2 from Rest to Contractions. Experimental Biology, Chicago, IL, 2017.

19. **Craig J.C.**, J.H. Merino, D.M. Hirai, T.D. Colburn, A. Tabuchi, J.T. Caldwell, C.J. Ade, T.I. Musch, and D.C. Poole. Critical Speed in Heart Failure Rats: The Central Determinant of Performance. American College of Sports Medicine, Minneapolis, MN, 2018.

20. Colburn, T.D., **J.C. Craig**, D.M. Hirai, T.I. Musch, and D.C. Poole. Recovery Interstitial PO_2 Dynamics Following Contractions in Healthy Skeletal Muscle of Different Oxidative Capacity. American College of Sports Medicine, Minneapolis, MN, 2018.

21. Hirai, D.M., T.D. Colburn, **J.C. Craig**, A. Tabuchi, T.I. Musch, and D.C. Poole. Dynamics of Skeletal Muscle Interstitial PO_2 During Recovery from Contractions. American College of Sports Medicine, Minneapolis, MN, 2018.

22. **Craig J.C.**, T.D. Colburn, J.T. Caldwell, D.M. Hirai, A. Tabuchi, J.H. Merino, C.J. Ade, T.I. Musch, and D.C. Poole. Central Cardiac Determinants of the Speed-duration Relationship in Heart Failure Rats. Experimental Biology, San Diego, CA, 2018.

23. Colburn T.D., **J.C. Craig**, D.M. Hirai, A. Tabuchi, K.S. Hageman, T.I. Musch, and D.C. Poole. Interstitial PO_2 Dynamics During Contractions in Healthy Skeletal Muscle: Relationship to Oxidative Capacity and Nitric Oxide Bioavailability. Experimental Biology, San Diego, CA, 2018.

24. Hirai D.M., **J.C. Craig**, T.D. Colburn, A. Tabuchi, K.S. Hageman, T.I. Musch, and D.C. Poole. Regulation of Capillary Hemodynamics by K_{ATP} Channels in Resting Skeletal Muscle. Experimental Biology, San Diego, CA, 2018.

25. Caldwell J.T., **J.C. Craig**, H.K. Post, G.M. Lovoy, S.L. Sutterfield, H.R. Bannister, S.W. Copp, and C.J. Ade. Effect of Dietary Nitrate on Blood Pressure and Vascular Control in Post-Menopausal Hypertensive Women. Experimental Biology, San Diego, CA, 2018.

Scientific Presentations

1. Broxterman, R.M., C.J. Ade, S.L. Wilcox, **J.C. Craig**, and T.J. Barstow. Determination of appropriate physiological measurements for predicting EVA task-failure. NASA Human Research Program Workshop, Galveston, TX, 2014.

2. **Craig J.C.**, S.K. Ferguson, C.T. Holdsworth, T.D. Colburn, T.I. Musch, and D.C. Poole. Beetroot Supplementation Improves Microvascular Hemodynamics and Diffusive Oxygen Transport in Chronic Heart Failure Rats. American College of Sports Medicine, Boston, MA, 2016.

3. **Craig J.C.**, T.D. Colburn, J.T. Caldwell, D.M. Hirai, A. Tabuchi, J.H. Merino, C.J. Ade, T.I. Musch, and D.C. Poole. Central Cardiac Determinants of the Speed-duration Relationship in Heart Failure Rats. Experimental Biology, San Diego, CA, 2018.